Detrital zircon age patterns from turbidites of the Balagne and Piedmont nappes of Alpine Corsica (France): Evidence for a European margin source

Wei Lin, Philippe Rossi, Michel Faure, Xian-Hua Li, Wenbin Ji, Yang Chu

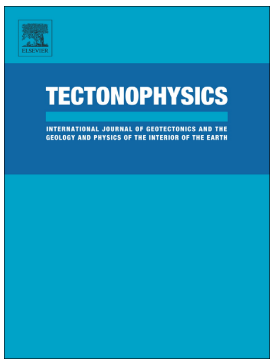

Detrital zircon age patterns from turbidites of the Balagne and Piedmont nappes of Alpine Corsica (France): Evidence for a European margin source

Wei Lin, Philippe Rossi, Michel Faure, Xian-Hua Li, Wenbin Ji, Yang Chu

PII: S0040-1951(17)30391-8
DOI: doi:10.1016/j.tecto.2017.09.015
Reference: TECTO 127628

To appear in: *Tectonophysics*

Received date: 19 March 2017
Revised date: 8 September 2017
Accepted date: 19 September 2017

Please cite this article as: Wei Lin, Philippe Rossi, Michel Faure, Xian-Hua Li, Wenbin Ji, Yang Chu , Detrital zircon age patterns from turbidites of the Balagne and Piedmont nappes of Alpine Corsica (France): Evidence for a European margin source. The address for the corresponding author was captured as affiliation for all authors. Please check if appropriate. Tecto(2017), doi:10.1016/j.tecto.2017.09.015

Detrital zircon age patterns from turbidites of the Balagne and Piedmont nappes of Alpine Corsica (France): evidence for an European margin source

Wei Lin [a, d*], Philippe Rossi [b], Michel Faure [c], Xian-Hua Li [a, d], Wenbin Ji [a, d], and Yang Chu [a, d]

[a] *State Key Laboratory of Lithospheric Evolution, Institute of Geology and Geophysics, Chinese Academy of Sciences, Beijing 100029, China*

[b] *CCGM-CGMW, 77 rue Claude-Bernard, 75005 Paris, France.*

[c] *ISTO, Université d'Orléans, UMR 7327, 45071 Orléans Cedex 2, France*

[d] *University of Chinese Academy of Sciences, Beijing 100049, China*

Corresponding author. Tel.: +86 10 82 998546; fax: +86 10 62 010846.

E-mail address: linwei@mail.iggcas.ac.cn (W. Lin).

Abstract.

In the front of metamorphic Cenozoic Alpine nappe of Schistes Lustrés, Western Corsica (France) exposes non-to very low grade metamorphic nappes, such as the Piedmont nappes and Upper nappes . Among these latter, the ophiolite-bearing Balagne nappe, tectonically overlying autochthonous Eocene conglomerates and sandstone, is composed of materials with nearly same age as the Piedmont-Ligurian Ocean, *i.e.*, ophiolites (pillow-lava and gabbro) with Jurassic and Earliest Cretaceous sedimentary turbidite (lydiennes bearing flysch) and, at the highest position in the nappe pile, the Eocene Annunciata turbidite. This latter formation was, in turn, overthrust by a Piedmont unit mainly composed of the Late Cretaceous "Narbinco" flysch. An European provenance for the the Balagne Nappe, previously questioned, is nowadays the most generally accepted view. In order to decipher the source of sediments, a

systematic U-Pb dating of 586 detrital zircon grains collected from the turbidites in the Balagne and Piedmont nappes has been performed. 494 points of Lu-Hf isotopic analysis carried out among these detrital zircons support that the continental crust in Corsica was derived from a recycled old crust. The zircon grains from all of the samples yield U-Pb age spectra ranging from Neoarchean to Late Paleozoic with age peaks at 2600 Ma, 2080 Ma, 1830 Ma, 910 Ma, 600 Ma, 560 Ma, 450 Ma, 330 Ma and 280 Ma with different continental model ages (T_{DM2}) from 3.5 Ga to 1.0 Ga. The variety of composition of the Corsican batholith, unique in its present Mediterranean environment, and in spite of Alpine transcurrent movements, provide a key to analyze the detrital zircon age distribution patterns of sedimentary rocks. These new results i) confirm the lack of any Cretaceous zircon that validates absence of any magmatic arc of this age, at least in the surroundings of the turbiditic formations from the Balagne and the Piedmont nappes; ii) fully support an European origin of the Balagne nappe, iii) put forward evidence that no ophiolitic zircon was contain in our cretaceous nor Eocene turbidites samples, and iv) question the possible deposition of the Piedmont Narbinco flysch on the Western Corsica vicinity located on the European margin.

Keywords: Detrital zircon provenance analysis, Balagne and Piedmont nappes, Alpine Corsica, Piedmont-Ligurian Ocean, European Tethyan Jurassic hyper-extended margin

1. Introduction

The island of Corsica (France), in the Western Mediterranean sea (Fig. 1), is part of the European continental margin of the Mesozoic Tethys. Corsica is classically subdivided into Variscan and Alpine domains in the West and East, respectively (Fig. 1). The Western part of Alpine Corsica is made of a stack of variously metamorphosed metasediments and ophiolites nappes that result from the Eocene continental subduction of the thinned European continental margin under the Piedmont-Ligurian accretionary wedge. Weakly metamorphosed turbidites and ophiolites nappes, exposed in the Balagne and Nebbio areas, were called Upper Nappes, or "nappes supérieures" (Durand-Delga, 1984; Molli, 2008; Molli and Malavieille, 2011; Malusà et al., 2015).

The continental marginal environment before and during the closure of the Tethys Piedmont-Ligurian Ocean remains debated because subduction was oblique to the trend of the passive European margin (e.g. Malusà et al., 2015, 2016a). If the presence of the Piedmont-Ligurian Ocean to the East of Corsica-Sardinia is now accepted, the global palinspastic reconstruction of the islands is still under discussion. Some authors refer i) to the presence, on the Western side of Corsica-Sardinia, of the Valais ocean (Stampfli and Borel, 2002; Turco et al., 2012; Advokaat et al., 2014) whereas others ii) consider the formations referred to as the Valaisan ocean may simply indicate that the Tethyan ocean was not completely subducted and still existed to the NE until the late Eocene (Malusà et al., 2015) and iii) or emplace series of sedimentary basins developed on a thinned continental crust bridging the gap between the Valais ocean and the North Pyrenean basins, opened as pull-aparts and formed during the transcurrent to transtensional movement of the Iberian microplate along the North Pyrenean Fault, during the opening of the Bay of Biscay (Choukroune and Mattauer, 1978; Handy et al., 2010). The subduction of the Piedmont-Ligurian Ocean began in Late Cretaceous but both the provenance of the continental material included in the oceanic formations and the direction of the subduction were disputed among following proposals: i) (1) eastward (or "Alpine"; Mattauer and Proust, 1976) under Adria or AlKaPeCa (Alboran, Kabylies, Peloritan, and Calabria) continental margin or ii) (2) westward (or "Apenninic"; Principi and Treves, 1984) under European margin or iii) a succession of (1) and (2) events (Réhault et al., 1984; Molli and Malavieille, 2011); this latter model (3) was recently supported in the light of thermochronological evidence (Malusà et al., 2016b). Presently, no remnant of any hypothetic Cretaceous arc volcanism related with the oceanic subduction was ever documented up to now.

More than one century of geological studies and detailed mapping (Rossi et al., 2001, and Molli and Malavieille, 2011 for the most recent period) led to build up a robust structural model of the complex geology of the Alpine Corsica in which the following main structural domains were defined from bottom to top of the pile: the Autochtonous and Parautochtonous, the Piedmont domains the Schistes Lustrés and the Nappes supérieures in highest structural position. Many paleogeographic sketches of possible location of each domain have been proposed according to an Ocean - Continent transition (OCT) paleogeography (*e.g.* Magné and Durand-Delga, 1983; Molli and

Malavieille, 2011; Vitale-Brovarone et al., 2011a, 2013; Meresse et al., 2012; Beltrando et al., 2013; Li et al., 2014; Seymour et al., 2016).

2. Aim of the paper

The present study focuses on three different tectonic units, in which Alpine deformation and metamorphism are weak: i) the Westernmost Balagne nappe of the "Nappes supérieures" unit, ii) the Piedmont Bas-Ostriconi and Santa-Lucia nappes that were respectively overthrust by the Balagne and the Schistes Lustrés nappes and iii) the Neoproterozoic basement with Panafrican micaschist underlying the Balagne nappe. We systematically performed U-Pb geochronology, and Lu-Hf isotopes analyzes on detrital zircon from silicic-clastic sedimentary rocks in order to contribute to: i) identify the provenance of the syn-tectonic turbiditic formations exposed in the Balagne, Bas-Ostriconi and Santa-Lucia nappes; ii) provide arguments to better constrain their original paleogeographic location with a peculiar focus on the Balagne nappe, and iii) to propose a possible emplacement of the Balagne ophiolite and Upper Cretaceous and Eocene turbidites in a schematic reconstruction of the Tethys margin.

3. Geological outline of Corsica

The present position of the Corsica-Sardinia continental block is due to the Early Miocene opening of the Ligurian-Provençal basin in the Western Mediterranean (Ashworth and Nairn, 1965) accommodated by 45° counterclockwise rotation of the Corsica-Sardinia block that mainly occurred between 20.5 and 15 Ma (Gattacecca et al., 2007). Before that time, the Corsica-Sardinia block formed part of the southern realm of the Variscan chain (Vialon, 1990; Rossi et al. 2009 and references therein; Malusà et al. 2016b).

3.1. Pre-Mesozoic Corsica

The Variscan rocks and structures are well developed in Western Corsica (Fig. 1). They are mainly represented by Carboniferous to lower Permian granitoids collectively called the Corsica-Sardinia Batholith (Orsini, 1976; Rossi and Cocherie, 1991). Northern Corsica exposes a non-metamorphosed Ordovician to Devonian sedimentary succession unconformably overlying Neoproterozoic micaschist and amphibolites (Barca et al., 1996) related to the Variscan hinterland (Rossi et al., 2009). U-Pb analyses

(Avigad et al., 2015) revealed a preponderance of zircons of Neoproterozoic ages between 0.72-0.53 Ga with major peaks at 0.59 Ga and 0.65 Ga. A few zircons yielded Grenvillian (0.9-1.1 Ga) as well as older Mesoproterozoic ages (1.3-1.6 Ga), and a number of detrital zircons yielded 2.2-1.9 Ga (Paleoproterozoic, Eburnian) ages. The oldest zircons detected yield 2.7 and 2.9 Ga ages (Avigad et al., 2015). The Neoproterozoic and Paleozoic formations were thrust over the Variscan Internal Zone composed mainly of anatectic (at ca. 350 Ma) high-grade metamorphic formations (with protoliths dated mainly of Ordovician) that crop out from central Corsica to northern Sardinia (Giacomini et al., 2008; Faure et al., 2014). The Variscan Internal Zone, which was interpreted as the Eo-Variscan suture (Rossi et al., 2009), was intruded in Corsica by several generations of granitoids (*e.g*. Cocherie et al., 2005b). The early magmatic suite, the U1 Mg-K monzonitic association, dated from ca. 340 Ma to 330 Ma (Paquette et al., 2003; Li et al., 2014), was followed, from 305 to 275 Ma, by the emplacement of the U2 calc-alkaline granodiorite and monzogranite plutons (Rossi et al., 2015) the end of U2 magmatism being contemporaneous with the U3 alkaline to per-alkaline volcanic-plutonic suite and by a voluminous tholeiitic magmatism (Paquette et al., 2003; Cocherie et al., 2005a; Li et al., 2014). Among these magmatic suites, the U1 Mg-K magmatism that outcrops in Bohemia, Vosges, Alpine External Massifs, and Western Corsica is characteristic of the Variscan Internal zone (Tabaud et al., 2015). Up to now, these granites were neither recognized in Calabria nor in Kabilia that belong to the Apulian continent (Malusà et al., 2015, 2016a). Then, the U1 signal should characterize the European plate, and the triplet U1, U2/U3 are well discriminates the Corsican batholith.

3.2. Alpine Corsica

The Eastern part of the island, or "Alpine Corsica", represents the southward prolongation of the Penninic zones of the Western Alps. The origin, geochronology and available models for the evolution of Alpine Corsica are extensively discussed in Vitale-Brovarone et al., (2013 and references therein). Only some relevant elements dealing with this paper are briefly presented hereafter. Several paleogeographic and tectonic units were recognized from West to East.

3.2.1. Autochtonous and para-autochthonous units

Scattered remnants of Triassic to Jurassic carbonates with a Briançonnais affinity are normally covered by Middle to Late Eocene turbiditic formations. These formations correspond to the Eastern passive margin of the European continent. The analogy of those turbidites with the Annot Sandstones (Grès d'Annot in SE France) (Joseph and Lomas, 2004) was remarked since Maury (1931). In this respect, these Middle to Late Eocene turbiditic formations can be considered as the equivalent on the southern flank of the Maures-Esterel-Corsica-Sardinia massif (prior to the Oligocene drifting) as proposed by Ferrandini et al. (2010). In Balagne, Eocene turbidite is overthrust by an ophiolitic nappe and its Late Jurassic to Eocene cover (Fig. 2). Those Eocene sandstone and conglomerate contains numerous tectonic slices (Durand-Delga, 1972) and olistoliths (Nardi, 1968) composed of Late Proterozoic micaschist, Carboniferous and Permian granite and arkose and sandstone, Permian volcanic-sedimentary series, and Triassic and Jurassic limestone, supplied from the European continental margin (Rossi et al., 2001; Malasoma and Marroni, 2007).

The Piedmont Santa-Lucia nappe

NE of Corte, the Santa-Lucia nappe (Ritsema, 1952; De Booy, 1954) tectonically overlies an Eocene Pre-Piedmont turbiditic formation and is thrust by the Schistes Lustrés nappe (Fig. 3). The Santa-Lucia nappe is composed, from base to top, of high-temperature granulites, mafic and intermediate plutonic rocks (Libourel, 1985) overlain by a up to 500 m thick polygenetic conglomerate, followed by an Upper Cretaceous (Coniacian-Maastrichtian [89-66 Ma]) “Tralonca Flysch” formation composed of well-bedded marly-calcareous sandstone-mudstone alternation (Rieuf, 1980). The LP-HT formations of the basement of the Santa-Lucia were intensively studied. (Libourel, 1985) and Caby and Jacob (2000) proposed that the LP-HT rocks represented a small crustal fragment of the deep crustal part of an aborted Permian-Mesozoic rift that may have opened at the southeastern margin of the western European paleocontinent. These formations were then identified as a part of the Jurassic Ocean-continent transition

(OCT) of the Piedmont-Ligurian Ocean (Rossi et al., 2006; Zibra et al., 2009; Beltrando et al., 2013; Seymour et al., 2016).

The Piedmont "Bas Ostriconi" nappe

The Bas Ostriconi nappe directly overlies the Eocene cover of the "autochthonous" basement in the north whereas it was overthrusted by the Balagne Nappe system. This late thrust is considered as a splay of the Ostriconi sinistral strike-slip fault system Malavielle et al. (2011). The Late Cretaceous Narbinco Formation that constitutes the main part of the Bas-Ostriconi nappe is essentially formed by a so called "flysch" (Nardi et al., 1978; Magné and Durand-Delga, 1983) and described as carbonatic turbidites with lenses of coarse-grained polymict conglomerates. The turbidites display a mixed siliciclastic-carbonatic composition and are affected by a polyphasic deformation (Pandolfi et al., 2016) and contains microconglomerates with granite and micaschist clasts.

Both the Piedmont Tralonca and Narbinco flysch formations may have been deposited in an abyssal plain, in a trench during Alpine subduction, or in listric fault-bounded basins, near the continent-ocean boundary (Sagri et al., 1982; Magné and Durand-Delga, 1983). Argnani et al. (2006) proposed an interpretation where the deposits of the Bas Ostriconi nappe were sedimented in a basin located along a transform fault zone separating two subduction zones with opposite dipping.The Santa-Lucia (with a continental basement) and the Bas-Ostriconi (with abundant clasts of continental material) nappes are the two main remnants of an ancient Piedmont nappe now dismembered, other remnants being the Macinaggio and the Pediquercio nappes exposed in Cap Corse and in Southern Corsica, respectively (Fig. 1). These turbiditic units that have been correlated with the Elba flysch (Marino et al., 1995), were contemporaneous with the Apenninic and Alpine "Flysch à Helmintoïdes". A European provenance has been proposed for these Piedmont Upper Cretaceous siliciclastic turbidites as is the case for the turbiditic siliciclastic material present from the Albian-Cenomanian until Eocene in the non-metamorphic ophiolitic units of Corsica e.g. in Balagne (Rossi et al., 2001; Principi, 2005; Durand-Delga et al., 2005; Danelian et al., 2008).

3.2.2. The Internal metamorphic zone

This domain represents the deepest one of Alpine Corsica stack of nappes. It consists of a complex tectonic imbrication of stacked units with ophiolites and sedimentary rocks ("Schistes Lustrés" Formation), and kilometer-scale slivers of continental crust. The ophiolites are relics of the Piedmont-Ligurian Ocean floor, and the sedimentary rocks represent the Jurassic to Early-Middle Cretaceous supra-ophiolitic cover. Most units record a high pressure-low temperature metamorphic evolution reaching lawsonite-blueschist or glaucophane-eclogite facies (Lahondère, 1996; Vitale-Brovarone et al., 2011b). The blueschist or eclogite facies rocks are partly retrogressed into greenschist facies conditions. This highly ductilely deformed "Schistes Lustrés" Nappe with ophiolites, and continental crust slices was thrust Westward onto the European Variscan continental basement during the Late Eocene (Bartonian, 40-37 Ma; Mattauer and Proust, 1975, 1976, Faure and Malavieille, 1981; Malavieille et al., 2011; Vitale-Brovarone et al., 2013).

3.3. The upper units of Balagne and Nebbio Nappes-"Nappes Supérieures" of Alpine Corsica

The Balagne nappe, cropping out about 100 km² to the southeast of Ile-Rousse, is the westernmost allochthonous unit among the "Nappes Supérieures" of Alpine Corsica. It forms like a large synform overthrust the autochthonous Eocene formations (Nardi et al., 1978; Rossi et al., 2001). The Ostriconi NW-SE trending brittle fault (Rossi et al., 2001; Molli, 2008) cuts the Eastern part of the Balagne nappe and separates the Balagne Nappe from the Tenda massif that consists of Alpine reworked Neoproterozoic to Paleozoic rocks that suffered Alpine blueschist metamorphism and deformation (Stam, 1952; Mattauer and Proust, 1976; Lahondère, 1996; Tribuzio and Giacomini, 2002; Molli and Tribuzio, 2004; Maggi et al., 2012; Vitale-Brovarone et al., 2013). The almost unmetamorphosed Balagne succession (Nardi et al., 1978; Durand-Delga, 1984; Marroni and Pandolfi, 2003) consists from bottom to top of: i) ophiolitic basalts and a few gabbro); ii) a radiolaritic sedimentary cover, dated from Late Dogger to Late Malm, which is locally associated with limestone and Early Cretaceous (so called 'Palombini' formation); iii) predominantly turbiditic Middle to Upper Cretaceous continental-

derived formations and namely the Albian-Cenomanian (Marino et al., 1995) lydiennes bearing flysch. From Albian to Cenomanian, the supra-ophiolitic sediments of the Balagne units were laden with continental detritus (sandstones, conglomerates, olistoliths), derived from rocks similar to those known in autochthonous Western Corsica (Carboniferous and Permian granites, Permian volcanics, metamorphic rocks and also basaltic debris).

The structural position of the Balagne nappe, in front of the Alpine belt, and to the West of the internal metamorphic zone, led to the assumption of a distant Eastern origin, up to east of the "Schistes Lustrés nappe" (e.g. Staub, 1928; Mattauer and Proust, 1975; Nardi et al., 1978; Jourdan, 1988). Dallan and Nardi (1984) assumed that, during the Mid-Cretaceous, the Balagne ophiolitic material had been tectonically transported westwards, near the West European continent, which served as the source of clastic input. Field observation suggests the part of the Piedmont-Ligurian Ocean presently included in the Balagne nappe situated close to a continent hypothesized as the European plate since Late Jurassic. (Durand-Delga et al., 1997; Peybernès et al., 2001a, b; Marroni and Pandolfi, 2003; Danelian et al., 2008). In particular, i) the Upper Malm limestone lay on the ophiolites and contains abundant clasts of different components (mainly granites) derived from the continental basement displaying the same characteristics as the Corsican basement; ii) zircon-bearing sandstones are interbedded within pillow-lavas in which these zircons are identical to those of the granites from the neighboring Western Corsica Variscan batholith (Rossi and Durand-Delga, 2001).

Three models, all based on a Balagne basin originally situated in the ocean-continent boundary, have been proposed: i) firstly, the Balagne formed an individual basin opened inside the thinned European margin on a thinned continental crust and bounded to the East by a microcontinental block, variably isolated from the Piedmont-Ligurian Ocean (Lahondère, 1996; Rossi et al., 2002); ii) alternatively, the Balagne basin might have formed the Westernmost part of the Piedmont-Ligurian Ocean (Durand-Delga, 1984; Marroni and Pandolfi, 2007); iii) the Balagne basin was close to an Eastern continental microblock, and thus representing the upper-plate of the subduction (Molli, 2008; Molli and Malavieille, 2011; Li et al., 2015).

The opening of the Ligurian-Piedmont Ocean

As the Tethys' Piedmont-Ligurian Ocean opened during Upper Dogger within the Variscan continental crust, one can argue that similar Paleozoic magmatic and metamorphic rocks should crop out on each side of the Piedmont-Ligurian Ocean. This would imply that the continental breakup resulted of lithologically similar conjugate margins and that the split line was not superimposed onto, or inherited from, a previous paleogeographic boundary. The reconstruction of the Jurassic Piedmonte-Ligurian basin along the Northern Apennines-Alpine-Corsica transect (Marroni and Pandolfi, 2007) suggests an asymmetric architecture for the Piedmont- Ligurian basin where extension of the lithosphere occurred along an east-dipping detachment fault system. The opening of the South China Sea provides a remarkable example of the development of a hyper extended margin onto a batholith (Savva et al., 2014). There low-angle faults reactivate older structures and their strike varies according to the orientation of the pluton boundaries. Those pluton boundaries controlled the geometry of large-scale crustal boudins. Similarly, one can think that the Eastern lithological or structural limits of the Corsican batholith were probably reworked as low-angle faults during the opening of the Piedmont-Ligurian Ocean resulting in a structural asymmetry between the European and Adria margins in the same way as the mechanism described for the opening of the Piedmont-Ligurian Ocean in the Alps (Lemoine et al., 1986; Marroni and Pandolfi, 2007). Because the rifting was asymmetric, the lower crust is generally exposed on the Adriatic margin and the upper crust in the European margin after Malusà et al. (2015).

4. Sampling

Detrital zircon analysis uses the interpreted provenance of the zircon to develop a geological history of sedimentary basins and their surrounding source regions. Ideally, the analyzed sample would completely represent geological history by including evidence of all the possible provenances. Therefore, the age spectra, established from a large number of detrital zircon grains, can be used to assess the distribution of source rocks in the provenance, and detrital zircons identified to be of igneous origin. Such an approach requires a relevant knowledge of the magmatic, metamorphic, and tectonic events that took place in the source regions (Condie et al., 2009). Conversely, the analysis of detrital zircon age spectra might help to improve the understanding of the

geological evolution of the source areas by revealing unexpected, or poorly documented, magmatic or metamorphic events.

Since the abundance of zircon (in terms of numbers of grains) does not change drastically during sediment transport, owing to the inherent stability of zircon, detrital zircon geochronology has received particular attention as a single-mineral provenance tool on the base of robust analysis of potential sources. Of course, the detrital geochronological work needs cautious quantification of hydraulic sorting effects and of the variable abundance (fertility) of datable minerals in different parent rocks like suggestion by Malusà et al. (2013, 2016c). The in situ Hf-isotope analysis of single zircon grain has proven to be a useful tool for reconstructing the tectonic evolution of continental blocks (Griffin et al., 2000; Condie et al., 2009). As a syntectonic sedimentary formation, resulting of erosion, transportation and deposition in active tectonic settings, turbidite records much information even it may lose some information due to late stage omission in orogenic belt (Gehrels, 2014; Malusà et al., 2011, 2016a). Thus, an integration of the different analytical datasets applied to detrital zircons in sedimentary basins offers the possibility to assess the tectonic evolution history of the orogen from which the sediments were derived in terms of ages, rock types and source materials (Wysoczanski et al., 1997; Carter and Moss, 1999; Bruguier et al., 1997; Cawood et al., 2012). Detrital zircon age patterns and Lu-Hf isotopic analysis were recently used to unravel the origin of terrigenous sediments and the growth of the crusts in the Western Alps in a situation close to Alpine Corsica environment (Bütler et al., 2011; Beltrán-Triviño et al., 2013; Malusà et al., 2013, 2016a; Manzotti et al., 2015, 2016; Chu et al., 2016 and references therein; Anfinson et al., 2016).

4.1. The Balagne nappe

4.1.1. The Annunciata Formation (Middle to Late-Middle Eocene)

The Annunciata formation was thrust onto the autochthonous Eocene formations in the NW part of the Balagne region (Fig. 2). Sediments of the Annunciata formation (foreland basin) contain reworked Late Lutetian nummulites constraining the nappe emplacement as Bartonian or younger (Rossi et al., 2001). Some authors assumed that

this formation was deposited close to its present position (Bodenhausen and Spijer, 1962; Nardi, 1968; Nardi et al., 1978). Other authors considered that the Annunciata Formation represents the upper part of the Autochthonous Eocene from which it is separated by a disharmonic contact (Jourdan, 1988; Égal, 1989). Malavieille et al. (2011) pointed out that the tight sedimentological analogies and the similarities in age between the Autochthonous Eocene and the Annunciata Formation "represent a key point in the long standing debate about the Balagne region".

Two samples were collected in the Annunciata Formation on each side of the Balagne nappe synform. These samples were chosen to provide arguments to balance between the two hypotheses previously exposed. The first sample, 11CO87 (42°37'32.28"; 09°05'57.28"), was picked up on the Eastern limb of the Balagne synform, to the North of Novella. As a fine-grained sandstone, the grains in 11CO87 sized around 0.1-0.3 mm, with turbiditic rhythms (Fig. 4A). The major detrital components are quartz, plagioclase, muscovite, and sedimentary and volcanic lithic fragments. In thin section, poorly rounded quartz with undulatory extinction represents 65-75% of the detrital component, plagioclase is about 15-20%, and muscovite is rarely observed less than 5% (Fig. 5A). The second sample, a fine-grained quarzo-feldspathic sandstone 11CO68 (42°35'0.74"; 09°03'5.85"), was collected on the Western limb of the syncline, East of Belgodere, close to the Variscan metamorphic basement (Fig. 4B). The major detrital components consist of quartz, plagioclase, mica, and detritus: metamorphic and volcanic lithoclast fragments (Fig. 5B). In thin section, poorly rounded quartz monocrysts around 0.1-0.4 mm in size with undulatory extinction represent about 75% of the detrital component; plagioclase around 0.2-0.4 mm in size and represent about 15% of the detrital component; and muscovite is less than 2%.

4.1.2. The lydienne bearing turbidite

This formation was sampled in order to identify what were the major alimentation sources of the lydiennes bearing flysch, postulated as highly heterogeneous, as revealed by the great compositional diversity of the olistoliths. The lydiennes bearing flysch of Albian-Cenomanian age is a turbiditic formation where decimetric beds of black chert, or lydiennes, are interlayered with sandstone and clayed pelite. It contains olistoliths of

various compositions, both from oceanic and continental origins, such as pillow-lavas, Malm limestone, calcareous sandstone, and granite. Sample 11CO69 (42°34'47.39"; 09°04'39.11") was collected in the lydiennes bearing flysch at the San Colombano pass. It is a fine grained quartz-sandstone alternating with black chert and laminated limestone (Fig. 4C). Quartz, lithic fragments (mostly volcanic rocks), and plagioclase represent the main detrital components of the sandstone. In thin section, poorly rounded quartz form 70% of the detrital component with grains around 0.04-0.1 mm in size, plagioclase around 0.03-0.08 mm with the maximum 0.2 mm in size and represent about 15% of the detrital component (Fig. 5C). In thin section, late fractures are filled with calcite and siliceous material.

4.2. The Piedmont nappes

Sample 11CO52 (42°20'40.7"; 09°11'59.47") was picked-up NNE of Corte (Fig. 3), in the Tralonca Formation that belongs to the Santa-Lucia nappe. This formation is characterized by metric beds of coarse sandstones, interbedded with dark pelites and conglomeratic lenses. It overlies the 200 to 300 m thick, so called Tomboni Late Cretaceous conglomerate, composed of roughly rounded elements of granite, micaschist, rhyolite and basic rocks. The analyzed sample is a coarse grained, deformed in ductile conditions, quartzo-feldspathic sandstone (Fig. 4D). The major detrital components are quartz, plagioclase, and sedimentary, metamorphic or volcanic lithic fragments. In thin section, more than 30% of the rock is occupied by a cement material, which mostly consists of calcite. In the lithic fragments, quartz, plagioclase, and muscovite represent about 75%, 15%, and less than 5%, respectively (Fig. 5D).

Sample 11CO55A (42°39'22.51"; 09°03'21.33") was collected in the Narbinco Formation from the “Bas-Ostriconi” nappe near Peraiola on the national road along the seashore East of Ile-Rousse (Fig. 2). The Narbinco “flysch” Formation of Cenomanian to Coniacian-Maastrichtian age is mainly composed of alternating beds of quartz bearing marly or compact platty limestone, micaceous and pelite bearing marl, and calcareous sandstone with polygenetic microbreccia reworking micaschist and granite. Sample 11CO55A is a fine grained graywacke (Fig. 4E). The major detrital content represents 45% of the rock with the grains size around 0.05-0.2mm (Fig. 5E). The quartz, plagioclase, muscovite, calcite, pyroxene and lithic fragments are the main

components. In thin section, poorly rounded quartz monocrysts forms 80% of the detrital component.

The large content in feldspar in all these formations and the presence of olistoliths and lithic fragments (in lydiennes bearing turbidite, Tralonca and Narbinco flysch) provides constrains to a relative vicinity and/or a rapid transfer of the sediments from the source to the basin(Pandolfi et al., 2016).

4.3. The basement of the Balagne nappe

It is formed by Eocene conglomeratic formations that lay on the Variscan batholith and host rocks, these latter being formed by the Eovariscan metamorphic gneisses of Belgodere and the Neoproterozoic micaschists of the Vezzo Pass, to the West and East, respectively. These micaschists were sampled to the East of the Vezzo pass (sample 1999 Vezzo).

5. Analytical procedures

5.1. Zircon U-Pb dating

Zircons were separated from each ca. 2 kg of samples using standard heavy liquid and magnetic separation techniques. Handpicked zircon grains were mounted in epoxy resin and then polished to reveal the cores for analysis. Zircon grains, together with standard 91500 and Temora zircons were cast in an epoxy mount, which were then polished to section the crystals in half to reveal the interiors for analysis. Those grains were randomly selected in difference sizes to avoid the age bias on those size-dependent grains. Zircons were documented with transmitted and reflected light micrographs and cathodoluminescence (CL) images were obtained by a CAMECA electron microscope in order to reveal their internal structures. On the basis of these anlyzed photographs, the various grains were selected for anlyzing.Measurements of U, Th, and Pb isotopes for sample 1999 Vezzo from the metamorphic basement of Corsica were conducted using the Cameca IMS-1280 SIMS at the Institute of Geology and Geophysics, Chinese Academy of Sciences in Beijing. U-Th-Pb ratios and absolute abundances were determined relative to the standard zircon 91500 (Wiedenbeck et al., 1995), analyses of

which were interspersed with those of unknown grains, using operating and data processing procedures similar to those described by Li et al. (2009). Each measurement consists of 7 cycles, and the total analytical time is ca. 12 minutes. Correction of common lead was made by measuring ^{204}Pb. An average Pb of present-day crustal composition (Stacey and Kramers, 1975) is used for the common Pb assuming that the common Pb is largely surface contamination introduced during sample preparation. Uncertainties on individual analyses in data tables are reported at a 1σ level. SIMS zircon U-Pb isotopic data are presented in Table 1.

Zircon U-Pb dating for five sandstone sample (prefixed with 11CO) was analyzed using a quadrupole ICP-MS (Agilient 7500a) equipped with an UP-193 Solid-State laser (193nm, New Wave Research Inc.) at the Geological Laboratory Centre, Chinese University of Geosciences in Beijing. Analytical procedures are similar to those reported by Song et al. (2010). Calibrations for zircon analyses were carried out using NIST 610 glass as an external standard and Si as internal standard. U-Th-Pb ratios and absolute abundances were determined relative to the standard zircon 91500 (Wiedenbeck et al., 1995). Zircon standard Temora (Black et al., 2004) and Qinghu (Li et al., 2013) were analyzed as unknowns to ascertain the veracity of Pb/U calibration. Correction of common lead was followed the method described by Andersen (2002). Data processing was carried out using the GLITTER program (van Achterbergh et al., 2001). LA-ICPMS zircon U-Pb analytical data are presented in Table 2. Data plot was carried out using the Density Plotter program (Vermeesch, 2012).

5.2. Zircon Lu-Hf isotopes

Zircon Lu-Hf isotopic analysis was carried out in situ on a Neptune multi-collector ICP-MS equipped with a Geolas-193 laser ablation system at the Institute of Geology and Geophysics, Chinese Academy of Sciences. Previously analyzed zircon grains for U-Pb isotopes were chosen for Lu-Hf isotopic analyses, with ablation pits of 44 or 63 μm in diameter, ablation time of 26 seconds, repetition rate of 10 Hz, and laser beam energy density of 10 J/cm^2. The detailed analytical procedures were similar to those described by Wu et al. (2006). Measured ^{176}Hf/^{177}Hf ratios were normalized to ^{179}Hf/^{177}Hf = 0.7325. Zircon standards Mud Tank and GJ-1 were analyzed alternately with the unknowns. During the course of this study, we obtained^{176}Hf/^{177}Hf ratio of 0.282504 ± 0.000032 (2σ, n=58) and 0.282022 ± 0.000051 (2σ, n=58) for Mud Tank

and GJ-1, respectively, in good agreement within errors with the recommended values of 0.282507 ± 0.000006 (Woodhead and Hergt, 2005) and 0.282000 ± 0.000005 (Morel et al., 2008).

6. Analytical results

In situ U-Pb data for zircons from one micaschist, and five sandstones are presented in Tables 1 & 2. All zircons were documented imaged with transmitted and reflected light micrographs as well as cathodoluminescence (CL) images to reveal their internal textures, and the mount was vacuum-coated with high-purity gold to reach <20 Ω resistance prior to SIMS and ICP-MS analyses (Figs 6 & 7). U-Pb ages are plotted in figures 6 & 8. Analyses that were >10% discordant (by comparison of $^{206}Pb/^{238}U$ and ^{207}Pb-^{206}Pb ages) are not considered nor discussed further (Malusà et al., 2013). Zircon ages younger than 1000 Ma were based on $^{206}Pb/^{238}U$ ratios, and ages older than 1000 Ma were based on ^{207}Pb-^{206}Pb ratios. Lu-Hf isotopic results are listed in Table 3, and diagrams of $\varepsilon_{Hf}(t)$ and Hf crustal model ages are shown in Fig. 9.

6.1. Zircon U-Pb age of the Vezzo micaschist

A total of 12 SIMS analyses of 10 zircon grains were conducted on this sample (Fig 6). Concentric zoning is poorly developed in zircons, indicating a metamorphic origin. Th/U rations range 0.190 to 0.709 (Table 1). The measured $^{207}Pb/^{206}Pb$ ages range from 2056 to 2155 Ma, with a lower intercept at 225 ± 210 Ma and an upper intercept at 2107 ± 22 Ma. A weighted mean age of ten analyses is calculated at 2081 ± 11 Ma (except spots 6 and 12, Fig. 6).

A larger population of zircon was analyzed on samples collected in the vicinity of the sample 1999Vezzo. A part of the results published during the course of this work, such as Avigad et al. (2015) fits with the Late-Paleoproterozoic group of ages bracketed from 2056 to 2155 Ma that has nevertheless to be extended up to 1.9 Ga (Eburnian) whereas new groups of ages at 1.6-1.0 Ga (Mesoproterozoic) and 0.63-0.54 Ga (Ediacaran) ages

were also found. These complementary younger ages could be explained by the heterogeneity of the Panafrican formations and the higher number of zircons analyzed.

6.2. Overview on the total results of the allochthonous formations

The plot of total data from 5 samples of the turbidite provides some key information about: i) the lack of data on a hypothetic Cretaceous arc; ii) the lack of any reworking of Jurassic zircon from ophiolite even if zircon fertility of the ophiolite is low (Malusà et al., 2016c), excepted for ferrogabbro and trondhjemite and iii) an overview of the ages of the main magmatic events within the Variscan basement (Fig. 8). By order of importance, the main sources where U1 (peaking at 330), U2-U3 (peaking at 282), Ordovician (peaking at 450) and Cadomian (peaking at 560-600) magmatisms with a few Proterozoic and Archean inheritance (Figs. 8 & 10).

6.2.1. The Balagne nappe

6.2.1.1. Sample 11CO87 (Eocene Annunciata turbidite, NW of Novella)

A total of 106 analyses on 106 grains was undertaken, 99 of which are concordant within uncertainties (Fig. 8). Zircons size ranges between 50-300 μm with prismatic or rounded shape. The grains have oscillatory zones or are homogeneous and light colored in CL images. Th/U ratios range from 0.01 to 2.33. The measured U /Pb ages range from 287 to 2586 Ma (Table 2). Two major peaks can be identified at ca. 327 Ma and 296 Ma, with a subordinate age peak at ca. 452 Ma. A small peak at ca. 501 Ma and an age group from 599 to 630 Ma are also revealed. A low background of dispersed ages ranges from Neoarchean to Neoproterozoic (Fig. 8).

6.2.1.2. Sample 11CO68 (Eocene Annunciata turbidite, East of Belgodere)

A total of 120 points on 120 grains was analyzed, and 117 concordant within uncertainties grains were kept as valid (Fig 8). Concentric zoning is distinctly

demonstrated in euhedral zircon grains with 100 to 250 μm in length, and length-width ratios of 2:1 to 3:1. Th/U ratios range from 0.003 to 1.83. The measured U /Pb ages range from 273 to 2076 Ma (Table 2). The population is essentially bimodal with one major peak at ca. 330 Ma, a second minor peak at ca. 452 Ma and an age group from 560 to 638 Ma is also revealed. A background between Paleoproterozoic to Late Neoproterozoic with a small peak at 900 Ma is also exhibited. This result have a little difference with the sample of 11CO87 (Fig. 8). Perhaps this might simply suggest that these Eocene turbidites have not the same age.

6.2.1.3. Sample 11CO69 (lydiennes bearing flysch at the San Colombano pass)

A total of 120 points on 120 grains was analyzed and 109 grains were kept as valid, 109 of which are concordant within uncertainties (Fig. 8). Zircons are mostly euhedral to subhedral, transparent and colorless, ranging from 50 to 250 μm in length, and have length to width ratio between 1.5:1 and 4:1. Concentric zoning is common in most crystals in CL images (Fig. 7). Th/U ratios range from 0.05 to 2.59. The measured $^{206}Pb/^{238}U$ ages (<1000 Ma) and $^{207}Pb/^{206}Pb$ age (>1000 Ma) range from 292 to 2889 Ma (Table 2). One major peak can be identified at ca. 556 Ma (a narrow range from 536 to 568 Ma), along with subordinate age peaks at ca. to 658 Ma, 619 Ma, 602 Ma, 478 Ma, 328 Ma, and 295 Ma, and minor peaks at 930 Ma and 436 Ma. A significant background of ages ranges from Neoarchean to Mesoproterozoic (Fig. 8).

6.2.2. The Piedmont nappe

6.2.2.1. Sample from 11CO52, (Tralonca Formation, NNE of Corte)

A total of 120 analyses of 120 grains were undertaken, 119 points of analysis were kept as valid, all of which are concordant within uncertainties (Fig 8). Zircons range in size between 50 to 300 μm with prismatic or rounded shape. They have oscillatory zones or are homogeneous and light in CL images (Fig. 7). Th/U ratios range from 0.13 to 1.38. The measured $^{206}Pb/^{238}U$ ages range from 256 to 968 Ma (Table 2). One major peak can be identified at ca. 281 Ma with a limited subordinate age peak at 333 Ma (Fig

8). It is worth to mention that the largest part of the zircon dates exhibit a Variscan age neither any Neoarchean nor Mesoproterozoic age are preserved in the analyzed grains like other samples (Fig. 3).

6.2.2.2. Sample 11CO55A (Late Cretaceous Narbinco flysch)

Of the 120 analyses conducted on 120 zircons for this sample, 119 points of analysis were effective and all of them are concordant within uncertainties (Fig. 8). Zircons separated from these samples are mostly euhedral to subhedral, transparent and colorless, ranging from 50 to 250 μm in length, and have length to width ratio ranging from 1:1 to 4:1; concentric zoning is common in most crystals in CL image (Fig. 7). Th/U ratios range from 0.08 to 1.78. Detrital zircons from 11CO55A sample of the Narbinco Formation lead to a single major peak (nearly 80% of analyses) pointing to 332 Ma with 109 zircon ages among 119 analyses dated between 356 Ma and 282 Ma. The other 6 zircon ages range from 2778 to 409 Ma. Zircon dates are essentially Variscan, one can nevertheless point out 2 isolated analyses pointing to 230 and 250 Ma that could echoed to the lower Triassic volcanism described in the environment of the Piedmont (Durand-Delga, 1984).

6.3. In situ Hf isotopes

494 dated zircon grains from five samples were selected for in situ Hf isotopes (Table 3). LA-MC-ICPMS zircon Hf-isotope measurements were performed after the U-Pb isotope analyses. The results are presented graphically in Fig. 9. Overall, the measured $\varepsilon_{Hf}(t)$ values exhibit a wide range from negative to positive (-22.9 to 12.3) with $^{176}Hf/^{177}Hf$ ratios varying from 0.280849 to 0.282796 (Fig. 9). The Hf isotopic composition for detrital zircons from Piedmont nappes clustering between 280 and 630 Ma show a consistent range of $\varepsilon_{Hf}(t)$ values from -10 to +10 whereas the $\varepsilon_{Hf}(t)$ values of Balagne nappe scatter more widely from -15 to +10 (Fig. 9). The crustal model age (T_{DM2}) was calculated assuming that the parental magma was produced from an average continental crust ($^{176}Lu/^{177}Hf=0.015$) that was originally derived from the depleted mantle (Griffin et al., 2004). The samples from the Balagne nappe (11CO87, 11CO68,

and 11CO69), and the Piedmont nappes (11CO55A and 11CO52) did not show many much differences on the continental model ages around Mesoproterozoic (T_{DM2}, Fig. 9).

7. Interpretation of the results

According to our new data from Alpine Corsica, five major age peaks were identified from these sediments at 630-590 Ma (~600 Ma), 580-530 Ma (~560 Ma), 470-430 Ma (450 Ma), 340-320 Ma (~330 Ma) and 300-270 Ma (~280 Ma), which are respectively related to Cadomian (Neoproterozoic), Early Paleozoic (Ordovician-Silurian), and Late Variscan (Carboniferous-Permian) events, respectively. A small peak around 890-920 Ma (~910 Ma) was also identified (Figs 11 & 12). A composite pre-Alpine history of magmatic and metamorphic events has been recorded in both the European and the Adriatic plates. It is thus necessary to discuss our new data in detail to unravel the possible provenance for these samples. However, one can keep in mind Maluski et al. (1973) discussion about possible left-lateral transcurrence that could have displaced, as a minimum of 60 km, the Alpine metamorphic wedge compared to Variscan Corsica, but at plate scale (Schetino and Turco, 2006) reconstructions have to account with large major (dextral) NE-trending transcurrent fault separating Sardinia in two blocks and to offset southeast Corsica with respect to the main Corsica block. In any case, the unique triplet of U1-U2-U3 granitic sequence which characterizes Corsica (Rossi et al., 2009) is a powerful tool to trace the Corsican provenance through zircon dating.

7.1. The Balagne Nappe

7.1.1. The Middle to Late (?) Eocene Annunciata Formation

The two main peaks identified at ca. 327 Ma and 296 Ma in sample 11CO87 are characteristic of the U1 and U2 magmatic units of the Corsican batholith, respectively (Paquette et al., 2003; Cocherie et al., 2005a; Li et al., 2014; Fig. 8). The subordinate age peak at ca. 452 Ma corresponds to the first Cambrian to Lower Ordovician transitional alkaline magmatism widespread in the entire Variscan belt including the nearby Sardinia and Calabria (Gaggero et al., 2012; Fig. 8). In the Belgodère area that bounds the Balagne nappe to the West, orthogneiss yields zircons dated at 476±8 Ma interpreted as the protolith age (Rossi et al., 2009). The minor peak at ca. 501 Ma might

correspond to the Cambrian alkaline magmatism, interpreted as evidence for an aborted rifting, also recorded in several places of the Variscan belt, as for instance in the French Massif central (Cocherie et al., 2005b; Bé Mézème et al., 2006; Faure et al., 2010). Alternatively, this age together with the secondary peaks at 599 to 630 Ma and those from 600 Ma argue for the signature of Neoproterozoic rocks formed during the Cadomian orogeny and its Lower Paleozoic magmatic cover (Rossi et al., 2009; Avigad et al., 2015; Fig. 8). In any case, the whole zircon ages yielded by this pattern are identical to the ages of the formations that immediately surround the Annunciata formation in its present position to the East of Novella.

In sample 11CO68, collected to the east of Belgodere, the bimodal age population with one major peak at ca. 330 Ma, and a second lower peak at ca. 452 Ma, and a background between Late Neoproterozoic to Paleoproterozoic can be compared to the previous one. The 330 Ma peak represents the U1 Mg-K magmatism that crops out immediately to the West. It is worth to note the total absence of the ca. 300 Ma peak and correlatively, the lack of U2 granitoids in the nearby basement west of the Balagne nappe (as it is presently the case). Minor peaks from 2.2 Ga to 452 Ma can be interpreted as for the previous sample. It is worth to emphasize the contrast of feeding in the Annunciata Formation from Variscan granites: there is a strong U1 age peak at 330 Ma but no significant age peak around 300-280 Ma (U2 and U3) in sample 11CO68 (to the West of the basin) whereas there is no U1 age peak but a large 300-280 Ma (U2 and U3) peak in sample 11CO87 to the East of the basin. This dissymmetry reflects the present position of the respective U1 to the West and U2/U3 granites *vs.* the Annunciata basin (Fig. 2)

To conclude, for both samples, the zircon population of the Annunciata Formation is the exact image of the rocks that presently crop out nearby the Balagne nappe. These results support the hypothesis of a deposition of the sediments in the present position of the nappe as previously proposed (Bodenhausen and Spijer, 1962; Nardi, 1968; Nardi et al., 1978), and the Annunciata Formation could represent the upper part of the Autochthonous Eocene series as previously suggested by Jourdan (1988) and Égal (1989). In the Annunciata Formation, the feeding polarity of the respective basins from the granitic sources exactly mirrors their present position whenever the distance of transportation of the sediments that could reach some hundreds of km, as is the case of the Aveto Formation of the Adriatic foredeep in Italy (Anfinson et al., 2015).

7.1.2. The lydiennes bearing flysch (Late Lower to Lower Late Cretaceous)

In the sample 11CO69 collected at the San Colombano pass, the detrital zircon age pattern displays several characteristic peaks representing every formation from the batholith i.e. U1 at 328 Ma, U2 at 295 Ma, Ordovician (478 Ma), and Neoproterozoic (602 Ma). It is worth to note that the major peak around 536-568 Ma (Fig. 8), that was not well marked in other samples, might correspond to the Late Neoproterozoic-Early Cambrian tectonothermal events along the northern peri-Gondwana regions that formed the Cadomian belt (von Raumer et al., 2003; Linnemann et al., 2007, 2008). This large variety of ages perfectly fits with the observation of meter scale to kilometer scale olistoliths of various lithologies. Then, in agreement with previous lithostratigraphic and paleontological data (Durand-Delga et al., 1997; Rossi et al., 2002), the basin of the lydiennes bearing flysch was located in the vicinity of the Variscan Corsica.

7.2. The Piedmont nappes

7.2.1. The Tralonca Formation of the Santa-Lucia nappe

From the analysis of the detrital zircon ages measured in sample 11CO52, the main peak identified at ca. 281 Ma represents the U2 and U3 magmatic episode whereas, a subordinate age peak at 333 Ma that can be related to the U1 episode.

The Tomboni conglomerate, that underlies the Tralonca flysch, results from an important erosion of the basement that was active during the Late Cretaceous. This shows that the batholith was already widely cropping out. The zircon population of the Tralonca flysch with a U3 peak at 281 Ma and a U1 peak at 333 Ma does not provide a complete image of the composition of the batholith. The lack of any representative peak at ca. 300 Ma that would represent the U2 calcalkaline episode could be caused by the large areal extension of U3 ignimbritic nappes that covered a large part of the batholith (Vellutini, 1977) prior to the Oligocene to Miocene uplift (Jakni et al., 2000; Danišik et al., 2007; Malusà et al., 2016b). This distribution supports the previously proposed paleogeographic location of the Santa-Lucia nappe in a para-autochthonous position to the East of the granitic batholith (Durand-Delga, 1984); or on the Ocean-Continent Transition (Fig. 14; Rossi et al., 2006; Beltrando et al., 2013; Seymour et al., 2016).

7.2.2. The Narbinco Formation of the Bas-Ostriconi nappe

In sample 11CO55A, collected near the coast the 332 Ma peak unequivocally represents the age of the U1 Mg-K granites that widely and exclusively crop out along the Western coast of Corsica, immediately to the West of the present position of the Narbinco turbidite. If the sample 11CO55A is representative of a large part of the formation, this very unique and monogenetic alimentation constrains the original position of the "Piedmont" Narbinco flysch at the immediate vicinity of the U1 Mg-K granites i.e. not very far from to its present position. This could explain that it did not receive zircon populations from U2 and from the host rocks of the batholith i.e. from the Eo-Variscan metamorphic rocks, the Neoproterozoic Cadomian basement, and Paleozoic cover. One could make the assumption that the Narbinco Formation could have been located on the Western side of Corsica (Durand-Delga, 1984; Fig. 13 a, b). It is worth to note that two grains of zircon pointing to 230 and 250 Ma that could echoed to the lower Triassic volcanism described in the environment of the Piedmont formations to the North of Corte (Ritsema, 1952).

Detrital zircons from Balagne and Piedmont Nappes from Alpine Corsica reveal the possible provenance of these Eocene and late Cretaceous flysch (Fig. 11). Detrital zircon U-Pb dating from Balagne Nappe falls into six main groups peaking around 907 Ma, 600 Ma, 560 Ma, 450 Ma, 330 Ma, and 296 Ma that correspond respectively to the Lower Tonian, Cadomian (Neoproterozoic), Ordovician, and U1 and U3 magmatism of Variscan (Carboniferous) events widespread in western and central Europe (Fig. 11). The analytical results from Piedmont nappes display two peaks: 326 Ma and 286 Ma that fit with the U3, U2 and U1 magmatic episode of the Variscan with a gap around 310 Ma (Fig. 11). It was worth to note that not so many Precambrian detrital zircons were found in the Piedmont nappes indicating that the tectonothermal events that occurred along the northern peri-Gondwana regions during the Late Neoproterozoic-Early Cambrian and the Late Cambrian-Ordovician are not well marked(Fig. 11). One can also consider that the host basement of the batholith had been widely eroded at this time.

7.3. Interpretation of the Hf isotopes

Hf isotopic data emphasize evidence of the predominance of crustal *vs.* mantle derived sources in the Variscan acidic to intermediate magmatism (Fig. 9) as it was already pointed out by Nd isotopic data (Cocherie et al., 1994). As indicated by Condie (1998), 75-80% of juvenile continental crust had been extracted from the mantle during the Archean and the Paleoproterozoic. After Downes and Duthou (1988), Pin and Duthou (1990), the Variscan contribution mainly consisted in a recycling of older crust. Arndt and Goldstein (1987) draw attention that all Nd model ages are not necessarily "crust-formation ages", because they represent a mixture of material derived from the mantle at various times, corresponding to major orogenic events. In any case, there is no indication of Variscan mantle derived material as claimed by Bonin (2007) for the U3 granites (Fig. 10).

Hf values for Ordovician rocks fit with the bimodal sources of the volcanism from the neighboring Sardinia where three main events were recognized according to Gaggero et al. (2012): i) a first transitional alkaline Cambrian to Lower Ordovician (492-480 Ma); ii) a second Mid-Ordovician bimodal calc-alkaline at ca. 465 Ma and a third Ordovician to Silurian alkali mafic (ca. 440 Ma). The data on Cadomian rocks fit with the results obtained by (Avigad et al., 2015) who consider a significant input from Cadomian arcs that resided within or at the vicinity of the proto-Cadomian basin in which the protolith of micaschist was deposited.

Our new zircon data show five distinct groups of concordant ages at 630-590 Ma, 580-530 Ma, 470-430 Ma, 340-320 Ma and 300-270 Ma (Fig.12), whereas the Hf model ages show a relatively concentrated distribution around 1.5 Ga (Figs. 9 and 10), which is consistent with results obtained in the Alps (Schaltegger and Gebauer, 1999; Chu et al., 2016). All the analyses of zircon are below the curve of the depleted mantle, suggesting that the magmas from which most of zircons crystallized, formed by partial melting of pre-existing crustal rocks, rather than from a juvenile source (Fig. 9). Similarly, In Fig. 10, most of the zircon Hf model ages (T_{DM2}) are much older than their crystallization ages, indicating a formation from remelting of older crustal rocks crystallized during the previous Cadomian, pre-Variscan, and Variscan crust formation events. The samples from the Balagne nappe (11CO87, 11CO68, and 11CO69) and the Piedmont nappes (11CO55A and 11CO52) show the similar continental model ages around 1.4-1.6 Ga (Fig. 9, 10). These estimations fit with those previously calculated

from Nd isotope geochemistry (Cocherie et al., 1994) that pointed to an age about 1 Ga for the continental crustal protolith of the U1 and U2 granitic series of the Corsican batholith.

8. Discussion

The lack of any reworking of Jurassic zircon from ophiolite, even if zircon fertility of the ophiolite is low, reveals that upper Cretaceous to Eocene turbidites were only fed by continental formations. Detrital zircon evidence in every of the Balagne's turbidite analyzed display, in very varying proportions however, the same range of ages and this fit with Pandolfi et al. (2016)'s statement that the Narbinco flysch and the turbidite sedimentary cover of the Balagne Nappe have common source areas and stratigraphic features.

8.1. The Balagne Nappe, the Annunciata Eocene turbidite

It was known that the nature of the various detritus in the Annunciata Eocene turbidite was similar to the formations outcropping at the immediate surroundings of the present Balagne nappe. The zircon age distribution fits with the nature of the metamorphic basement from Corsica- Sardinia- Maures massifs but demonstrates that the Eocene turbidite was fed by granites from the Corsican batholith. The Eastern (11CO87) and the Western (11CO68) age distribution curves give a representative image of the respective sources with a peak of U1 (330 Ma) granite on the Western and U2 (282 Ma) granite on the Eastern part of the Eocene basin and then constrain this formation deposited not far from its present position prior to its tectonic emplacement even if turbidite can travel over a long distance. This conclusion complies with previous ones arguing that the Annunciata formation constituted the upper part of the Autochtonous Eocene thrusted on the lower part of the Eocene formation (Bodenhausen and Spijer, 1962; Nardi, 1968; Nardi et al., 1978; Jourdan, 1988; Égal, 1989).

In the "lydiennes bearing flysch", the zircon age distribution in the "Middle" Cretaceous turbidite (sample 11CO69) reveals the importance of a sedimentary flux supplied by a Neoproterozoic basement (peaks from 2.9 Ga to 536 Ma), and an Ordovician cover (peaks at 478 and 436 Ma). Nowadays, the Ordovician formations

able to provide such zircons are restricted in Corsica to the Agriates area of for Neoproterozoic, and south of Calvi, for Neoproterozoic and Lower Paleozoic but are still widespread in the Maures massif (Bellot, 2005) and Northeastern Sardinia (Gaggero et al., 2012). The presence of U1 (330 Ma) and U2 (295 Ma) zircon population testifies however a feeding from the batholith, even if the flux was weak.

8.2. The Piedmont units

The European provenance of the turbiditic siliciclastic material present from the Albian-Cenomanian until Eocene in the non-metamorphic ophiolitic units of Corsica was agreed (Durand-Delga, 1984; Padoa and Durand-Delga, 2001; Principi, 2005) and Pandolfi et al. (2016)'s conclusions assigned to the Narbinco Flysch a deposition onto the Piedmont- Ligurian oceanic basin, in an area located close to the European continental margin. The Piedmontformations and the Balagne basin were fed, from Upper Lower Cretaceous to Eocene, by continental formations having the same characteristics than those outcropping in their present environment. If the zircon population of the Tralonca flysch fits with a provenance from the Eastern part of the batholith, the very unique and monogenic population of zircon from U1 could constrain a Western provenance of the Narbinco flysch and its deposition in a basin situated within U1 granitic suite on the Western (or Northwestern in the reconstructed paleoposition) side of the Corsica batholith.

On fig. 14, a reconstruction at Late Cretaceous position of the Piedmont basins *v.s* the Corsica Sardinia block s drawn taking into account that a series of basins opened within a thinned continental crust. These basins, the opening of which was controlled by the left-lateral North Pyrenean fault, and a series of normal faults: i.e. Cévennes, Nimes, Durance faults, appear as pull-aparts bridging the gap between the Pyrenées and the Valais ocean.

On the section (Fig. 14) the original position of the Balagne is situated between the Pigno block and the Santa-Lucia Piedmont basin as previously proposed in Lahondère (1996) and Li et al. (2015) and is now moreover supported by the zircon patterns of the Cretaceous lydiennes bearing flysch in the present study. Note that the presence of

remnants of continental crust under the Balagne oceanic basin was constrained by the presence in trondhjemites of the Balagne ophiolitic complex of Ordovician and Archean inherited zircons (Rossi et al., 2002).

9. Conclusion

Detrital zircon U-Pb dating results from five samples in the Corsica Alps demonstrate major age peaks at 630-590 Ma (~600 Ma), 580-530 Ma (~560 Ma), 470-430 Ma (450 Ma), 340-320 Ma (~330 Ma), 300-270 Ma (~280 Ma) -that correspond to Pre-Cadomian, Cadomian, Cambrian, Ordovician, Variscan, and Permian magmatic events, respectively. A smaller peak, around 890-920 Ma (~910 Ma) was also recognized. The Piedmont flyschs and the turbidite sedimentary cover of the Balagne Nappe have common source areas and stratigraphic features and the lack of any evidence of ophiolitic Jurassic zircon in the turbidite point to an intracontinental environment for the sedimentation. Hf isotopic data indicate that these events did not give rise to significant continental growth through generation of juvenile crust. These results fit, at a local scale, with the earth scaleproposal that 75 to 80 % of the juvenile continental crust was still extracted from the mantle as soon as the end of Proterozoic (Condie, 1998).

One can underline the lack of any Cretaceous zircon that rules out any hypothesis of a Cretaceous magmatic arc, at least in the surroundings of the turbiditic formations from the Balagne and the Piedmont nappes. Two main arguments could be taken into account to constrain a European origin of the Balagne nappe, in agreement with the sedimentological arguments already exposed (Durand-Delga et al., 1997): i) the systematic presence of variously represented age peaks, known in the Variscan basement of Corsica, Sardinia and the Maures massif, and ii) the systematic presence of zircons from Visean U1 granites that up to now were only described in the Variscan belt preserved in the European plate. Among the different formation that have been analyzed here, and that fit with a deposition in the margin of the Piedmont-Ligurian Ocean, the monogenic U1 zircon population of the Narbinco Piedmont flysch should constrain a Western batholith provenance and a deposition on the Western side of the Corsican batholith. This emphasizes the key place of the Balagne area in the paleogeographic framework of the Alpine belt of Corsica.

Acknowledgments

This work is supported by the DREAM project of MOST China (2016YFC0600401, 2016YFC0600102) and NSFC (41225009, 41502215,41472193). We present our sincere thanks to Prof. Marco G. Malusà and another anonymous reviewer and Prof. Z.X. Li (Editor) for their constructive suggestions and detail reviews.

References

Advokaat, E. L., van Hinsbergen, D. J. J., Maffione, M., Langereis, C.G., Vissers, R.L.M., Cherchi, A., Schroeder, R., Madani, H. Columbu, S., 2014. Eocene rotation of Sardinia, and the paleogeography of the Western Mediterranean region. Earth and Planet. Sci. Lett. 401, 183-195.

Andersen, T., 2002. Correction of common lead in U- Pb analyses that do not report ^{204}Pb. Chem. Geol. 192, 59-79.

Anfinson, O.A., Malusà, M.G., Ottria, G., Dafov, L., Stockli, D.F., 2016. Tracking coarse-grained gravity flows by LASS-ICP-MS depth-profiling of detrital zircon (Aveto Formation, Adriatic foredeep, Italy). Marine and Petroleum Geology 77, 1163-1176.

Argnani, A., Fontana, D., Stefani, C., Zuffa, G.G., 2006. Palaeogeography of the Upper Cretaceous-Eocene carbonate turbidites of the Northern Apennines from provenance studies. In: Moratti, G., Chalouan, A. (Eds.), Tectonics of the Western Mediterranean and North Africa. Geol. Soc. London, Spec. Publ. 262, pp. 259-275.

Arndt, N.T., Goldstein, SL., 1987. Use and abuse of crust-formation ages. Geology 15, 893-895.

Ashworth, T.P., Nairn, A.E.M., 1965. An anomalous pole from Corsica. Paleogeogr., Paleoclim., Paleoecol. 1, 119-125.

Avigad, D., Rossi, Ph., Gerdes, A., 2015. Origin of "Pan-African" micaschist from Variscan Corsica: detrital zircon U-Pb-Hf constrains on provenance and Cadomian paleogeography. Géol. de la France 1, 13.

Barca, S., Durand-Delga, M., Rossi, Ph., Štorch, P., 1996. Les micaschistes panafricains de Corse et leur couverture paléozoïque : leur interprétation au sein de l'orogène varisque sud-européen. C. R. Acad. Sci. Paris 322, IIa, 982-989.

Bé Mézème, E., Cocherie, A., Faure, M., Legendre, O., Rossi, P., 2006. Electron microprobe monazite geochronology: a tool for evaluating magmatic age domains, examples from the Variscan French Massif Central. Lithos 87, 276-288.

Bellot, J.P., 2005. The Paleozoic evolution of the Maures massif (France) and its potential correlation with others areas of the Variscan belt: a review. J. of the Virtual Explorer (Electronic Edition) 19, Paper 4.

Beltrando, M., Zibra, I., Montanini, A. and Tribuzio, R., 2013. Crustal thinning and exhumation along a fossil magma-poor distal margin preserved in Corsica: A hot rift to drift transition? Lithos 168-169, 99-112.

Beltrán-Triviño, A., Winkler, W., von Quadt, A., 2013. Tracing Alpine sediment sources through laser ablation U-Pb dating and Hf-isotopes of detrital zircons. Sedimentology 60, 197-224.

Black, L.P., Kamo, S.L., Allen, C.M., Davis, D.W., Aleinikoff, J.N., Valley, J.W., Mundil, R., Campbel, I.H., Korsch, R.J., Williams, I.S., Foudoulis, C., 2004. Improved $^{206}Pb/^{238}U$ microprobe geochronology by the monitoring of a trace-element-related matrix effect; SHRIMP, ID-TIMS, ELA-ICP-MS and oxygen isotope documentation for a series of zircon standards. Chem. Geol. 205, 115-140.

Bodenhausen, J.W.A., Spijer, S.B., 1962. On the Nappe structure of the Balagne (NW Corsica). Proc. Koninkl Nederl Akad. Wetensch. Amsterdam, ser. B, 65, 35-45.

Bonin, B., 2007. A-type granites and related rocks: Evolution of a concept, problems and prospects. Lithos 97, 1-29.

Bruguier, O., Lancelot, J.R., Malavieille, J., 1997. U-Pb dating on single detrital zircon grains from the Triassic Songpan-Ganze flysch (Central China): provenance and tectonic correlations. Earth and Planet. Sci. Lett. 152, 217-231.

Bütler, E., Winkler, W., Guillong, M., 2011. Laser ablation U/Pb age patterns of detrital zircons in the Schlieren Flysch (Central Switzerland): New evidence on the detrital sources. Swiss J. Geosci. 104, 225-236.

Caby, R., Jacob, C., 2000. La transition croûte/manteau dans la nappe de Santa-Lucia di-Mercurio (Corse alpine) : les racines d'un rift permien. Géol. de la France 1, 21-34.

Carter, A., Moss, S.J., 1999. Combined detrital-zircon fission-track and U-Pb dating: a new approach to understanding hinterland evolution. Geology 27, 235-238.

Cawood, P.A., Hawkesworth, C.J., Dhuime, B., 2012. Detrital zircon record and tectonic setting. Geology 40, 875-878.

Choukroune, P., Mattauer, M., 1978. Tectonique des plaques et Pyrénées : Sur le fonctionnement de la faille transformante nord-pyrénéenne; comparaison avec les modèles actuels. Bull. Soc. Géol. Fr. 20, 689-700.

Chu, Y., Lin, W., Faure, M., Wang, Q., 2016. Detrital zircon U-Pb ages and Hf isotopic constraints on the terrigenous sediments of the Western Alps and their paleogeographic implications. Tectonics 35, doi:10.1002/2016TC004276.

Cocherie, A., Baudin, T., Autran, A., Guerrot, C., Fanning, M., Laumonier, B., 2005b. U-Pb zircon (ID-TIMS and SHRIMP) evidence for the early Ordovician intrusion of metagranites in the late Proterozoic Canaveilles Group of the Pyrenees and the Montagne Noire (France). Bull. Soc. géol. Fr. 176, 269-282.

Cocherie, A., Rossi, Ph., Fanning, C.M., Guerrot, C., 2005a. Comparative use of TIMS and SHRIMP for U-Pb zircon dating of A-type granites and mafic tholeiitic layered complexes and dykes from the Corsican Batholith (France). Lithos 82, 185-219.

Cocherie, A., Rossi, Ph., Fouillac, A.M., Vidal Ph., 1994. Crust and mantle contributions to granite genesis. An example from the Variscan batholith of Corsica studied by trace element and Nd-Sr-O isotope systematics. Chem. Geol. 115, 173-211.

Condie, K.C., 1998. Episodic continental growth and supercontinents: a mantle avalanche connection? Earth and Planet. Sci. Lett. 163, 97-108.

Condie, K.C., Belousova, E., Griffin ,W.L., Sircombe, K.N., 2009. Granitoid events in space and time: constraints from igneous and detrital zircon age spectra. Gondwana Res. 15, 228-242.

Dallan, L., Nardi, R., 1984. Ipotesi sulle evoluzione dei domini 'Iiguri' della Corsica nel quadro della paleogeographia e delle tettonica delle unità alpine. Bol. Soc. Geol. It. 103, 515-527.

Danelian, T., de Wever, P., Durand-Delga, M., 2008. Revised radiolarian ages for the sedimentary cover of the Balagne ophiolite (Corsica, France). Implications for the palaeoenvironmental evolution of the Balano-Ligurian margin. Bull. Soc. géol. Fr. 179, 289 - 296.

Danišik, M., Kuhlemann, J., Dunkl, I., Székely, B., Frisch, W., 2007. Burial and exhumation of Corsica (France) in the light of fission track data. Tectonics 26, TC1001, doi:10.1029/2005TC001938

De Booy, T., 1954. Géologie de la région de Francardo (Corse) (Ph.D. thesis) Univ. Amsterdam.

Downes, H., Duthou, J.L., 1988. Isotopic and trace-element arguments for the lower-crustal origin of Hercynian granitoids and pre-Hercynian orthogneisses, Massif Central (France). Chem. Geol. 68, 291-308.

Durand-Delga, M., 1972. Impressions sur l'édifice alpin de la Corse. Livre Jub. Prof. D. Andrusov : "Tectonic Problems of the Alpine System", M. Mahel (édit). Bratislava, p. 203-229.

Durand-Delga, M., 1984. Principaux traits de la Corse alpine et corrélation avec les Alpes ligures. Mem. Soc. Geol. It., 28, pp. 285-329.

Durand-Delga, M., Fondecave-Wallez, M.J., Rossi, Ph., 2005. L'unité ophiolitique de Pineto (Corse) : signification du détritisme continental dans sa couverture de flysch albo-cénomanien. C. R. Geoscience 337, 1084-1095.

Durand-Delga, M., Peybernès, B., Rossi, Ph., 1997. Arguments en faveur de la position, au Jurassique, des ophiolites de Balagne (Haute-Corse, France) au voisinage de la marge continentale européenne. C. R. Acad. Sci., Paris. 324, 973-981.

Égal, E., 1989. Tectonique de l'Éocène en Corse (Ph.D. thesis) Géol. Univ. Claude-Bernard, Lyon.

Faure, M., Cocherie, A., Bé Mézème, E., Charles, N., Rossi, P., 2010. Middle Carboniferous crustal melting in the Variscan belt: New insights from U-Th-Pb_{tot} monazite and U-Pb zircon ages of the Montagne Noire Axial Zone (southern French Massif Central). Gondwana Res. 18, 653-673.

Faure, M., Malavieille, J., 1981. Etude structurale d'un cisaillement ductile. Le charriage ophiolitique corse dans la région de Bastia. Bull. Soc. Geol. Fr. 23, 335-343.

Faure, M., Rossi, Ph., Gaché, J., Melleton, J., Frei, D., Li, X. H., Lin, W., 2014. Variscan orogeny in Corsica: new structural and geochronological insights, and its place in the Variscan geodynamic framework. Int. J. Earth Sci. (Geol. Rundsch.) 103, 1533-1551.

Ferrandini, J., Ferrandini, M., Rossi, Ph., Savary-Sismondini, B., 2010. Définition et datation de la Formation de Venaco (Corse): dépôt d'origine gravitaire d'âge Priabonien. C. R. Geosciences 342, 921-929.

Gaggero, L., Oggiano, G., Funedda, A. Buzzi, L., 2012. Rifting and Arc-Related Early Paleozoic Volcanism along the North Gondwana Margin: Geochemical and Geological Evidence from Sardinia (Italy). The Journal of Geology 120, 273-292.

Gattacecca, J., Deino, A., Rizzo, R., Jones, D.S., Henry, B., Beaudoin, B., Vedeboin, F., 2007. Miocene rotation of Sardinia: new paleomagnetic and geochronological constraints and geodynamic implications. Earth Planet. Sci. Lett. 258, 359-377.

Gehrels, G., 2014. Detrital Zircon U-Pb Geochronology Applied to Tectonics. Annu. Rev. Earth Planet. Sci. 42, 127-149.

Giacomini, F., Dallai, F., Carminati, E., Tiepolo, M., Ghezzo, C., 2008. Exhumation of a Variscan orogenic complex: insights into the composite granulitic-amphibolitic metamorphic basement of south-east Corsica (France). J. metamorphic Geol. 26, 403-436.

Griffin, W.L., Belousova, E.A., Shee, S.R., Pearson, N.J., O'reilly, S.Y., 2004. Archean crustal evolution in the northern Yilgarn Craton: U-Pb and Hf-isotope evidence from detrital zircons. Precambrian Res. 131, 231-282.

Griffin, W.L., Pearson, N.J., Belousova, E.A., Jackson, S.E., van Achterbergh E., O'Reilly, S.Y., Shee, S.R., 2000. The Hf isotope composition of cratonic mantle: LAM-MC-ICPMS analyses of zircon megacrysts in kimberlites. Geochimica et Cosmochimica Acta 64, 133-147.

Handy, M.R., Schmid, S.M., Bousquet, R., Kissling, E., Bernoulli, D., 2010. Reconciling plate-tectonic reconstructions of Alpine Tethys with the geological-geophysical record of spreading and subduction in the Alps. Earth-Science Reviews 102, 121-158.

Jakni, B., Poupeau, G., Sosson, M., Rossi, Ph., Ferrandini, J., Guennoc, P., 2000. Dénudations cénozoïques en Corse : une analyse thermochronologique par traces de fission sur apatites. C. R. Acad. Sci., Paris 331, 775-782.

Joseph, P., Lomas, S.A., 2004. Deep-water sedimentation in the Alpine Foreland Basin of SE France: New perspectives on the Grès d'Annot and related systems—an introduction. In: Joseph, P., Lomas, S.A. (Eds.), Deep-Water Sedimentation in the Alpine Basin of SE France: New Perspectives on the Grès d'Annot and Related Systems. Geol. Soc. London, Spec. Publ. 221, pp. 1-16.

Jourdan, C., 1988. Balagne orientale et massif du Tenda (Corse septentrionale). Étude structurale, interprétation des accidents et des déformations, reconstitutions géodynamiques (Ph.D. thesis) Univ. Paris XI (Orsay).

Lahondère, D., 1996. Les schistes bleus et les éclogites à lawsonite des unités continentales et océaniques de la Corse alpine (Ph.D. thesis) Univ. Montpellier (USTL), Doc. BRGM 240.

Lemoine, M., Bas, T., Arnaud-Vanneau, A., Arnaud, H., Dumont, T., Gidon, M., Bourbon, M., De Graciansky, P.C., Rutkiewicz, J.L., Mégard-Galli, J., Tricart, P., 1986. The continental margin of the Mesozoic Tethys in the Western Alps. Marine Petroleum Geol. 3, 179-199.

Li, X.H., Faure, M., Lin, W., 2014. From crustal anatexis to mantle melting in the Variscan orogen of Corsica (France): SIMS U-Pb zircon age constraints. Tectonophysics 634, 19-30.

Li, X.H., Faure, M., Rossi, Ph., Lin, W., Lahondère, D., 2015. Age of Alpine Corsica ophiolites revisited: Insights from in situ zircon U-Pb age and O-Hf isotopes. Lithos 220-223, 179-190.

Li, X.H., Liu, Y., Li, Q.L., Guo, C.H., Chamberlain, K.R., 2009. Precise determination of Phanerozoic zircon Pb/Pb age by multicollector SIMS without external standardization, Geochem. Geophys. Geosyst. 10, Q04010, doi:10.1029/2009GC002400

Li, X.H., Tang, G.Q., Gong, B., Yang, Y.H., Hou, K.J., Hu, Z.C., Li, Q.L., Liu, Y., Li, W.X., 2013. Qinghu zircon: A working reference for microbeam analysis of U-Pb age and Hf and O isotopes. China Sci. Bull. 58, 4647-4654.

Libourel, G., 1985. Le complexe de Santa-Lucia-di-Mercurio (Corse). Ultramafites mantelliques, intrusion basique stratifiée, paragneiss granulitiques. Un équivalent possible des complexes de la zone d'Ivrée (Thèse Doct. 3e cycle) Univ. Toulouse.

Linnemann, U., Francisco, P., Jeffries, T.E., Drost, K., Gerdes, A., 2008. The Cadomian Orogeny and the opening of the Rheic Ocean: The diacrony of geotectonic processes constrained by LA-ICP-MS U-Pb zircon dating (Ossa-Morena and Saxo-Thuringian Zones, Iberian and Bohemian Massifs). Tectonophysics 461, 21-43.

Linnemann, U., Gerdes, A., Drost, K., Buschmann, B., 2007. The continuum between Cadomian Orogenesis and opening of the Rheic Ocean: Constraints from LA-ICP-MS U-Pb zircon dating and analysis of plate-tectonic setting (Saxo-Thuringian Zone, NE Bohemian massif, Germany) . In: Linnemann, U., Nance, R.D., Kraft, P., and Zulauf, G., (Eds.), The Evolution of the Rheic Ocean: From Avalonian-Cadomian Active Margin to Alleghenian-Variscan Collision. Geol. Soc. Am. Spec. Pap. 423, pp. 61-96.

Maggi, M., Rossetti, F., Corfu, F., Theye, T., Andersen, T.B., Faccenna, C., 2012. Clinopyroxene-Rutile Phyllonites from the East Tenda Shear Zone (Alpine Corsica, France): Pressure-Temperature-Time Constraints to the Alpine Reworking of Variscan Corsica. Journal of the Geological Society, 169(6), 723-732.

Magné, J., Durand-Delga, M., 1983. Mise au point sur le Sénonien de Corse. Géol. Médit., Marseille 10, 403-410.

Malasoma, A., Marroni, M., 2007. HP/LT metamorphism in the Volparone Breccia (Northern Corsica, France): evidence for involvement of the Europe/Corsica continental margin in the Alpine subduction zone. J. Met. Geol. 25, 529-545.

Malavieille, J., Molli, G., Ferrandini, M., Ferrandini, J., Ottaviani, S.M., Vitale-Brovarone, A., Beyssac, O., Ciancaleoni, L., Maggi, M., Rossetti, F., 2011. General Architecture and tectonic evolution of Alpine Corsica. Insights from a transect between Bastia and the Balagne region. In: Malavieille, J., Molli, G., Vitale-Brovarone, A., Beyssac, O., (Eds.), Corse Alp 2011 - Field Trip Guidebook, J. of the Virtual Explorer, 39, paper 3.

Malusà, M.G., Danišík, M., Kuhlemann, J., 2016b. Tracking the Adriatic-slab travel beneath the Tethyan margin of Corsica-Sardinia by low-temperature thermochronometry. Gondwana Res. 31, 135-149.

Malusà, M.G., Faccenna, C., Baldwin, S.L., Fitzgerald, G., Rossetti F., Balestrieri, M. L., Danišik, M., Ellero, A., Ottria, G., Piromallo, C., 2015. Contrasting styles of (U)HP rock exhumation along the Cenozoic Adria-Europe plate boundary (Western Alps, Calabria, Corsica), Geochem. Geophys. Geosyst., 16, 1786-1824, doi:10.1002/ 2015GC005767.

Malusà, M.G., Resentini, A., Garzanti, E., 2016c. Hydraulic sorting and mineral fertility bias in detrital geochronology. Gondwana Res., 31, 1-19.

Malusà, M.G., Anfinson, O.A., Dafov, L.N., Stockli, D.F., 2016a. Tracking Adria indentation beneath the Alps by detrital zircon U-Pb geochronology: Implications for the Oligocene-Miocene dynamics of the Adriatic microplate. Geology 44, 155-158.

Malusà, M.G., Carter, A., Limoncelli, M., Villa, I.M., Garzanti, E., 2013. Bias in detrital zircon geochronology and thermochronometry. Chem. Geol. 359, 90-107.

Malusà, M.G., Villa, I.M., Vezzoli, G., Garzanti, E., 2011. Detrital geochronology of unroofing magmatic complexes and the slow erosion of Oligocene volcanoes in the Alps. Earth Planet. Sci. Lett. 301, 324-336.

Maluski, H., Mattauer, M., Matte, P., 1973. Sur la présence de décrochements alpins en Corse. C.R. Acad. Sc. Paris, 276, 709-712.

Manzotti, P., Ballèvre, M., Poujol, M., 2016. Detrital zircon geochronology in the Dora-Maira and Zone Houillére: a record of sediment travel paths in the Carboniferous. Terra Nova 28, 279-288.

Manzotti, P., Poujol, M., Ballèvre, M., 2015. Detrital zircon geochronology in blueschist facies meta conglomerates from the Western Alps: implications for the late Carboniferous to early Permian palaeogeography. Int. J. Earth Sci. (Geol. Rundsch.) 104,703-731.

Marino, M., Monechi, M., Principi, G., 1995. New calcareous nannofossils data on Cretaceous-Eocene age corsican turbidites. Rev. Ital. Paleont. Strat. 101, 49-62.

Marroni, M., Pandolfi, L., 2001. Mafic rocks from the sedimentary breccias associated to the Balagne ophiolitic nappe (Northern Corsica): geochemical features and geological implications. Ofioliti, 26, 2b, 433-444.

Marroni, M., Pandolfi, L., 2003. Deformation history of the ophiolite sequence from the Balagne Nappe, northern Corsica: insights in the tectonic evolution of Alpine Corsica. Geol. J. 38, 67-83.

Marroni, M., Pandolfi, L., 2007. The architecture of the Jurassic Ligure-Piemont oceanic basin: tentative reconstruction along the Northern Apennine- Alpine Corsica transect, Int. J. Earth Sci. (Geol. Rundsch.) 96, 1059-1078.

Mattauer, M., Proust, F., 1975. Arguments microtectoniques en faveur de l'origine ultra des nappes de Balagne et de Saint-Florent (Corse). Réun. ann. Sci. Terre, Montpellier, p. 253.

Mattauer, M., Proust, M., 1976. La Corse alpine: un modèle de genèse du métamorphisme haute pression par subduction de croûte continentale sous du matériel océanique. C. R. Acad. Sci., Paris 282, 1249-1251.

Maury, E., 1931. Les nappes de la région du col de San Colombano (Corse). Bull. Serv. Carte Geol. Fr. 34, 157-182.

Meresse, F., Lagabrielle, F., Malavieille, J., Ildefonse, B., 2012. A fossil Ocean-Continent Transition of the Mesozoic Tethys preserved in the Schistes Lustrés nappe of northern Corsica. Tectonophysics 579, 4-16.

Molli, G., Malavieille, J., 2011. Orogenic processes and the Corsica/Apennines geodynamic evolution: insights from Taiwan. Int. J. Earth Sci. (Geol. Rundsch.) 100, 1207-1224.

Molli, G., 2008. Northern Apennine-Corsica orogenic system: an updated overview. In: Siegesmund, S., Fügenschuh, B. Froitzheim, N. (Eds.) Tectonic Aspects of the Alpine-Dinaride-Carpathian System. Geol. Soc. London Spec. Publ. 298, pp. 413-442.

Molli, G., Tribuzio, R., 2004. Shear zones and metamorphic signature of subducted continental crust as tracers of the evolution of the Corsica/Northern Apennine orogenic system. In: Alsop, G.I., Holdsworth, R.E., McCaffrey, K.J.W., Hand, M. (Eds), Flow Processes in Faults and Shear Zones. Geol. Soc. London, Spec. Publ. 224, pp. 321-335.

Morel, M.L., Nebel, A.O., Nebel-Jacobsen, Y.J., Miller, J.S., Vroon, P.Z., 2008. Hafnium isotope characterization of the GJ-1 zircon reference material by solution and laser-ablation MC-ICPMS. Chem. Geol. 255, 231-235.

Nardi, R., 1968. Contributo alla geologia della Balagna (Corsica nord occidentale). Mem. Soc. Geol. It. 7, 471-429.

Nardi, R., Puccinelli, A., Verani, M., 1978. Carta geologica della Balagne « sedimentaria » (Corsica) alla scala 1/25 000 e note illustrative. Boll. Soc. Geol. It. 97, 3-22.

Orsini, J.B., 1976. Les granitoïdes hercyniens corso-sardes: mise en évidence de deux associations magmatiques. Bull. Soc. géol. Fr., (7), XVIII, 1203-1206.

Padoa, E., Durand-Delga, M., 2001. L'unité ophiolitique du Rio Magno en Corse alpine, élément des Ligurides de l'Apennin septentrional. C. R. Acad. Sci. Paris IIa 333, 285-293.

Pandolfi, L., Marroni, M., Malasoma, A., 2016. Stratigraphic and structural features of the Bas Ostriconi unit (Corsica): Palaeogeographic implications. C.R. Geosciences 348, 630-640.

Paquette, J.L., Ménot, R.P., Pin, C., Orsini, J.B., 2003. Episodic and short-lived granitic pulses in a postcollisional setting: evidence from precise U-Pb zircon dating through a crustal cross section in Corsica. Chem. Geol. 198, 1-20.

Peybernès, B., Durand-Delga, M., Cugny, P., 2001a. Reconstitution, en Corse, au Jurassique moyen-supérieur, de la marge européenne de l'océan Liguro-Piémontais, grâce à des niveaux repères à Praekurnubia crusei (foraminifère). C.R. Acad. Sci., Paris 332, 499-506.

Peybernès, B., Durand-Delga, M., Rossi, Ph., Cugny, P., 2001b. Nouvelles datations micropaléontologiques dans les séquences intra- et post-ophiolitiques de la nappe de Balagne

(Corse) et essai de reconstitution d'un segment de la marge occidentale de l'océan liguro-piémontais. Eclogae Geol. Helv. 94, 95-105.

Pin, C., Duthou, J.L., 1990. Sources of Hercynian granitoids from the French Massif Central: Inferences from Nd isotopes and consequences for crustal evolution. Chem. Geol. 83, 281-296.

Principi, G., 2005. About the early Late Cretaceous siliciclastic turbidites in Corsica and northern Apennine ophiolitic successions. C.R. Geoscience 337, 1393-1394.

Principi, G., Treves, B., 1984. Il sistema Corso-Appenninico come prisma d'accrezione. Riflessi sul problema generale del limite Alpi-Appennini. Mem. Soc. Geol. It. 28, 549-576.

Réhault, J.P., Boillot, G., Mauffret, A.,1984. The Western Mediterranean Basin geological evolution. Marine Geol. 55, 447-477.

Rieuf, M., 1980. Étude stratigraphique et structurale des unités au Nord-Est de Corte (Corse) (Ph.D. thesis) Univ. Toulouse.

Ritsema, L., 1952. Géologie de la région de Corte (Corse) (Ph.D. thesis) Univ. Amsterdam.

Rossi, P., Oggiano, G., Cocherie, A., 2009. A restored section of the "Southern Variscan realm" across the Corsica-Sardinia microcontinent. C.R. Geosciences 341, 224-238.

Rossi, Ph., Cocherie, A., 1991. Genesis of a Variscan batholith: field, mineralogical and geochemical evidence from the Corsica-Sardinia batholith. Tectonophysics 195, 319-346.

Rossi, Ph., Cocherie, A., Fanning, C.M., 2015. Evidence in Variscan Corsica of a brief and voluminous Late Carboniferous to Early Permian volcanic-plutonic event contemporaneous with a high-temperature/low-pressure metamorphic peak in the lower crust. Bull. Soc. géol. Fr. 186, 171-192.

Rossi, Ph., Cocherie, A., Fanning, M. C., Deloule E., 2006. Variscan to eo-Alpine events recorded in European lower-crust zircons sampled from the French Massif Central and Corsica, France, Lithos 87, 235-260.

Rossi, Ph., Cocherie, A., Lahondère, D., Fannin,g C.M., 2002. La marge européenne de la Téthys jurassique en Corse: datation de trondhjémites de Balagne et indices de croûte continentale sous le domaine balano-ligure. C.R. Acad. Sci., Paris, Geosciences 334, 313-332.

Rossi, Ph., Durand-Delga, M., 2001. Signification du dépôt de sables quartzeux au sein des basaltes jurassiques océaniques de Balagne (Corse). Ofioliti 26, 169-174.

Rossi, Ph., Durand-Delga, M., Lahondère, J.C., Lahondère, D., 2001. Carte géol. France à1/50000, feuille Santo-Pietro-di-Tenda (1106) - Orléans: BRGM. Notice explicative par Ph. Rossi, M. Durand-Delga, J.C. Lahondère, D. Lahondère.

Rossi, Ph., Oggiano, G., Cocherie, A., 2009. A restored section of the "southern Variscan realm" across the Corsica-Sardinia microcontinent. C.R. Geosciences 341, 224-238.

Sagri, M., Aiello, E., Cortini, L., 1982. Le unità torbiditiche cretacee della Corsica. Rend. Soc. Geol. It. 27, 87-92.

Savva, D., Pubellier, M., Franke, D., Chamot-Rooke, N., Meresse, F., Steuer, S., Auxietre, J.L., 2014. Different expressions of rifting on the South China Sea margins. Marine and Petroleum Geol. 58 (B), 579-598.

Schaltegger, U., Gebauer, D., 1999. Pre-Alpine geochronology of the central, Western and Southern Alps, Schweiz. Mineral. Petrogr. Mitt. 79, 79-87.

Schettino, A., Turco, E., 2006. Tectonics and geodynamics Plate kinematics of the Western Mediterranean region during the Oligocene and Early Miocene. Geophys. J. Int. 166, 1398-1423.

Seymour, N.M., Stockli, D.F., Beltrando, M., Smye, A.J., 2016. Tracing the thermal evolution of the Corsican lower crust during Tethyan rifting, Tectonics, 35, 2439-2466,.

Song, S.G., Niu, Y.L., Wei, C.J., Ji,J., Su, L., 2010. Metamorphism, anatexis, zircon ages and Tectonic evolution of the Gongshan block in the northern Indochina continent: An eastern extension of the Lhasa Block. Lithos 120, 327-346.

Stacey, J.S., Kramers, J.D., 1975. Approximation of terrestrial lead isotope evolution by a two-stage model. Earth Planet. Sci. Lett. 26, 207-221.

Stam, J. C., 1952. Géologie de la région du Tenda septentrional (Corse). Thèse, univ. Amsterdam, n° 203. Van Gorcum et comp. N. V., 96 p.

Stampfli, G.M., Borel, G.D., 2002. A plate tectonic model for the Paleozoic and Mesozoic constrained by dynamic plate boundaries and restored synthetic oceanic isochrons. Earth and Planet. Sci. Lett. 196, 17-33.

Staub, R., 1928. Der Deckenbau Korsikas und sein Zusammenhang mit Alpen und Apennin. Vierteljahrsschrift der Naturf. Gesellschaft in Zürich 298-347.

Tabaud, A.S., Janousek, V., Schulmann, K., Rossi, Ph., Skrzypek, E., Whitechurch, H., Guerrot, C., Paquette, J.L., 2015. Chronology, petrogenesis and heat sources for successive Carboniferous magmatic events in the southern-central Variscan Vosges Mts (NE France). J. Geol. Soc. London 172, 87-102.

Tribuzio R., Giacomini F., 2002. Blueschist facies metamorphism of peralkaline rhyolites from the Tenda crystalline massif (northern Corsica): evidence for involvement in the Alpine subduction event? J. metamorphic Geol. 20, 513-526.

Turco, E., Macchiavelli, C., Mazzoli, S., Schettino, A., Pierantoni, P.P., 2012. Kinematic evolution of Alpine Corsica in the framework of Mediterranean mountain belts. Tectonophysics 579, 193-206.

van Achterbergh, E., Ryan, C., Jackson, S., Griffin, W.L., 2001. Appendix 3 data reduction software for LA-ICP-MS. In: Sylvester, P. (Ed.), Laser-ablation-ICPMS in the Earth Sciences. Mineralogical Association of Canada. Short Courses 29, pp. 239-243.

Vellutini, P., 1977. Le magmatisme permien de la Corse du Nord-Ouest, son extension en Méditerranée occidentale (Ph.D. thesis) Univ. Marseille.

Vermeesch, P., 2012. On the visualisation of detrital age distributions, Chem. Geol. 312-313, 190-194.

Vialon, P., 1990. Deep Alpine structures and geodynamic evolution: an introduction and outline of a new interpretation. Mém. de la Soc. Géol. de Fr. 156, 7-14.

Vitale-Brovarone, A., Beltrando, M., Malavieille, J., Giuntoli, F., Tondella, E., Groppo, C., Beyssac, O., Compagnoni, R., 2011a. Inherited ocean-continent transition zones in deeply subducted terranes: insights from Alpine Corsica. Lithos 124, 273-290.

Vitale-Brovarone, A., Groppo, C., Hetenyi, G., Compagnoni, R., Malavieille, J., 2011b. Coexistence of lawsonite-bearing eclogite and blueschist: phase equilibria modelling of Alpine Corsica metabasalts and petrological evolution of subducting slabs. J. Metamorph. Geol. 29, 583-600.

von Raumer, J.F., Stampfli, G.M., Bussy, F., 2003. Gondwana-derived microcontinents-the constituents of the Variscan and Alpine collisional orogens, Tectonophysics 365, 7-22.

Wiedenbeck, M., Allé, P., Corfu, F., Griffin, W.L., Meier, M., Oberli, F., von Quadt, A., Roddick, J.C., Spiegel, W., 1995. Three natural zircon standards for U-Th-Pb, Lu-Hf, trace element and REE analysis. Geostand. Newsletter 19, 1-23.

Woodhead, J.D., Hergt, J.M., 2005. A preliminary appraisal of seven natural zircon reference materials for in situ Hf isotope determination. Geostand. Geoanal. Res. 29, 183-195.

Wu, F.Y., Yang, Y.H., Xie, L.W., Yang, J.H., Xu, P., 2006. Hf isotopic compositions of the standard zircons and baddeleyites used in U-Pb geochronology. Chem. Geol. 234, 105-126.

Wysoczanski, R.J., Gibson, G.M., Ireland, T.R., 1997. Detrital zircon age patterns and provenance in late Paleozoic-early Mesozoic New Zealand terranes and development of the paleo-Pacific Gondwana margin. Geology 25, 939-942.

Zibra, I., Kruhl, H., Braga, R., 2009. Late Palaeozoic deformation of post-Variscan lower crust: shear zone widening due to strain localization during retrograde shearing. Int. J. Earth Sci. (Geol. Rundsch.) 99, 973-991.

Figure captions

Fig. 1. Simplified geological map of the Corsica Island.

Fig. 2. Geological map and related cross section of the Balagne nappe and its basement with location of the analyzed samples.

Fig. 3. Geological map and related cross section of the Santa-Lucia nappe, North of Corte area, indicating the location of the Cretaceous turbidite (Tralonca flysch) and the location of the sample.

Fig. 4. Field pictures of the different outcrops of turbidites of the Balagne nappe (A. and B. Eocene Annunciata turbidite and C. Lydiennes bearing flysch); the Piedmont formations (D. Tralonca Formation, and E. Narbinco flysch).

Fig. 5. Microscope thin sections representative of dated rocks: A. and B. Eocene Annunciata turbidite, C. Lydiennes bearing flysch, D. Tralonca Formation, E. Narbinco flysch.

Fig. 6. Representative cathodoluminescence (CL) images for zircons from the Neoproterozoic micaschist and the concordia diagram.

Fig. 7. Representative cathodoluminescence (CL) images of selected detrital zircons with a wide range in size and morphology from the Alpine turbidites of Corsica. The circles represent U-Pb analytical sites, numbers and ages presented in figure 8.

Fig. 8. Cumulative probability plots and U-Pb concordia diagrams for detrital zircons from the Alpine turbidites of Corsica. See Figs. 2 and 3 for location, Table 2 for a list of zircon ages.

Fig. 9. Plots of $\varepsilon_{Hf}(t)$ value versus U-Pb age for detrital zircons of this study. Dash lines show evolution of typical zircons with depleted mantle model ages between 1.1 Ga, 1.8 Ga and 2.5 Ga; and the model ages of the dated zircon.

Fig. 10. The two stage model Hf age T_{DM2} versus age plot for detrital zircons, showing the source of zircons. The zircon Hf model ages are older than their crystallization ages, revealing a formation from remelting of the older crust rocks crystallized during the previous events.

Fig. 11. Synthetic and comparison of the cumulative probability plots of detrital zircon U-Pb ages from the Balagne nappe and the Piedmont nappe. Histograms of all the concordant detrital zircon ages obtained in this study.

Fig. 12. Synthetic and comparison of the cumulative probability plots of detrital zircon U-Pb ages from the Alpine turbidites of Corsica. Histograms of all the concordant detrital zircon ages obtained in this study.

Fig. 13. Synthetic and comparison of the cumulative probability plots of detrital zircon U-Pb ages from the Alpine turbidites between Late Cretaceous to middle Eocene. Histograms of all the concordant detrital zircon ages obtained in this study. Inside figure shows that some of the zircons from U1 display a Th/U ratio higher than those of U2 and U3.

Fig. 14. Plate reconstruction of the Western Tethyan region in the Upper Cretaceous modified from Handy et al. (2010). Line is the trace of the sections ~~B1 and B2~~ showing ~~two~~ the possible position~~s~~ of the Balagne and the basin of th Narbinco flyschs within the

European margin of the Piedmont-Ligurian ocean (the drawings of the section was adapted from Meresse et al., 2012).

Table 1 SIMS U-Pb analytical results for zircon of the 1999 Vezzo from the metamorphic basement of Corsica

Table 2. Zircon U-Pb analytical data of the detrital zircons. Discordance (percentage) is calculated as (1) 100%*(($^{207}Pb/^{206}Pb$ age -$^{206}Pb/^{238}U$ age)/($^{207}Pb/^{206}Pb$ age)), if the $^{206}Pb/^{238}U$ age is older than 1000 Ma; (2) 100%*(($^{207}Pb/^{235}U$ age -$^{206}Pb/^{238}U$ age)/($^{206}Pb/^{238}U$ age)), if the $^{206}Pb/^{238}U$ age is younger than 1000 Ma.

Table 3. LA-ICP-MS zircon Lu-Hf isotopic data. Age is the same from Table 2
T(DM) and T(DM2) are one-stage and two-stage Hf model ages, respectively.
$^{176}Hf/^{177}Hf$ (CHUR, t) = 0.282772-(0.0332*(EXP (0.01867*Age/1000)-1)). $^{176}Hf/^{177}Hf$ (DM, t) = 0.28325-(0.0384*(EXP (0.01867*Age/1000)-1))). T_{DM1}= (1/0.01867)*LN (1+ (($^{176}Hf/^{177}Hf$-0.28325)/ ($^{176}Lu/^{177}Hf$-0.0384))). T_{DM2}= (Age/1000) + ((1/0.01867)*LN (1+ (($^{176}Hf/^{177}Hf$ (σ, t)-$^{176}Hf/^{177}Hf$ (DM, t))/(0.015-0.0384))))).

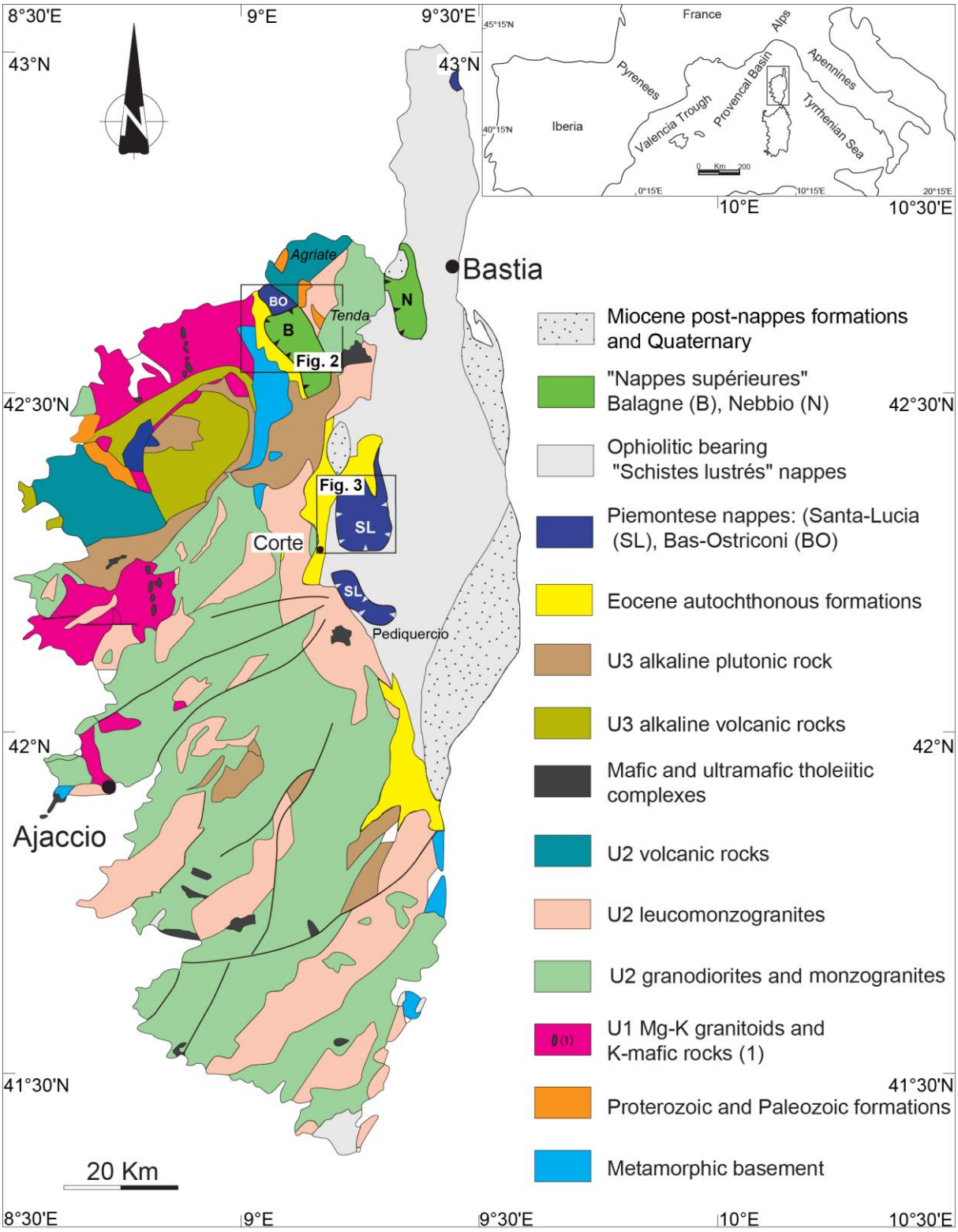

Fig. 1. Simplified geological map of Corsica

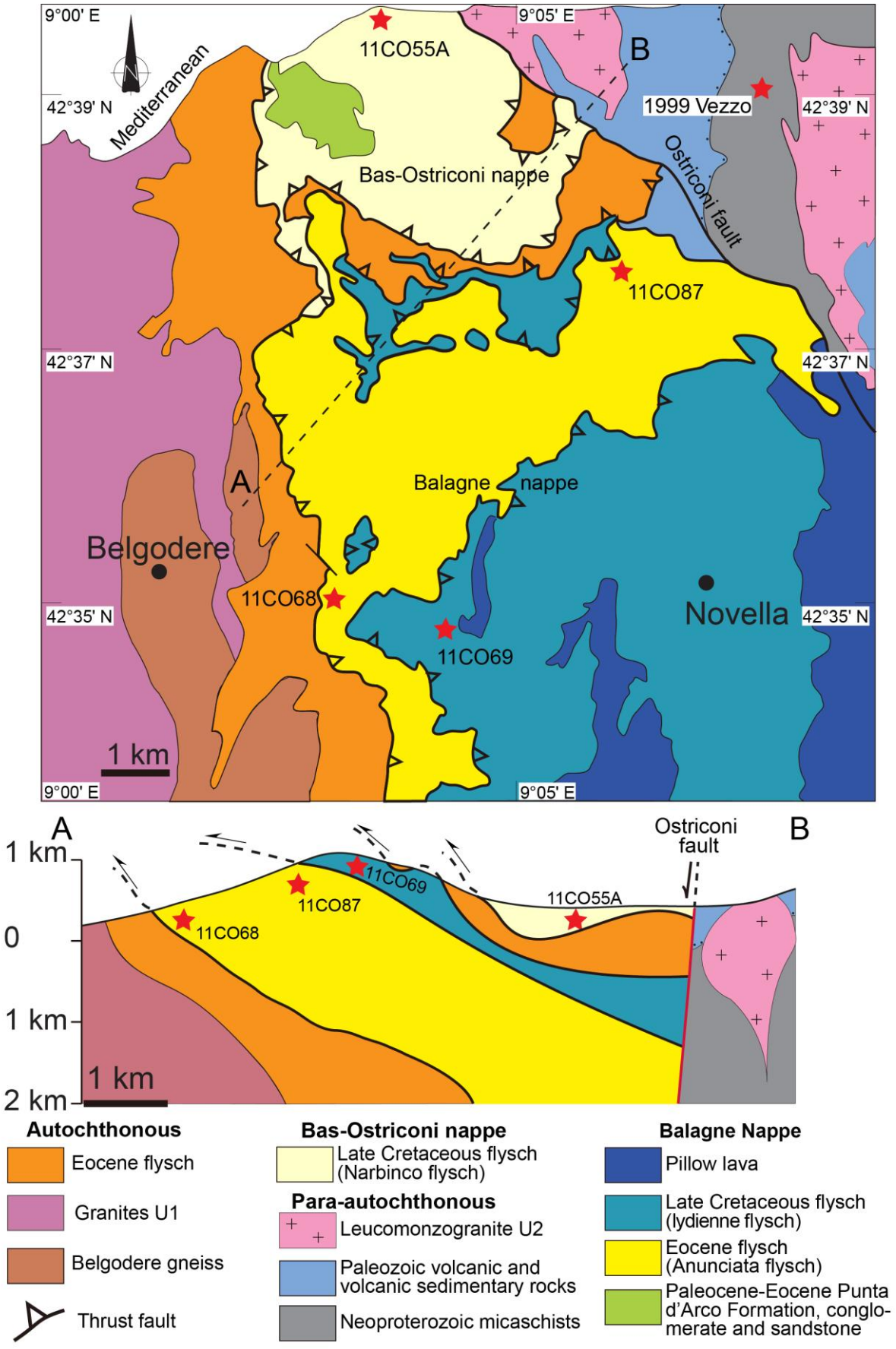

Fig. 2. Geological map and related cross section of the Balagne nappe and its basement with location of analyzed samples.

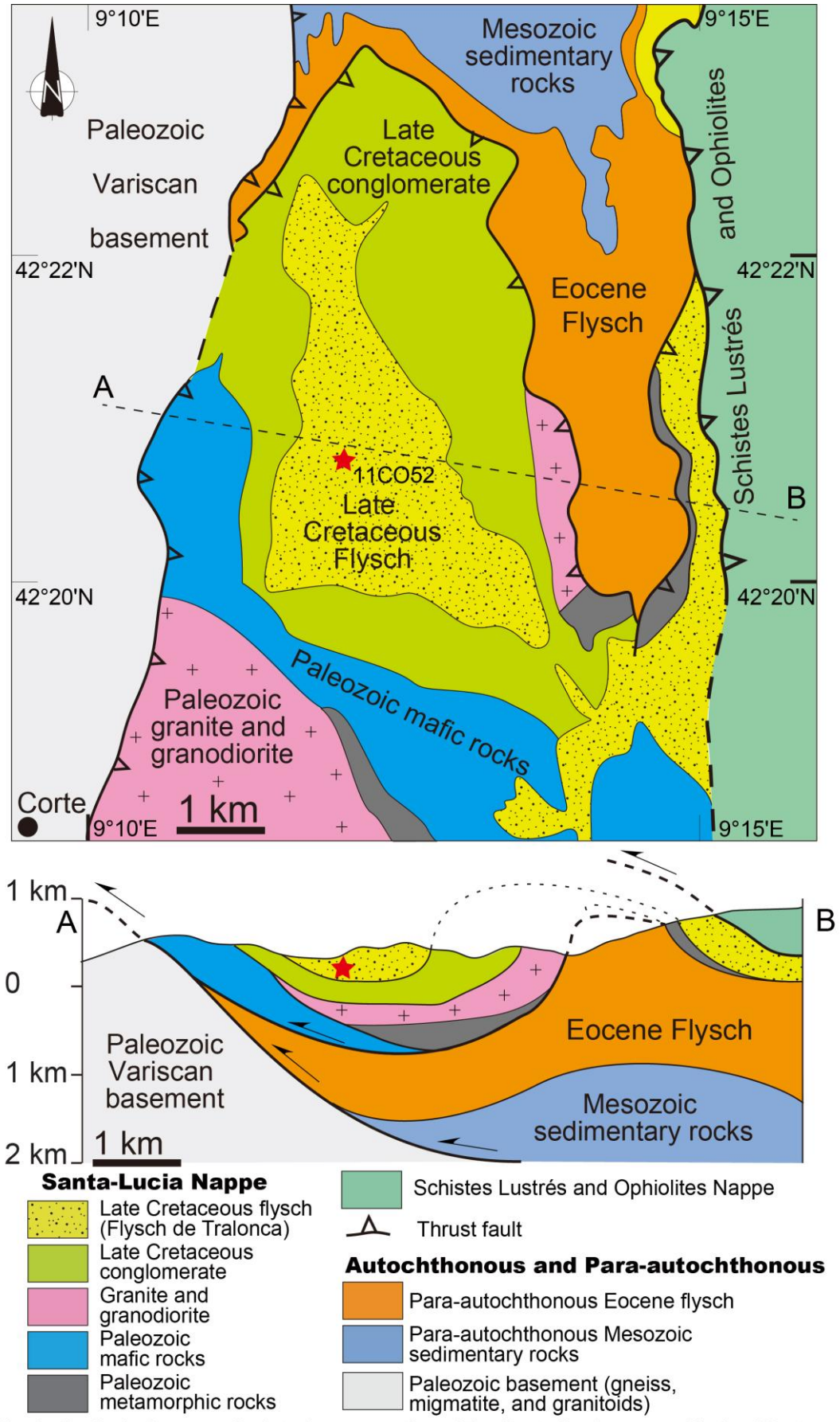

Fig. 3. Geological map and related cross section of the Santa-Lucia nappe, North of Corte area, indicating the location of Cretaceous turbidite (Tralonca flysch) and analyzed sample.

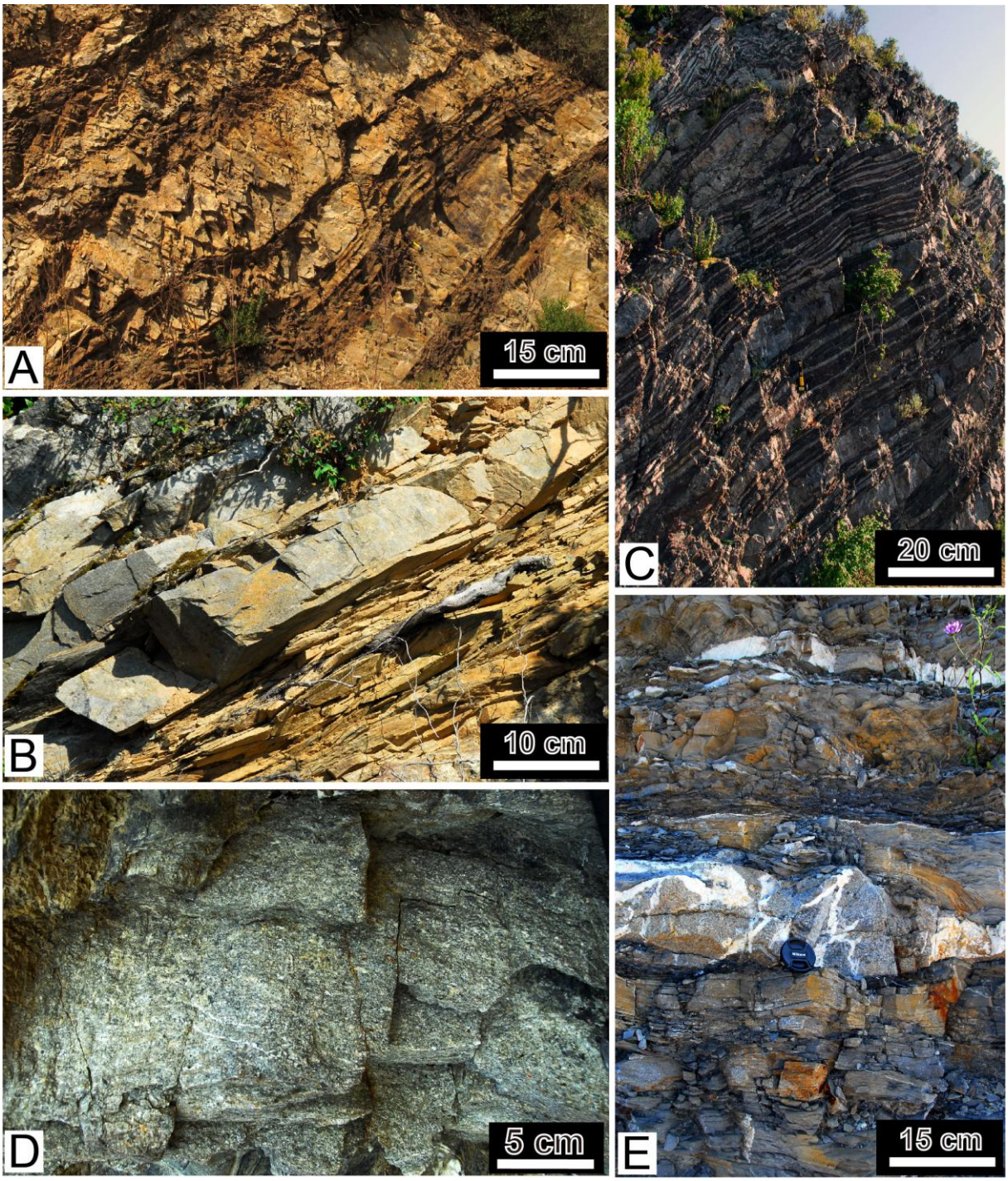

Fig. 4. Field pictures of the different outcrops of turbidites of the Balagne nappe (A. and B. the Eocene Annunciata turbidite and C. Lydite bearing flysch); the Piemontese formations (D. Tralonca Formation, and E. Narbinco flysch).

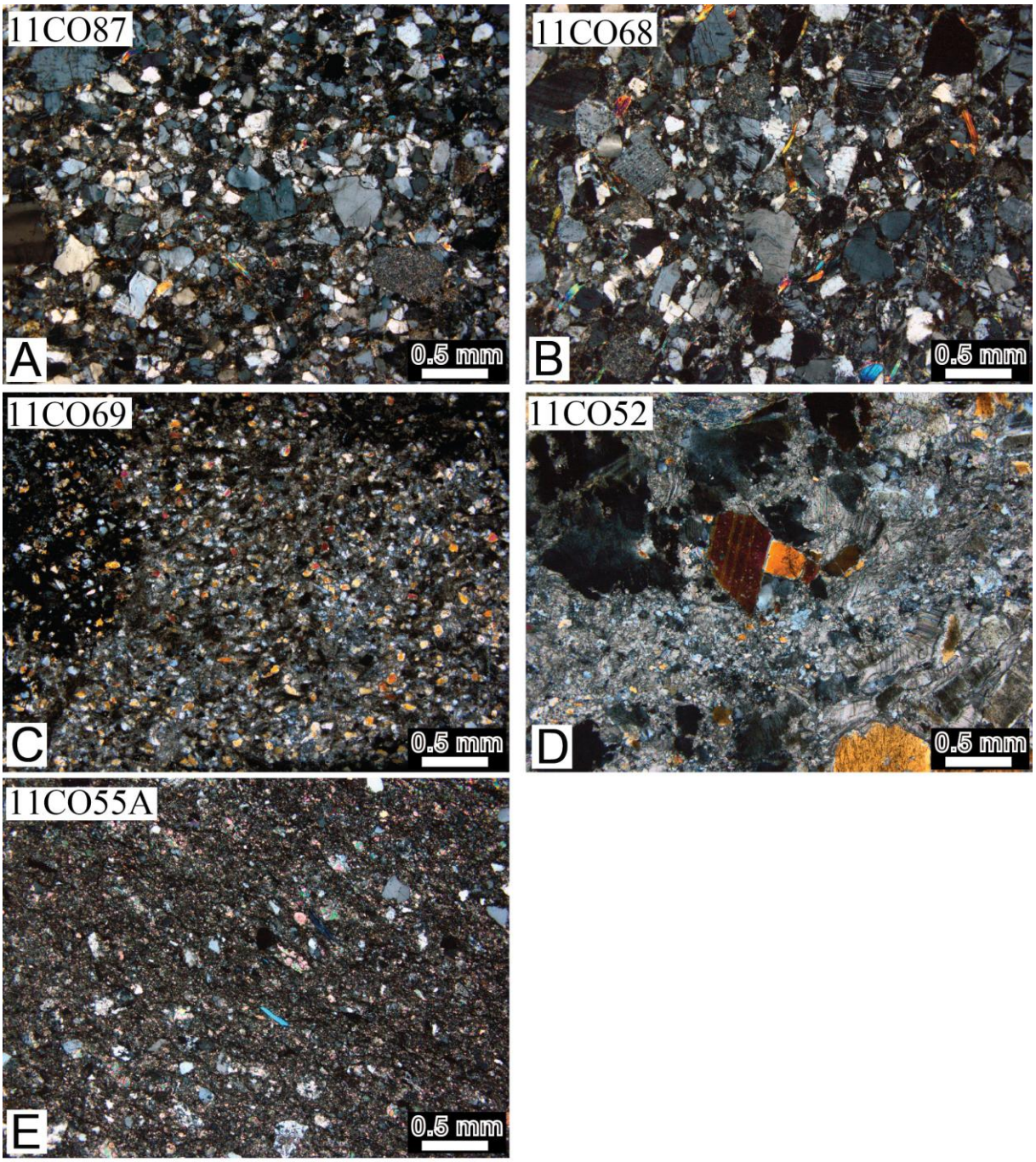

Fig. 5. Microscope thin sections representative of dated rocks: A. and B. the Eocene Annunciata turbidite, C. Lydite bearing flysch, D. Tralonca Formation, E. Narbinco flysch.

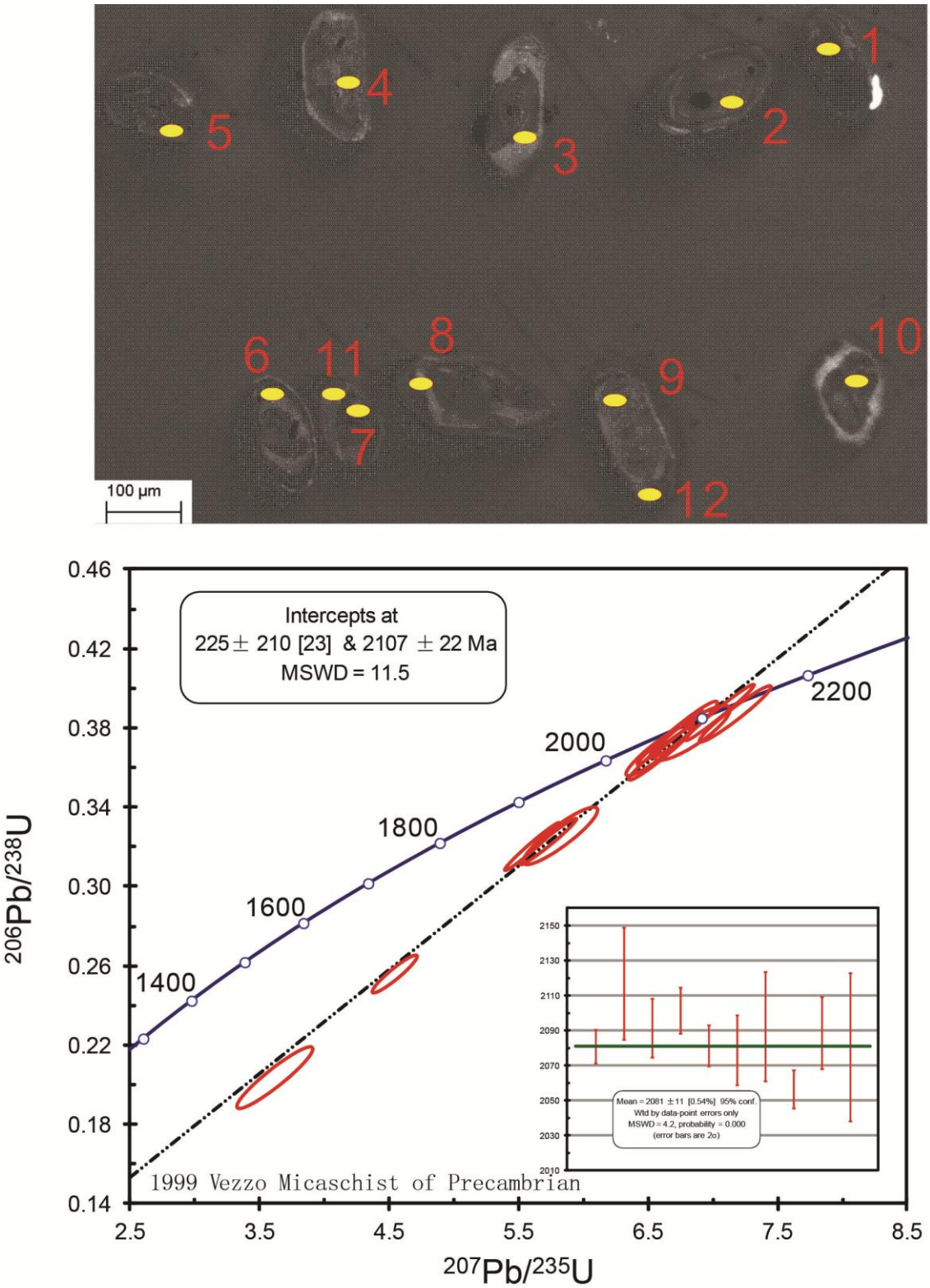

Fig. 6. Representative cathodoluminescence (CL) images for zircons from the Neoproterozoic micaschist and the concordia diagram.

Fig. 7. Representative cathodoluminescence (CL) images of selected detrital zircons with a wide range in size and morphology from the Alpine turbidites of Corsica. The circles represent U-Pb analytical sites, numbers and ages presented in figure 8.

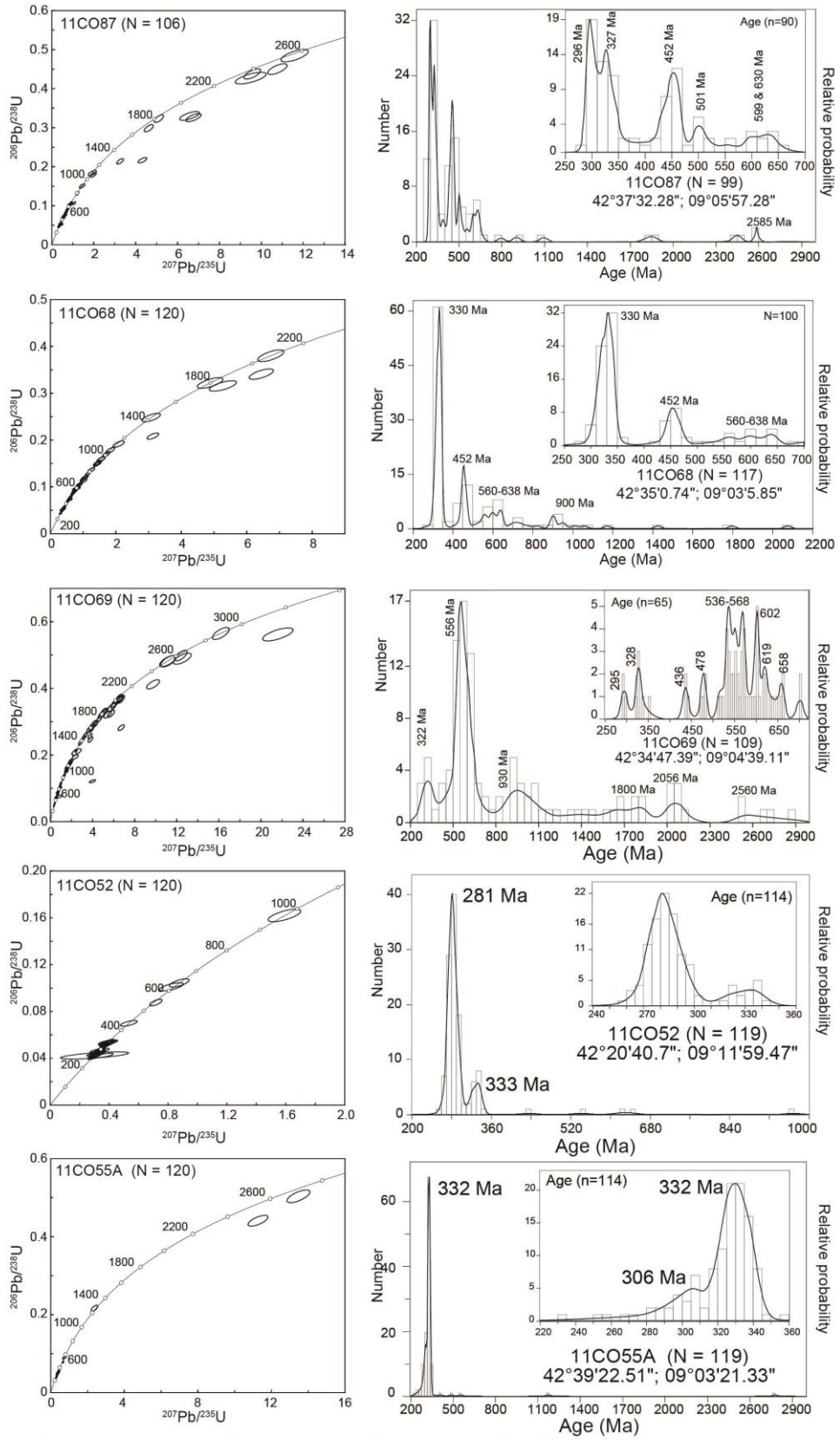

Fig. 8. Cumulative probability plots and U-Pb concordia diagrams for detrital zircons from the Alpine turbidites of Corsica. See Figs. 2 and 3 for location, Table 2 for a list of zircon ages.

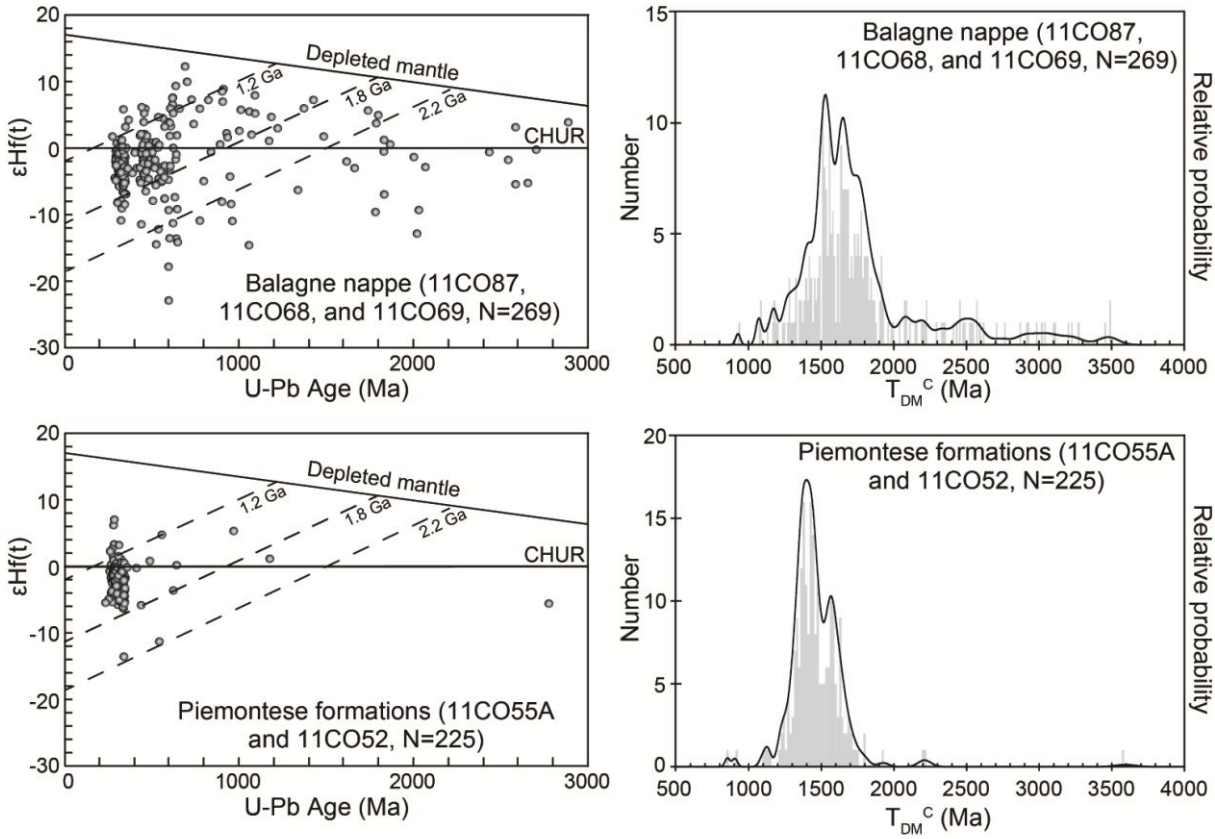

Fig. 9. Plots of ε_{Hf} (t) value versus U-Pb age for detrital zircons of this study. Dash lines show evolution of typical zircons with depleted mantle model ages between 1.1 Ga, 1.8 Ga and 2.5 Ga; and the model ages of the dated zircon.

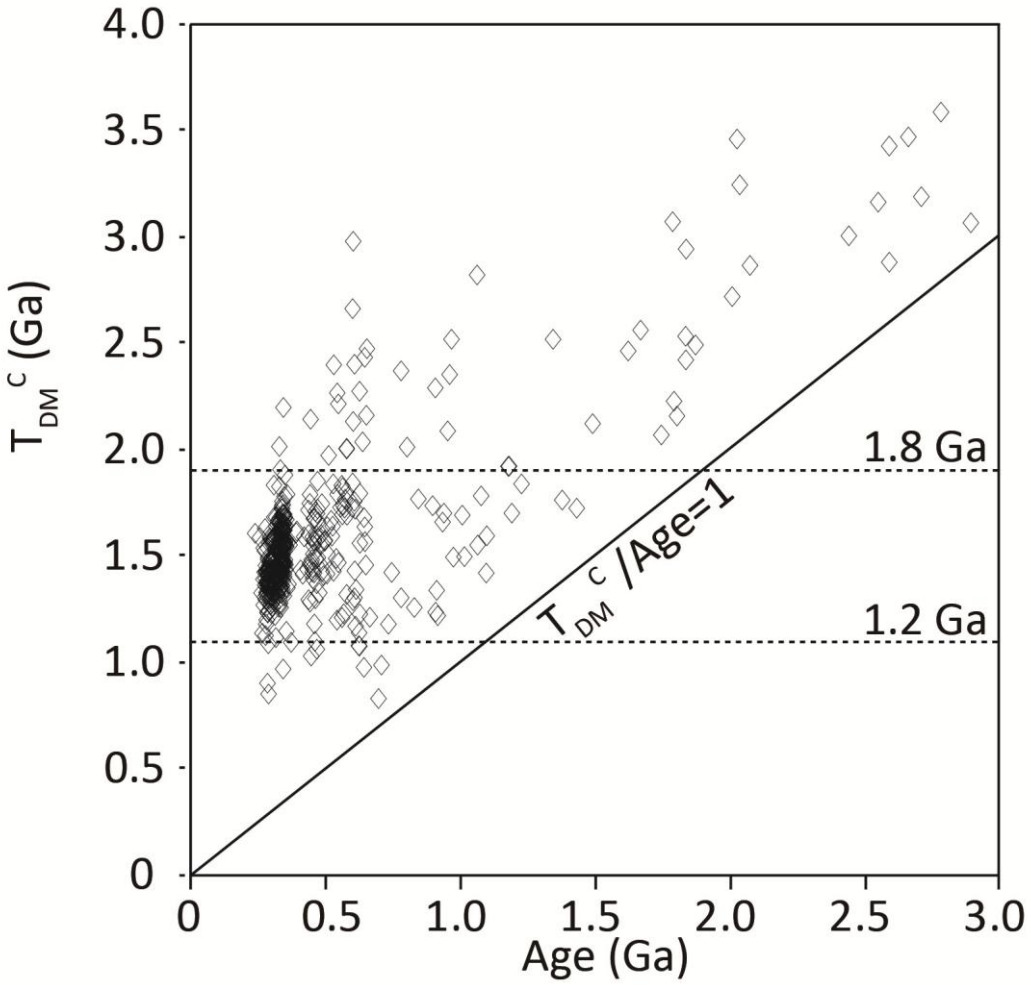

Fig. 10. The two stage model Hf age T_{DM2} versus age plot for detrital zircons, showing the source of zircons. The zircon Hf model ages are older than their crystallization ages, revealing a formation from remelting of the older crust rocks crystallized during the previous events.

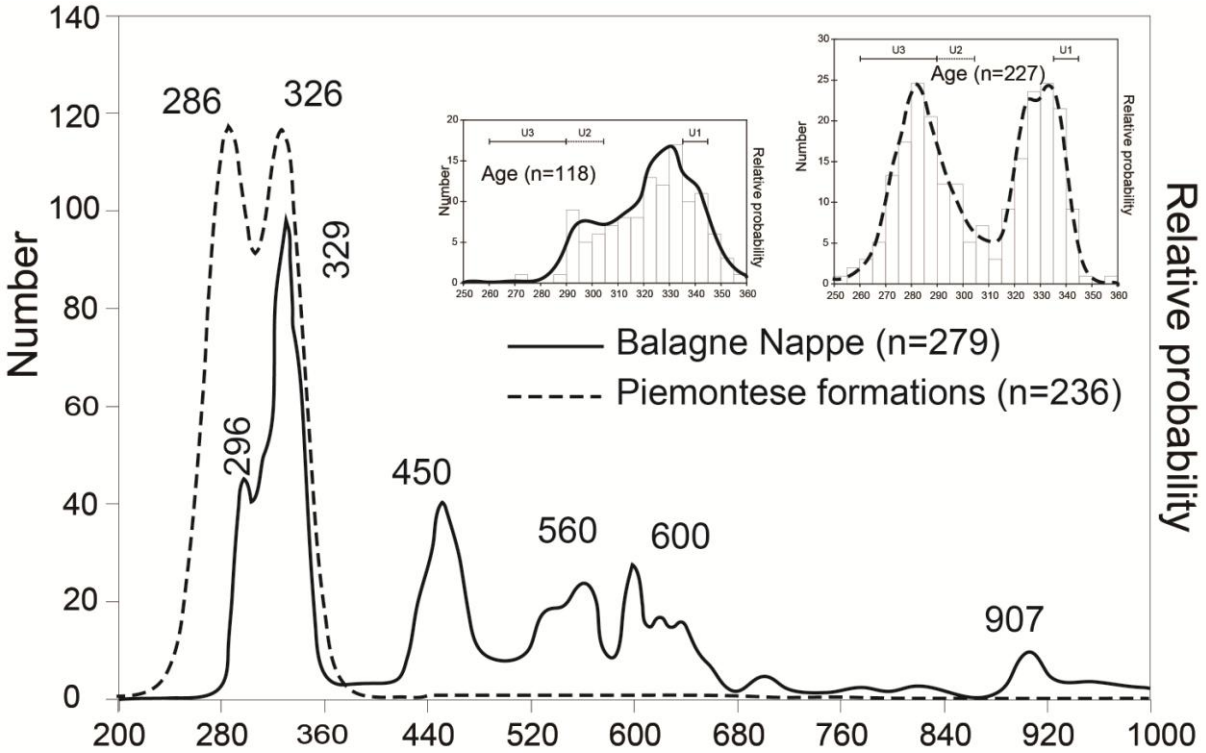

Fig. 11. Synthetic and comparison of the cumulative probability plots of detrital zircon U-Pb ages from the Balagne nappe and the Piemontese nappe. Histograms of all the concordant detrital zircon ages obtained in this study.

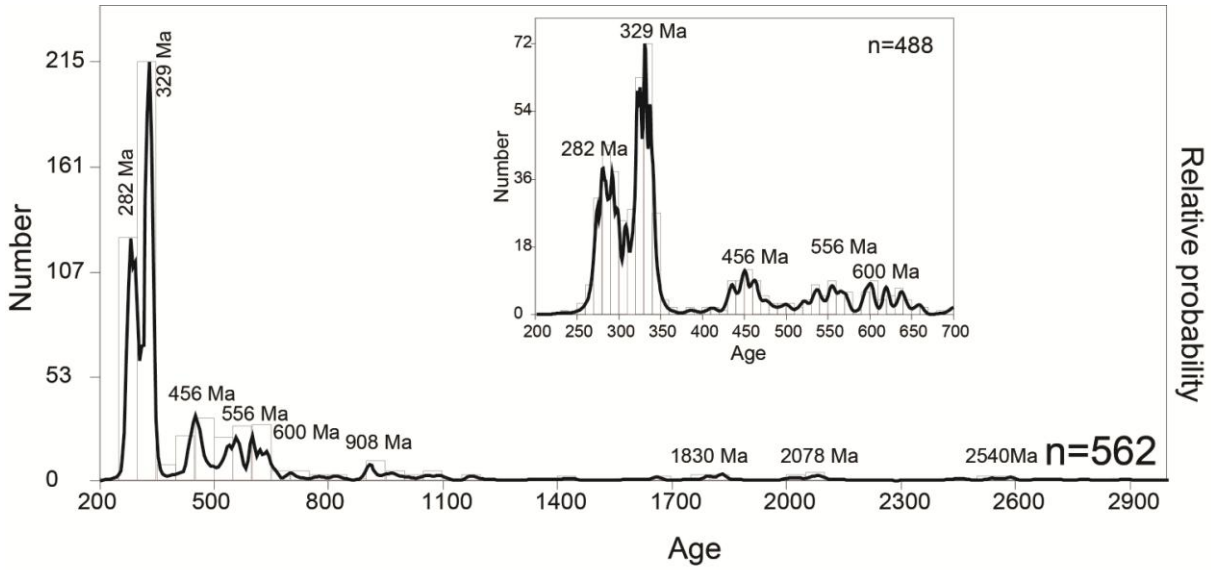

Fig. 12. Synthetic and comparison of the cumulative probability plots of detrital zircon U-Pb ages from the Alpine turbidites of Corsica. Histograms of all the concordant detrital zircon ages obtained in this study.

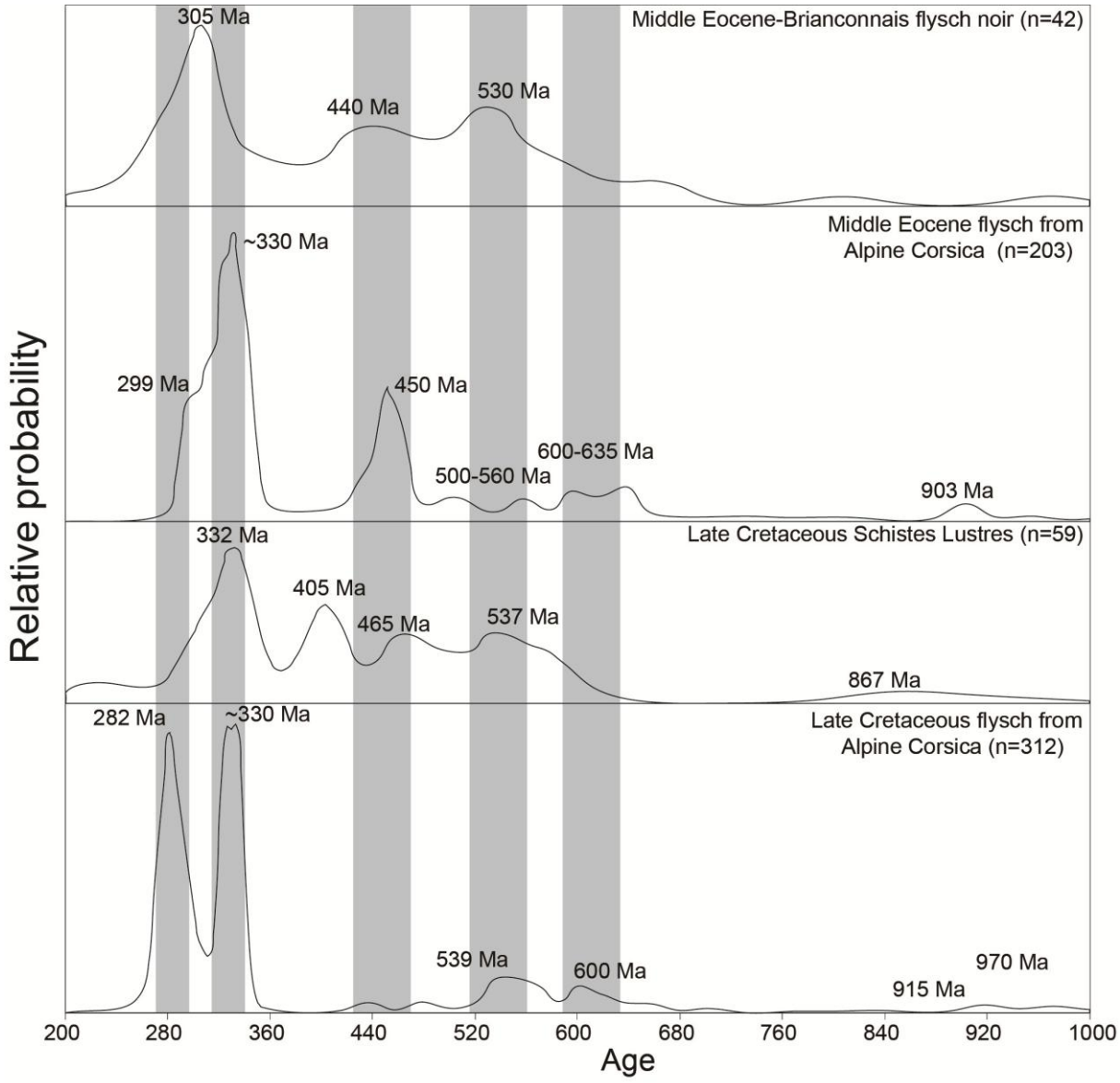

Fig. 13. Synthetic and comparison of the cumulative probability plots of detrital zircon U-Pb ages from the Alpine turbidites of Corsica. Histograms of all the concordant detrital zircon ages obtained in this study. Inside figure shows that some of the zircons from U1 display a Th/U ratio higher than those of U2 and U3.

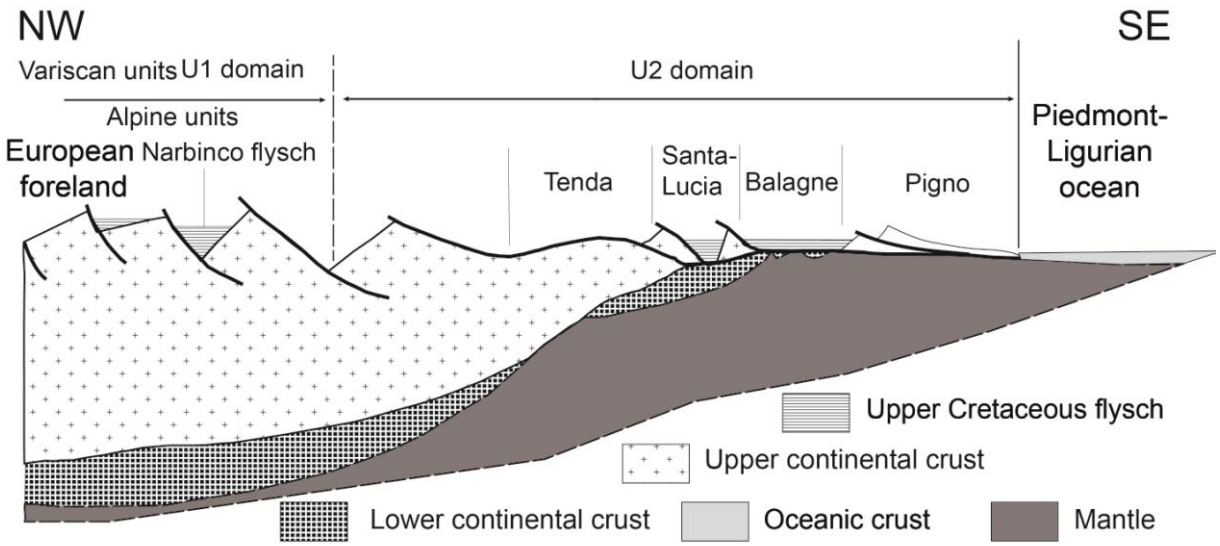

Fig. 14. Plate reconstruction of the Western Tethyan region in the Upper Cretaceous modified from Handy et al. (2010). Line is the trace of the section showing the possible position of the Balagne and the basin of th Narbinco flyschs within the European margin of the Piedmont-Ligurian ocean (the drawings of the section was adapted from Meresse et al., 2012).

Table 1 SIMS U–Pb analytical results for zircon of the 1999 Vezzo from the metamorphic basement of Corsica

Sample/ spot #	[U] ppm	[Th] ppm	[Pb] ppm	Th/U meas	$^{207}Pb/^{206}Pb$	±s %	$^{207}Pb/^{235}U$	±s %	$^{206}Pb/^{238}U$	±s %	r	$^{207}Pb/^{206}Pb$	±s	$^{207}Pb/^{235}U$	±s	$^{206}Pb/^{238}U$	±s	f_{206}%
54550@1	1464	278	651	0.190	0.12874	0.27	6.66331	1.53	0.3754	1.50	0.98376	2080.8	4.8	2067.8	13.6	2054.7	26.5	{0.01}
54550@2	430	295	214	0.686	0.13140	0.92	6.84228	1.76	0.3777	1.50	0.85260	2116.8	16.0	2091.2	15.7	2065.3	26.6	{3.20}
54550@3	465	291	230	0.627	0.12953	0.48	6.77481	1.58	0.3793	1.50	0.95225	2091.6	8.4	2082.4	14.1	2073.2	26.7	{0.45}
54550@4	654	430	316	0.658	0.13026	0.38	6.59582	1.55	0.3672	1.50	0.96998	2101.5	6.6	2058.8	13.7	2016.4	26.1	{0.17}
54550@5	1191	227	455	0.191	0.12878	0.34	5.73018	1.54	0.3227	1.50	0.97579	2081.3	5.9	1935.9	13.4	1803.0	23.7	{0.44}
54550@6	435	534	141	1.229	0.12859	0.57	4.54092	1.61	0.2561	1.50	0.93542	2078.7	10.0	1738.5	13.5	1470.0	19.8	{1.08}
54550@7	898	244	411	0.272	0.13434	0.41	7.17084	1.56	0.3871	1.50	0.96427	2155.4	7.2	2132.9	14.0	2109.6	27.1	{0.70}
54550@8	711	147	328	0.206	0.13179	0.29	7.05109	1.53	0.3880	1.50	0.98231	2121.9	5.0	2117.9	13.7	2113.7	27.1	{0.11}
54550@9	680	482	293	0.709	0.12958	0.89	5.82013	2.02	0.3257	1.81	0.89684	2092.3	15.6	1949.4	17.6	1817.7	28.7	{2.20}
54550@10	1516	534	597	0.352	0.12697	0.31	5.60238	1.58	0.3200	1.55	0.98065	2056.5	5.4	1916.5	13.7	1789.8	24.2	{0.19}
54550@11	371	220	174	0.592	0.12931	0.59	6.58495	1.62	0.3693	1.51	0.93157	2088.7	10.3	2057.3	14.4	2026.2	26.3	{0.25}
54550@12	1300	1787	340	1.375	0.12872	1.21	3.61460	3.35	0.2037	3.12	0.93227	2080.5	21.2	1552.7	27.0	1195.0	34.2	{3.66}

Table 2 Zircon U-Pb analytical data of the detrital zircons

Sample#spot	Th (ppm)	U (ppm)	Th/U	Isotopic ratios						Age (Ma)						Disconcordance
				$^{207}Pb/^{206}Pb$	±σ	$^{207}Pb/^{235}U$	±σ	$^{206}Pb/^{238}U$	±σ	$^{207}Pb/^{206}Pb$	±σ	$^{207}Pb/^{235}U$	±σ	$^{206}Pb/^{238}U$	±σ	
11CO87																
11CO87#01	87	104	0.83	0.11014	0.00219	3.25218	0.06582	0.21401	0.00275	1802	19	1470	16	1250	15	44.16%
11CO87#02	52	115	0.45	0.05238	0.00399	0.34109	0.0259	0.04719	0.00072	302	145	298	20	297	4	0.34%
11CO87#03	78	122	0.64	0.05227	0.00236	0.33562	0.01501	0.04654	0.00068	297	75	294	11	293	4	0.34%
11CO87#04	20	308	0.06	0.15815	0.0033	9.56027	0.16228	0.43844	0.00532	2436	36	2393	16	2344	24	3.92%
11CO87#05	118	179	0.66	0.17295	0.00294	10.76012	0.19016	0.45095	0.00562	2586	14	2503	16	2399	25	7.79%
11CO87#06	132	287	0.46	0.11417	0.00197	5.1003	0.09145	0.32379	0.00403	1867	16	1836	15	1808	20	3.26%
11CO87#07	172	288	0.60	0.05279	0.00146	0.37619	0.01046	0.05166	0.00067	320	40	324	8	325	4	-0.31%
11CO87#08	87	159	0.55	0.05291	0.00219	0.38082	0.01571	0.05217	0.00073	325	68	328	12	328	4	0.00%
11CO87#09	91	222	0.41	0.05298	0.00177	0.37396	0.01246	0.05116	0.00069	328	51	323	9	322	4	0.31%
11CO87#10	25	55	0.46	0.06933	0.00253	1.44241	0.05247	0.15081	0.00212	909	52	907	22	906	12	0.11%
11CO87#11	39	187	0.21	0.14436	0.00275	4.31815	0.08421	0.21684	0.00279	2280	17	1697	16	1265	15	80.24%
11CO87#12	83	667	0.12	0.06743	0.00121	1.22199	0.02277	0.13137	0.00164	851	20	811	10	796	9	1.88%
11CO87#13	90	664	0.14	0.05224	0.00119	0.33459	0.00775	0.04643	0.00059	296	30	293	6	293	4	0.00%
11CO87#14	380	647	0.59	0.05248	0.00114	0.37208	0.00824	0.0514	0.00065	306	28	321	6	323	4	-0.62%
11CO87#15	77	165	0.46	0.05625	0.00174	0.57859	0.01794	0.07457	0.001	462	45	464	12	464	6	0.00%
11CO87#16	54	196	0.28	0.11197	0.00206	4.62089	0.08794	0.29918	0.00379	1832	17	1753	16	1687	19	8.60%
11CO87#17	94	228	0.41	0.05203	0.00182	0.32704	0.01141	0.04557	0.00062	287	55	287	9	287	4	0.00%
11CO87#18	65	110	0.59	0.05613	0.00261	0.56199	0.02602	0.07259	0.00103	458	77	453	17	452	6	0.22%
11CO87#19	232	289	0.81	0.05289	0.0015	0.37714	0.0110	0.05169	0.0006	324	42	325	8	325	4	0.00%

					4		5		9							
11CO87#20	65	150	0.44	0.05613	0.00205	0.56053	0.02044	0.0724	0.00099	458	56	452	13	451	6	0.22%
11CO87#21	52	164	0.32	0.05577	0.00196	0.53659	0.01887	0.06976	0.00095	443	54	436	12	435	6	0.23%
11CO87#22	91	114	0.80	0.05325	0.00239	0.39625	0.0177	0.05395	0.00079	339	75	339	13	339	5	0.00%
11CO87#23	33	137	0.24	0.05593	0.00213	0.55929	0.02128	0.07251	0.00101	450	60	451	14	451	6	0.00%
11CO87#24	60	232	0.26	0.05724	0.00149	0.63816	0.01677	0.08083	0.00107	501	35	501	10	501	6	0.00%
11CO87#25	514	959	0.54	0.05619	0.00117	0.53097	0.01131	0.06851	0.00087	460	26	432	8	427	5	1.17%
11CO87#26	73	648	0.11	0.05209	0.00128	0.33367	0.00834	0.04645	0.0006	289	34	292	6	293	4	-0.34%
11CO87#27	177	338	0.52	0.05231	0.00162	0.3409	0.01061	0.04725	0.00063	299	47	298	8	298	4	0.00%
11CO87#28	78	178	0.44	0.05312	0.00232	0.38579	0.01679	0.05266	0.00075	334	73	331	12	331	5	0.00%
11CO87#29	144	478	0.30	0.05593	0.00135	0.55795	0.01369	0.07234	0.00094	450	32	450	9	450	6	0.00%
11CO87#30	47	259	0.18	0.05744	0.00189	0.63803	0.02115	0.08054	0.00107	508	49	501	13	499	6	0.40%
11CO87#31	225	439	0.51	0.05229	0.00145	0.33351	0.00933	0.04625	0.00061	298	40	292	7	291	4	0.34%
11CO87#32	350	275	1.27	0.05293	0.00212	0.36612	0.01469	0.05016	0.00068	326	66	317	11	316	4	0.32%
11CO87#33	98	111	0.89	0.05984	0.00198	0.79865	0.02636	0.09677	0.00136	598	47	596	15	595	8	0.17%
11CO87#34	40	1498	0.03	0.0535	0.00108	0.41454	0.00861	0.05619	0.00071	350	25	352	6	352	4	0.00%
11CO87#35	74	141	0.52	0.05217	0.00286	0.34225	0.01864	0.04758	0.00071	293	97	299	14	300	4	-0.33%
11CO87#36	203	554	0.37	0.1501	0.00383	6.75571	0.1486	0.32644	0.00422	2347	45	2080	19	1821	21	28.89%
11CO87#37	142	172	0.82	0.05586	0.00193	0.55789	0.01925	0.07243	0.00101	447	52	450	13	451	6	-0.22%
11CO87#38	82	335	0.24	0.05703	0.00141	0.62138	0.01562	0.07901	0.00104	493	33	491	10	490	6	0.20%
11CO87#39	58	273	0.21	0.06136	0.00153	0.90859	0.023	0.10738	0.00142	652	32	656	12	658	8	-0.30%
11CO87#40	266	333	0.80	0.05287	0.00192	0.37591	0.01368	0.05156	0.0007	323	58	324	10	324	4	0.00%

11CO87#41	89	212	0.42	0.05306	0.00181	0.38587	0.01319	0.05274	0.00073	331	52	331	10	331	4	0.00%
11CO87#42	24	40	0.60	0.07582	0.00314	1.92524	0.07941	0.18415	0.00276	1090	58	1090	28	1090	15	0.00%
11CO87#43	188	448	0.42	0.05571	0.00134	0.55071	0.01349	0.07169	0.00094	441	32	445	9	446	6	-0.22%
11CO87#44	6	510	0.01	0.05776	0.00146	0.54987	0.01419	0.06905	0.0009	521	34	445	9	430	5	3.49%
11CO87#45	142	259	0.55	0.06046	0.00152	0.84136	0.02156	0.10093	0.00133	620	33	620	12	620	8	0.00%
11CO87#46	20	367	0.05	0.05615	0.00161	0.57048	0.01653	0.07369	0.00098	458	41	458	11	458	6	0.00%
11CO87#47	241	247	0.98	0.05309	0.00176	0.38639	0.01287	0.05279	0.00073	333	50	332	9	332	4	0.00%
11CO87#48	434	186	2.33	0.0597	0.00169	0.79766	0.02275	0.09691	0.00132	593	38	596	13	596	8	0.00%
11CO87#49	956	466	2.05	0.05994	0.00147	0.75146	0.01874	0.09092	0.00119	601	32	569	11	561	7	1.43%
11CO87#50	168	294	0.57	0.05232	0.00195	0.34054	0.0127	0.0472	0.00065	299	60	298	10	297	4	0.34%
11CO87#51	120	304	0.40	0.05246	0.00167	0.34523	0.01102	0.04773	0.00066	306	48	301	8	301	4	0.00%
11CO87#52	164	338	0.48	0.05203	0.00171	0.33681	0.01113	0.04695	0.00064	287	51	295	8	296	4	-0.34%
11CO87#53	117	160	0.73	0.0528	0.00224	0.38326	0.01621	0.05264	0.00077	320	69	329	12	331	5	-0.60%
11CO87#54	159	349	0.45	0.05258	0.00168	0.35932	0.01157	0.04957	0.00068	311	48	312	9	312	4	0.00%
11CO87#55	213	276	0.77	0.05745	0.00186	0.64542	0.02102	0.08148	0.0011	509	48	506	13	505	7	0.20%
11CO87#56	74	372	0.20	0.05981	0.0017	0.69314	0.01993	0.08405	0.00113	597	39	535	12	520	7	2.88%
11CO87#57	53	57	0.92	0.06074	0.00346	0.86812	0.0492	0.10365	0.00162	630	95	635	27	636	9	-0.16%
11CO87#58	39	385	0.10	0.05436	0.00163	0.46108	0.01396	0.06151	0.00084	386	44	385	10	385	5	0.00%
11CO87#59	387	568	0.68	0.05221	0.00148	0.33484	0.00963	0.04652	0.00062	295	41	293	7	293	4	0.00%
11CO87#60	77	159	0.48	0.0525	0.00247	0.35575	0.01665	0.04915	0.00073	307	79	309	12	309	4	0.00%
11CO87#61	53	77	0.69	0.17292	0.00387	11.5792	0.26648	0.48565	0.0065	2586	21	2571	22	2552	28	1.33%
11CO87#62	83	164	0.50	0.05629	0.0020	0.58099	0.0214	0.07486	0.0010	464	57	465	14	465	6	0.00%

					7		4		6							
11CO87#63	175	563	0.31	0.0597	0.00143	0.80228	0.01971	0.09746	0.00129	593	31	598	11	600	8	-0.33%
11CO87#64	105	197	0.53	0.14393	0.00465	6.56478	0.19124	0.3308	0.0046	2275	57	2055	26	1842	22	23.51%
11CO87#65	87	298	0.29	0.05749	0.00197	0.63965	0.02204	0.08069	0.00111	510	51	502	14	500	7	0.40%
11CO87#66	11	844	0.01	0.05304	0.00146	0.37487	0.01049	0.05126	0.00068	331	40	323	8	322	4	0.31%
11CO87#67	15	1138	0.01	0.0556	0.00134	0.53388	0.01318	0.06964	0.00092	436	32	434	9	434	6	0.00%
11CO87#68	184	645	0.28	0.05235	0.00155	0.34338	0.01032	0.04757	0.00064	301	44	300	8	300	4	0.00%
11CO87#69	66	318	0.21	0.05592	0.00187	0.555	0.01872	0.07198	0.001	449	50	448	12	448	6	0.00%
11CO87#70	188	419	0.45	0.054	0.00213	0.36186	0.01434	0.0486	0.00069	371	64	314	11	306	4	2.61%
11CO87#71	74	145	0.51	0.0564	0.00254	0.57452	0.02591	0.07388	0.00108	468	74	461	17	459	6	0.44%
11CO87#72	77	373	0.21	0.05244	0.00272	0.33486	0.01668	0.04631	0.00067	305	121	293	13	292	4	0.34%
11CO87#73	37	63	0.59	0.05623	0.00368	0.57504	0.03742	0.07416	0.00122	461	116	461	24	461	7	0.00%
11CO87#74	126	783	0.16	0.05694	0.00156	0.55755	0.01559	0.07102	0.00096	489	38	450	10	442	6	1.81%
11CO87#75	199	1200	0.17	0.05379	0.00148	0.34336	0.00966	0.04629	0.00062	362	39	300	7	292	4	2.74%
11CO87#76	32	152	0.21	0.05428	0.00225	0.4637	0.0192	0.06195	0.00092	383	66	387	13	387	6	0.00%
11CO87#77	53	290	0.18	0.07182	0.00208	1.05454	0.03104	0.10648	0.00146	981	38	731	15	652	9	12.12%
11CO87#78	22	281	0.08	0.06203	0.00208	0.65395	0.02213	0.07645	0.00106	675	49	511	14	475	6	7.58%
11CO87#79	37	165	0.22	0.05864	0.00216	0.72773	0.02689	0.09	0.00131	554	55	555	16	556	8	-0.18%
11CO87#80	194	243	0.80	0.05617	0.0019	0.57593	0.01962	0.07435	0.00105	459	50	462	13	462	6	0.00%
11CO87#81	70	266	0.26	0.0578	0.00184	0.67386	0.02174	0.08454	0.00119	522	46	523	13	523	7	0.00%
11CO87#82	106	484	0.22	0.05584	0.00222	0.51036	0.019	0.06629	0.00091	446	90	419	13	414	6	1.21%
11CO87#83	60	116	0.52	0.07971	0.00233	1.97149	0.0584	0.17936	0.00252	1190	36	1106	20	1063	14	11.95%

11CO87#84	663	791	0.84	0.05464	0.00157	0.41798	0.01225	0.05548	0.00076	398	41	355	9	348	5	2.01%
11CO87#85	211	263	0.80	0.06097	0.00178	0.87676	0.02602	0.10428	0.00145	638	40	639	14	639	8	0.00%
11CO87#86	123	255	0.48	0.05257	0.00198	0.35938	0.01358	0.04957	0.00072	310	59	312	10	312	4	0.00%
11CO87#87	418	437	0.96	0.05415	0.00194	0.38898	0.01404	0.05209	0.00073	377	56	334	10	327	4	2.14%
11CO87#88	638	889	0.72	0.16082	0.00561	9.48682	0.30196	0.42784	0.00613	2464	60	2386	29	2296	28	7.32%
11CO87#89	248	221	1.12	0.06097	0.00206	0.86526	0.02967	0.10291	0.00144	638	50	633	16	631	8	0.32%
11CO87#90	33	447	0.07	0.05541	0.0019	0.44694	0.01548	0.05849	0.00082	429	52	375	11	366	5	2.46%
11CO87#91	108	273	0.40	0.05473	0.00226	0.48423	0.02013	0.06416	0.00092	401	67	401	14	401	6	0.00%
11CO87#92	122	342	0.36	0.05259	0.00199	0.36209	0.01384	0.04992	0.00072	311	61	314	10	314	4	0.00%
11CO87#93	95	156	0.61	0.06055	0.00234	0.84148	0.03278	0.10076	0.00146	623	59	620	18	619	9	0.16%
11CO87#94	64	214	0.30	0.05371	0.0023	0.41081	0.01766	0.05545	0.00082	359	70	349	13	348	5	0.29%
11CO87#95	95	134	0.71	0.05263	0.00253	0.35829	0.01721	0.04936	0.00077	313	81	311	13	311	5	0.00%
11CO87#96	47	300	0.16	0.05281	0.00209	0.35506	0.01413	0.04874	0.00071	321	64	309	11	307	4	0.65%
11CO87#97	93	96	0.98	0.05299	0.00411	0.39385	0.0305	0.05389	0.00089	328	146	337	22	338	5	-0.30%
11CO87#98	162	440	0.37	0.06012	0.00203	0.57317	0.01963	0.06912	0.00099	608	49	460	13	431	6	6.73%
11CO87#99	306	398	0.77	0.05331	0.00203	0.40549	0.01564	0.05515	0.00079	342	61	346	11	346	5	0.00%
11CO87#100	195	501	0.39	0.05336	0.00178	0.40034	0.01358	0.0544	0.00077	344	51	342	10	341	5	0.29%
11CO87#101	27	65	0.41	0.05571	0.00365	0.53973	0.03518	0.07024	0.00118	441	116	438	23	438	7	0.00%
11CO87#102	43	351	0.12	0.05801	0.00251	0.59335	0.02419	0.07419	0.00106	530	97	473	15	461	6	2.60%
11CO87#103	276	477	0.58	0.06454	0.00393	0.46211	0.02724	0.05193	0.00081	759	132	386	19	326	5	18.40%
11CO87#104	48	937	0.05	0.05674	0.00229	0.37495	0.01418	0.04792	0.00068	482	91	323	10	302	4	6.95%
11CO87#105	73	226	0.32	0.05248	0.0022	0.35308	0.0149	0.04877	0.0007	306	69	307	11	307	5	0.00%

					1		3		4							
11CO87#106	238	421	0.57	0.05329	0.0019 4	0.39747	0.0146 5	0.05407	0.0007 8	341	57	340	11	339	5	0.29%
11CO68																
11CO68#01	162	643	0.25	0.05248	0.0014	0.35643	0.0096 4	0.04926	0.0006 5	306	38	310	7	310	4	0.00%
11CO68#02	249	695	0.36	0.05302	0.0012 8	0.38596	0.0095 3	0.05279	0.0007	330	33	331	7	332	4	-0.30%
11CO68#03	274	550	0.50	0.05297	0.0014 1	0.38254	0.0103 3	0.05237	0.0007	328	37	329	8	329	4	0.00%
11CO68#04	50	90	0.56	0.06659	0.0022 1	1.25027	0.0416 7	0.13615	0.0019 4	825	46	824	19	823	11	0.12%
11CO68#05	77	855	0.09	0.05575	0.0012 1	0.54884	0.0122 9	0.07139	0.0009 3	442	28	444	8	445	6	-0.22%
11CO68#06	80	243	0.33	0.05577	0.0018 7	0.5437	0.0183 5	0.0707	0.0009 7	443	51	441	12	440	6	0.23%
11CO68#07	151	268	0.56	0.0524	0.0019 6	0.34414	0.0128 7	0.04762	0.0006 7	303	59	300	10	300	4	0.00%
11CO68#08	126	201	0.62	0.05336	0.0021 2	0.40155	0.0159 6	0.05458	0.0007 8	344	64	343	12	343	5	0.00%
11CO68#09	382	479	0.80	0.05278	0.0013 7	0.3731	0.0098 2	0.05126	0.0006 9	319	36	322	7	322	4	0.00%
11CO68#10	73	841	0.09	0.05268	0.0012 2	0.36799	0.0087 7	0.05066	0.0006 7	315	31	318	7	319	4	-0.31%
11CO68#11	213	274	0.78	0.06074	0.0016 3	0.84293	0.0229 2	0.10063	0.0013 5	630	36	621	13	618	8	0.49%
11CO68#12	257	517	0.50	0.05322	0.0013 6	0.3874	0.0100 8	0.05278	0.0007	338	35	332	7	332	4	0.00%
11CO68#13	220	246	0.89	0.05278	0.0019 2	0.37087	0.0134 9	0.05095	0.0007 2	319	57	320	10	320	4	0.00%
11CO68#14	159	307	0.52	0.06044	0.0015 8	0.82241	0.0218 8	0.09868	0.0013 1	619	35	609	12	607	8	0.33%
11CO68#15	34	224	0.15	0.05656	0.0019 5	0.56144	0.0194 9	0.07198	0.0009 8	474	53	452	13	448	6	0.89%
11CO68#16	101	153	0.66	0.0579	0.0020 2	0.69344	0.0242 8	0.08686	0.0012	526	52	535	15	537	7	-0.37%
11CO68#17	229	167	1.37	0.0579	0.0017 3	0.67652	0.0203 9	0.08473	0.0011 7	526	42	525	12	524	7	0.19%
11CO68#18	252	511	0.49	0.05295	0.0013 6	0.37755	0.0098 8	0.05171	0.0006 9	327	36	325	7	325	4	0.00%
11CO68#19	38	353	0.11	0.0561	0.0015 5	0.56728	0.0158 5	0.07333	0.0009 9	456	38	456	10	456	6	0.00%
11CO68#20	18	935	0.02	0.05246	0.0012	0.36257	0.0086	0.05012	0.0006	306	31	314	6	315	4	-0.32%

11CO68#21	248	242	1.03	0.05302	0.00201 3	0.37627	0.01443	0.05146	0.00076 3	330	61	324	11	323	4	0.31%
11CO68#22	67	76	0.88	0.07061	0.0023	1.54034	0.05034	0.15821	0.00226	946	44	947	20	947	13	0.00%
11CO68#23	203	597	0.34	0.05272	0.00147	0.36564	0.01032	0.05029	0.00067	317	40	316	8	316	4	0.00%
11CO68#24	97	576	0.17	0.05299	0.00157	0.37486	0.01124	0.0513	0.00069	328	44	323	8	322	4	0.31%
11CO68#25	404	764	0.53	0.05409	0.0014	0.37022	0.00981	0.04964	0.00066	375	36	320	7	312	4	2.56%
11CO68#26	80	489	0.16	0.05316	0.00156	0.38551	0.01148	0.05259	0.00071	336	43	331	8	330	4	0.30%
11CO68#27	113	292	0.39	0.05607	0.00171	0.56045	0.01723	0.07249	0.00099	455	44	452	11	451	6	0.22%
11CO68#28	34	325	0.11	0.05614	0.00163	0.56487	0.01659	0.07297	0.00099	458	41	455	11	454	6	0.22%
11CO68#29	34	313	0.11	0.05678	0.00154	0.59242	0.01627	0.07566	0.00102	483	37	472	10	470	6	0.43%
11CO68#30	681	822	0.83	0.06401	0.00136	1.07185	0.02355	0.12142	0.00159	742	25	740	12	739	9	0.14%
11CO68#31	72	296	0.24	0.05599	0.00177	0.55198	0.01758	0.07149	0.00098	452	46	446	12	445	6	0.22%
11CO68#32	19	1117	0.02	0.05261	0.00132	0.35797	0.00916	0.04934	0.00066	312	34	311	7	310	4	0.32%
11CO68#33	464	1473	0.32	0.05285	0.00124	0.34979	0.00843	0.048	0.00063	322	32	305	6	302	4	0.99%
11CO68#34	419	418	1.00	0.05409	0.00201	0.37391	0.01395	0.05013	0.0007	375	59	323	10	315	4	2.54%
11CO68#35	32	349	0.09	0.06068	0.00157	0.85222	0.02236	0.10184	0.00137	628	34	626	12	625	8	0.16%
11CO68#36	2	649	0.00	0.05302	0.0014	0.37959	0.01017	0.05192	0.0007	330	37	327	7	326	4	0.31%
11CO68#37	250	514	0.49	0.05303	0.00143	0.38843	0.01067	0.05312	0.00072	330	38	333	8	334	4	-0.30%
11CO68#38	126	370	0.34	0.0532	0.00164	0.40145	0.01247	0.05472	0.00075	337	46	343	9	343	5	0.00%
11CO68#39	51	325	0.16	0.05341	0.00159	0.40738	0.01225	0.05531	0.00076	346	43	347	9	347	5	0.00%
11CO68#40	56	222	0.25	0.05669	0.00185	0.59067	0.01934	0.07555	0.00106	479	48	471	12	470	6	0.21%
11CO68#41	165	327	0.51	0.06861	0.00165	1.40217	0.03443	0.1482	0.00198	887	29	890	15	891	11	-0.11%

11CO68#42	92	182	0.50	0.05318	0.00213	0.39717	0.01585	0.05416	0.00079	336	64	340	12	340	5	0.00%
11CO68#43	105	405	0.26	0.06212	0.00218	0.98711	0.03198	0.11524	0.00155	678	77	697	16	703	9	-0.85%
11CO68#44	107	205	0.52	0.05579	0.00216	0.55217	0.02145	0.07177	0.00101	444	61	446	14	447	6	-0.22%
11CO68#45	161	438	0.37	0.05334	0.00153	0.39966	0.01158	0.05434	0.00074	343	41	341	8	341	5	0.00%
11CO68#46	352	547	0.64	0.05565	0.00153	0.53057	0.0148	0.06914	0.00093	438	38	432	10	431	6	0.23%
11CO68#47	133	158	0.84	0.13703	0.00315	6.44278	0.15208	0.34094	0.00456	2190	23	2038	21	1891	22	15.81%
11CO68#48	45	488	0.09	0.10897	0.0029	3.13155	0.0727	0.20843	0.0027	1782	50	1440	18	1220	14	46.07%
11CO68#49	312	220	1.42	0.0694	0.0018	1.45049	0.03831	0.15155	0.00205	911	32	910	16	910	11	0.00%
11CO68#50	96	128	0.75	0.1284	0.00303	6.73466	0.16263	0.38034	0.00512	2076	24	2077	21	2078	24	-0.10%
11CO68#51	47	447	0.11	0.05515	0.00164	0.50361	0.01518	0.06622	0.0009	418	43	414	10	413	5	0.24%
11CO68#52	128	343	0.37	0.05305	0.00174	0.39132	0.01293	0.05349	0.00075	331	49	335	9	336	5	-0.30%
11CO68#53	64	207	0.31	0.05604	0.00194	0.56675	0.01964	0.07334	0.00104	454	52	456	13	456	6	0.00%
11CO68#54	140	275	0.51	0.05309	0.00186	0.38859	0.01363	0.05308	0.00075	333	54	333	10	333	5	0.00%
11CO68#55	232	266	0.87	0.07282	0.00187	1.70263	0.04459	0.16956	0.0023	1009	31	1010	17	1010	13	-0.10%
11CO68#56	75	53	1.41	0.05976	0.00373	0.79209	0.04909	0.09611	0.00157	595	106	592	28	592	9	0.00%
11CO68#57	359	621	0.58	0.05261	0.00149	0.36846	0.01057	0.05078	0.00069	312	41	319	8	319	4	0.00%
11CO68#58	207	259	0.80	0.07027	0.00194	1.45506	0.04082	0.15016	0.00204	936	35	912	17	902	11	1.11%
11CO68#59	117	223	0.53	0.05174	0.00258	0.30813	0.01536	0.04319	0.00063	274	87	273	12	273	4	0.00%
11CO68#60	77	235	0.33	0.05979	0.0029	0.59987	0.0278	0.07277	0.00103	596	108	477	18	453	6	5.30%
11CO68#61	154	395	0.39	0.0528	0.00169	0.37409	0.01202	0.05138	0.00072	320	48	323	9	323	4	0.00%
11CO68#62	104	502	0.21	0.05304	0.00161	0.38588	0.01183	0.05275	0.00073	331	45	331	9	331	4	0.00%
11CO68#63	186	191	0.97	0.05318	0.00213	0.39236	0.0157	0.05351	0.00079	336	64	336	11	336	5	0.00%

11CO68#64	153	430	0.35	0.05318	0.00177	0.38746	0.01295	0.05283	0.00074	336	50	333	9	332	5	0.30%
11CO68#65	65	300	0.22	0.05259	0.00239	0.36434	0.01653	0.05024	0.00072	311	77	315	12	316	4	-0.32%
11CO68#66	352	565	0.62	0.06495	0.00177	1.14193	0.03163	0.12749	0.00173	773	36	773	15	774	10	-0.13%
11CO68#67	114	188	0.61	0.05323	0.00249	0.38959	0.01817	0.05307	0.00079	339	79	334	13	333	5	0.30%
11CO68#68	47	170	0.28	0.07462	0.00216	1.83285	0.05348	0.17811	0.00248	1058	36	1057	19	1057	14	0.09%
11CO68#69	232	305	0.76	0.05306	0.00185	0.38672	0.01347	0.05285	0.00076	331	53	332	10	332	5	0.00%
11CO68#70	125	356	0.35	0.05643	0.00195	0.58137	0.02016	0.07472	0.00105	469	52	465	13	465	6	0.00%
11CO68#71	84	183	0.46	0.05554	0.00224	0.41081	0.01647	0.05363	0.0008	434	63	349	12	337	5	3.56%
11CO68#72	75	337	0.22	0.05359	0.00186	0.41382	0.01441	0.056	0.0008	354	53	352	10	351	5	0.28%
11CO68#73	482	352	1.37	0.05307	0.00211	0.37787	0.01504	0.05163	0.00073	332	64	325	11	325	4	0.00%
11CO68#74	64	141	0.45	0.06931	0.00238	1.43382	0.04939	0.15002	0.00215	908	47	903	21	901	12	0.22%
11CO68#75	212	408	0.52	0.05252	0.00183	0.35542	0.0124	0.04907	0.0007	308	53	309	9	309	4	0.00%
11CO68#76	251	359	0.70	0.05257	0.00186	0.35158	0.01243	0.04849	0.0007	310	54	306	9	305	4	0.33%
11CO68#77	165	156	1.06	0.05369	0.00282	0.40905	0.02139	0.05525	0.00085	358	90	348	15	347	5	0.29%
11CO68#78	282	262	1.08	0.05307	0.00227	0.39104	0.0167	0.05343	0.00079	332	70	335	12	336	5	-0.30%
11CO68#79	171	304	0.56	0.0533	0.00207	0.39554	0.01535	0.05381	0.00078	342	61	338	11	338	5	0.00%
11CO68#80	51	269	0.19	0.05345	0.00255	0.40522	0.01931	0.05497	0.00081	348	81	345	14	345	5	0.00%
11CO68#81	316	191	1.66	0.06086	0.0022	0.87508	0.0316	0.10427	0.00151	634	53	638	17	639	9	-0.16%
11CO68#82	529	395	1.34	0.07093	0.00212	1.56027	0.04709	0.1595	0.00221	955	39	955	19	954	12	0.10%
11CO68#83	24	193	0.13	0.05645	0.00224	0.58385	0.02314	0.07501	0.00111	470	61	467	15	466	7	0.21%
11CO68#84	145	306	0.47	0.05898	0.00205	0.72987	0.02551	0.08974	0.00128	566	51	556	15	554	8	0.36%
11CO68#85	60	103	0.58	0.12102	0.0038	5.26914	0.1690	0.31572	0.0045	1971	37	1864	27	1769	22	11.42%

					7		2		7							
11CO68#86	160	701	0.23	0.053	0.0018 3	0.37684	0.0130 5	0.05156	0.0007 3	329	53	325	10	324	4	0.31%
11CO68#87	414	476	0.87	0.05326	0.0019 4	0.40267	0.0146 7	0.05483	0.0007 9	340	56	344	11	344	5	0.00%
11CO68#88	139	373	0.37	0.05635	0.0020 1	0.57528	0.0206 1	0.07403	0.0010 6	466	54	461	13	460	6	0.22%
11CO68#89	245	480	0.51	0.05686	0.0018 9	0.62102	0.0207 1	0.0792	0.0011 3	486	48	490	13	491	7	-0.20%
11CO68#90	175	634	0.28	0.05621	0.0018 9	0.57826	0.0195 1	0.07459	0.0010 5	461	50	463	13	464	6	-0.22%
11CO68#91	46	224	0.20	0.06132	0.0022	0.89301	0.0320 2	0.1056	0.0015 3	650	52	648	17	647	9	0.15%
11CO68#92	219	408	0.54	0.05265	0.0019 4	0.36291	0.0134	0.04998	0.0007 3	314	57	314	10	314	4	0.00%
11CO68#93	140	157	0.89	0.06132	0.0024 4	0.88656	0.0351 9	0.10484	0.0015 6	650	60	645	19	643	9	0.31%
11CO68#94	215	185	1.16	0.05405	0.0029 5	0.40176	0.0218 4	0.0539	0.0008 3	373	95	343	16	338	5	1.48%
11CO68#95	42	232	0.18	0.05878	0.0024 1	0.73404	0.0301	0.09055	0.0013 4	559	63	559	18	559	8	0.00%
11CO68#96	298	305	0.98	0.05292	0.0023 7	0.38312	0.0171 2	0.0525	0.0007 9	325	74	329	13	330	5	-0.30%
11CO68#97	56	125	0.45	0.06079	0.0024 8	0.86877	0.0353 2	0.10363	0.0015 8	632	61	635	19	636	9	-0.16%
11CO68#98	184	402	0.46	0.05294	0.0020 6	0.38391	0.0149 5	0.05259	0.0007 7	326	62	330	11	330	5	0.00%
11CO68#99	41	129	0.32	0.10991	0.0035 9	4.88201	0.1603 1	0.32208	0.0046 3	1798	39	1799	28	1800	23	-0.11%
11CO68#100	66	285	0.23	0.07901	0.0026 6	2.08542	0.0703 5	0.19141	0.0027 6	1172	44	1144	23	1129	15	3.81%
11CO68#101	132	338	0.39	0.053	0.0023 3	0.3711	0.0162 5	0.05077	0.0007 7	329	72	320	12	319	5	0.31%
11CO68#102	65	176	0.37	0.0599	0.0028 7	0.80648	0.0384 7	0.09763	0.0014 9	600	77	600	22	601	9	-0.17%
11CO68#103	222	548	0.41	0.05375	0.0020 5	0.36109	0.0137 5	0.04871	0.0007 1	361	59	313	10	307	4	1.95%
11CO68#104	290	348	0.83	0.05328	0.0023 4	0.39778	0.0174 3	0.05414	0.0008 1	341	72	340	13	340	5	0.00%
11CO68#105	233	382	0.61	0.05987	0.0021 9	0.79665	0.0292 1	0.09649	0.0014	599	54	595	17	594	8	0.17%
11CO68#106	483	263	1.83	0.0592	0.0023 9	0.74675	0.0300 9	0.09146	0.0013 5	574	62	566	17	564	8	0.35%

11CO68#107	101	225	0.45	0.05331	0.00298	0.39892	0.02222	0.05426	0.00084	342	98	341	16	341	5	0.00%
11CO68#108	144	274	0.53	0.05299	0.00236	0.3737	0.01658	0.05114	0.00078	328	73	322	12	322	5	0.00%
11CO68#109	118	350	0.34	0.05328	0.00224	0.39901	0.0167	0.0543	0.00081	341	68	341	12	341	5	0.00%
11CO68#110	197	542	0.36	0.0595	0.00221	0.76161	0.02831	0.09281	0.00136	585	55	575	16	572	8	0.52%
11CO68#111	488	520	0.94	0.05368	0.00217	0.39046	0.01577	0.05274	0.00077	358	65	335	12	331	5	1.21%
11CO68#112	277	419	0.66	0.05311	0.00209	0.3863	0.01515	0.05274	0.00079	333	62	332	11	331	5	0.30%
11CO68#113	149	444	0.33	0.05323	0.0021	0.40063	0.01581	0.05458	0.00081	339	62	342	11	343	5	-0.29%
11CO68#114	39	107	0.37	0.09003	0.00335	3.07925	0.11455	0.24801	0.00371	1426	48	1428	29	1428	19	-0.14%
11CO68#115	153	248	0.62	0.05276	0.00274	0.37739	0.01949	0.05187	0.0008	318	89	325	14	326	5	-0.31%
11CO68#116	246	349	0.71	0.0532	0.00221	0.3984	0.01651	0.0543	0.00082	337	66	340	12	341	5	-0.29%
11CO68#117	51	361	0.14	0.06535	0.00248	1.01754	0.03857	0.11291	0.00167	786	55	713	19	690	10	3.33%
11CO68#118	331	376	0.88	0.05233	0.00453	0.36977	0.03144	0.05125	0.00082	300	198	319	23	322	5	-0.93%
11CO68#119	44	156	0.28	0.0636	0.0026	1.04753	0.04261	0.11943	0.00182	728	60	728	21	727	10	0.14%
11CO68#120	166	456	0.36	0.05373	0.00213	0.42589	0.01681	0.05748	0.00086	360	62	360	12	360	5	0.00%
11CO69																
11CO69#01	63	125	0.51	0.11205	0.0026	3.80459	0.0905	0.24626	0.00333	1833	24	1594	19	1419	17	29.18%
11CO69#02	261	198	1.32	0.12448	0.00231	6.10361	0.11961	0.35561	0.00456	2021	18	1991	17	1961	22	3.06%
11CO69#03	56	105	0.54	0.0689	0.0024	1.31832	0.04622	0.13876	0.00195	896	49	854	20	838	11	1.91%
11CO69#04	97	219	0.44	0.05912	0.00189	0.70917	0.02292	0.08699	0.00116	572	47	544	14	538	7	1.12%
11CO69#05	178	273	0.65	0.06003	0.00153	0.8149	0.02129	0.09844	0.00129	605	34	605	12	605	8	0.00%
11CO69#06	41	551	0.07	0.17307	0.00382	6.73468	0.12295	0.28222	0.00351	2588	38	2077	16	1603	18	61.45%
11CO69#07	54	184	0.29	0.12903	0.00244	6.48073	0.12913	0.36426	0.0047	2085	18	2043	18	2002	22	4.15%

11CO69#08	112	131	0.86	0.12788	0.00251	6.53953	0.13448	0.37085	0.00485	2069	19	2051	18	2033	23	1.77%
11CO69#09	333	302	1.10	0.05998	0.00152	0.81012	0.02094	0.09795	0.00129	603	33	603	12	602	8	0.17%
11CO69#10	212	284	0.74	0.06073	0.00161	0.84696	0.0229	0.10114	0.00133	630	36	623	13	621	8	0.32%
11CO69#11	234	621	0.38	0.06135	0.00133	0.85582	0.01918	0.10116	0.00131	652	27	628	10	621	8	1.13%
11CO69#12	82	188	0.43	0.05967	0.00218	0.79452	0.02923	0.09657	0.00134	592	56	594	17	594	8	0.00%
11CO69#13	148	328	0.45	0.05851	0.0016	0.71792	0.02006	0.08898	0.00118	549	38	549	12	550	7	-0.18%
11CO69#14	43	397	0.11	0.06786	0.00177	1.1932	0.02725	0.12753	0.00161	864	55	797	13	774	9	2.97%
11CO69#15	71	182	0.39	0.05221	0.0026	0.33309	0.01659	0.04626	0.00066	295	88	292	13	292	4	0.00%
11CO69#16	40	59	0.68	0.07006	0.00237	1.49609	0.05059	0.15486	0.00226	930	45	929	21	928	13	0.11%
11CO69#17	35	447	0.08	0.12516	0.00227	6.042	0.11631	0.35008	0.00446	2031	17	1982	17	1935	21	4.96%
11CO69#18	63	265	0.24	0.05764	0.0019	0.61478	0.02043	0.07735	0.00106	516	49	487	13	480	6	1.46%
11CO69#19	105	173	0.61	0.10927	0.0022	4.66604	0.09791	0.30968	0.00403	1787	20	1761	18	1739	20	2.76%
11CO69#20	83	201	0.41	0.05922	0.00161	0.75866	0.02094	0.0929	0.00125	575	37	573	12	573	7	0.00%
11CO69#21	215	674	0.32	0.13284	0.0024	6.73634	0.12921	0.36773	0.00467	2136	17	2077	17	2019	22	5.79%
11CO69#22	57	175	0.32	0.0578	0.00225	0.67206	0.02631	0.08432	0.00118	522	61	522	16	522	7	0.00%
11CO69#23	146	480	0.30	0.06308	0.00137	0.93963	0.0211	0.10801	0.0014	711	26	673	11	661	8	1.82%
11CO69#24	152	175	0.87	0.18041	0.00335	12.40465	0.24339	0.4986	0.00642	2657	17	2636	18	2608	28	1.88%
11CO69#25	198	304	0.65	0.10649	0.00202	4.3214	0.08634	0.29428	0.00378	1740	19	1697	16	1663	19	4.63%
11CO69#26	351	386	0.91	0.06279	0.00158	0.78167	0.02014	0.09027	0.0012	701	33	586	11	557	7	5.21%
11CO69#27	100	252	0.40	0.06167	0.0015	0.83169	0.02068	0.09779	0.0013	663	31	615	11	601	8	2.33%
11CO69#28	199	142	1.40	0.05474	0.00204	0.42363	0.01577	0.05612	0.00081	402	57	359	11	352	5	1.99%
11CO69#29	139	371	0.37	0.10672	0.0020	3.77324	0.0759	0.25639	0.0032	1744	19	1587	16	1471	17	18.56%

					4		4		9							
11CO69#30	65	123	0.53	0.20789	0.00397	16.20458	0.32548	0.56525	0.00735	2889	17	2889	19	2888	30	0.03%
11CO69#31	253	246	1.03	0.07455	0.00161	1.7813	0.04001	0.17327	0.00225	1056	25	1039	15	1030	12	2.52%
11CO69#32	66	418	0.16	0.05954	0.0015	0.70801	0.01829	0.08623	0.00114	587	33	544	11	533	7	2.06%
11CO69#33	33	133	0.25	0.07542	0.00203	1.67165	0.04574	0.16073	0.00216	1080	34	998	17	961	12	3.85%
11CO69#34	200	688	0.29	0.07587	0.00152	1.77569	0.03718	0.16972	0.00218	1092	22	1037	14	1011	12	8.01%
11CO69#35	47	126	0.38	0.05893	0.00188	0.74648	0.02399	0.09185	0.00128	565	46	566	14	566	8	0.00%
11CO69#36	51	349	0.15	0.05943	0.00161	0.73978	0.02045	0.09027	0.0012	583	37	562	12	557	7	0.90%
11CO69#37	83	85	0.97	0.10212	0.0024	4.14057	0.10012	0.29401	0.00392	1663	26	1662	20	1662	20	0.06%
11CO69#38	347	286	1.21	0.05506	0.0018	0.39552	0.01304	0.05208	0.00071	415	49	338	9	327	4	3.36%
11CO69#39	470	333	1.41	0.05299	0.00154	0.38241	0.01123	0.05233	0.00071	328	42	329	8	329	4	0.00%
11CO69#40	114	123	0.93	0.10194	0.00229	3.90368	0.09046	0.27769	0.00371	1660	24	1614	19	1580	19	5.06%
11CO69#41	492	511	0.96	0.06179	0.00144	0.85471	0.02054	0.1003	0.00132	667	30	627	11	616	8	1.79%
11CO69#42	49	317	0.15	0.06148	0.00159	0.91031	0.02406	0.10736	0.00143	656	34	657	13	657	8	0.00%
11CO69#43	120	367	0.33	0.12957	0.0026	6.59398	0.13827	0.36902	0.00477	2092	20	2059	18	2025	22	3.31%
11CO69#44	766	1103	0.69	0.06414	0.00136	0.86834	0.01913	0.09817	0.00127	746	26	635	10	604	7	5.13%
11CO69#45	78	63	1.25	0.09964	0.0025	3.91898	0.1001	0.2852	0.00392	1617	28	1618	21	1617	20	0.00%
11CO69#46	53	226	0.24	0.05817	0.00165	0.69613	0.02009	0.08677	0.00117	536	40	536	12	536	7	0.00%
11CO69#47	169	132	1.28	0.07096	0.00211	1.47818	0.04447	0.15105	0.00208	956	39	921	18	907	12	1.54%
11CO69#48	78	116	0.67	0.08753	0.00226	2.86744	0.07533	0.23755	0.00325	1372	30	1373	20	1374	17	-0.15%
11CO69#49	39	382	0.10	0.09065	0.00193	3.12557	0.06897	0.25002	0.00326	1439	23	1439	17	1439	17	0.00%
11CO69#50	112	390	0.29	0.06105	0.00153	0.87398	0.02244	0.1038	0.00138	641	33	638	12	637	8	0.16%

11CO69#51	52	152	0.34	0.11184	0.00242	5.04101	0.11291	0.32683	0.0043	1830	22	1826	19	1823	21	0.38%
11CO69#52	384	739	0.52	0.07624	0.00163	1.60213	0.03547	0.15238	0.0019 8	1101	24	971	14	914	11	6.24%
11CO69#53	126	140	0.90	0.05923	0.00202	0.75838	0.02596	0.09284	0.0013	576	50	573	15	572	8	0.17%
11CO69#54	32	178	0.18	0.05877	0.00184	0.72017	0.02275	0.08886	0.0012 2	559	45	551	13	549	7	0.36%
11CO69#55	55	75	0.74	0.0739	0.00214	1.77805	0.05196	0.17445	0.0024 4	1039	37	1037	19	1037	13	0.19%
11CO69#56	46	150	0.31	0.05562	0.00191	0.54169	0.01869	0.07062	0.0009 9	437	52	440	12	440	6	0.00%
11CO69#57	50	36	1.40	0.08601	0.00655	2.48207	0.18354	0.20929	0.0038 6	1338	152	1267	54	1225	21	9.22%
11CO69#58	87	167	0.52	0.1717	0.00499	9.7598	0.25068	0.41226	0.0056 2	2574	50	2412	24	2225	26	15.69%
11CO69#59	29	377	0.08	0.05865	0.00163	0.70747	0.01999	0.08747	0.0011 7	554	38	543	12	541	7	0.37%
11CO69#60	203	353	0.58	0.0641	0.00166	0.95317	0.0252	0.10781	0.0014 4	745	34	680	13	660	8	3.03%
11CO69#61	62	150	0.41	0.05903	0.00184	0.75196	0.02359	0.09237	0.0012 9	568	44	569	14	570	8	-0.18%
11CO69#62	54	536	0.10	0.05824	0.00147	0.6941	0.0179	0.08641	0.0011 5	539	34	535	11	534	7	0.19%
11CO69#63	45	185	0.24	0.05655	0.00187	0.59881	0.01987	0.07678	0.0010 8	474	48	476	13	477	6	-0.21%
11CO69#64	28	294	0.10	0.06276	0.00161	0.99494	0.02608	0.11496	0.0015 5	700	33	701	13	701	9	0.00%
11CO69#65	92	94	0.97	0.06266	0.0021	0.99294	0.03335	0.11489	0.0016 3	697	47	700	17	701	9	-0.14%
11CO69#66	211	147	1.44	0.05991	0.002	0.81119	0.02729	0.09817	0.0013 7	600	49	603	15	604	8	-0.17%
11CO69#67	55	113	0.48	0.07017	0.00206	1.50766	0.04459	0.15578	0.0021 8	933	38	933	18	933	12	0.00%
11CO69#68	360	447	0.80	0.129	0.00291	5.76497	0.13432	0.32405	0.0042 7	2084	23	1941	20	1809	21	15.20%
11CO69#69	80	31	2.59	0.1687	0.00446	11.21078	0.29989	0.48183	0.007	2545	26	2541	25	2535	30	0.39%
11CO69#70	80	762	0.11	0.05559	0.00156	0.53612	0.01526	0.06992	0.0009 5	436	39	436	10	436	6	0.00%
11CO69#71	35	125	0.28	0.07253	0.00228	1.68509	0.0534	0.16846	0.0023 4	1001	42	1003	20	1004	13	-0.30%
11CO69#72	126	255	0.49	0.06265	0.0021	0.74103	0.0258	0.08576	0.0012	696	50	563	15	530	7	6.23%

11CO69#73	92	206	0.45	0.05969	0.00179	0.79676	0.02417	0.09679	0.00134	592	42	595	14	596	8	-0.17%
11CO69#74	104	291	0.36	0.05953	0.00191	0.70719	0.02285	0.08613	0.00119	587	46	543	14	533	7	1.88%
11CO69#75	61	75	0.82	0.05542	0.00469	0.53305	0.0449	0.06974	0.00117	429	160	434	30	435	7	-0.23%
11CO69#76	349	298	1.17	0.06003	0.00168	0.8082	0.02294	0.09762	0.00133	605	38	601	13	600	8	0.17%
11CO69#77	69	99	0.70	0.1119	0.00284	5.09141	0.13174	0.32991	0.0045	1831	28	1835	22	1838	22	-0.38%
11CO69#78	37	164	0.22	0.08043	0.00267	2.00828	0.06068	0.18108	0.00248	1208	67	1118	20	1073	14	12.58%
11CO69#79	26	50	0.52	0.05948	0.00316	0.78367	0.04126	0.09553	0.00158	585	85	588	23	588	9	0.00%
11CO69#80	40	112	0.36	0.10989	0.0028	4.86208	0.12633	0.32081	0.00437	1798	28	1796	22	1794	21	0.22%
11CO69#81	361	389	0.93	0.05887	0.00162	0.74468	0.0208	0.09172	0.00125	562	37	565	12	566	7	-0.18%
11CO69#82	136	329	0.41	0.05888	0.00185	0.74423	0.02355	0.09164	0.00127	563	45	565	14	565	7	0.00%
11CO69#83	66	174	0.38	0.12319	0.00314	5.82592	0.15162	0.3429	0.00467	2003	27	1950	23	1901	22	5.37%
11CO69#84	98	186	0.53	0.09284	0.00241	3.31265	0.08781	0.25873	0.00351	1485	30	1484	21	1483	18	0.13%
11CO69#85	208	317	0.65	0.27898	0.00859	21.63107	0.59038	0.56234	0.00801	3357	49	3167	26	2876	33	16.72%
11CO69#86	133	410	0.32	0.0529	0.0019	0.38134	0.01381	0.05227	0.00073	325	57	328	10	328	4	0.00%
11CO69#87	174	514	0.34	0.0642	0.0018	0.73537	0.02095	0.08305	0.00114	748	37	560	12	514	7	8.95%
11CO69#88	131	121	1.08	0.12274	0.0033	5.44677	0.14873	0.32177	0.00444	1996	29	1892	23	1798	22	11.01%
11CO69#89	39	51	0.75	0.07631	0.0037	1.81735	0.08773	0.17268	0.00271	1103	71	1052	32	1027	15	7.40%
11CO69#90	185	192	0.97	0.0592	0.00199	0.75784	0.02557	0.09281	0.00131	574	49	573	15	572	8	0.17%
11CO69#91	165	266	0.62	0.06121	0.00181	0.88863	0.0265	0.10527	0.00146	647	40	646	14	645	9	0.16%
11CO69#92	485	445	1.09	0.05939	0.0017	0.77009	0.02239	0.09402	0.00129	581	39	580	13	579	8	0.17%
11CO69#93	46	131	0.35	0.06081	0.00216	0.86147	0.03068	0.10272	0.00149	633	52	631	17	630	9	0.16%

11CO69#94	48	40	1.21	0.07174	0.00403	1.61327	0.09031	0.16305	0.00258	979	88	975	35	974	14	0.10%
11CO69#95	64	554	0.12	0.06085	0.00181	0.70095	0.02107	0.08352	0.00115	634	41	539	13	517	7	4.26%
11CO69#96	16	337	0.05	0.05271	0.00261	0.37155	0.0183	0.05111	0.00079	316	84	321	14	321	5	0.00%
11CO69#97	28	68	0.42	0.08099	0.00264	2.33972	0.07665	0.20947	0.00302	1221	42	1224	23	1226	16	-0.41%
11CO69#98	46	93	0.49	0.18577	0.00509	12.53963	0.34902	0.48942	0.00687	2705	28	2646	26	2568	30	5.33%
11CO69#99	260	395	0.66	0.05229	0.00176	0.34293	0.01162	0.04755	0.00068	298	51	299	9	299	4	0.00%
11CO69#100	55	353	0.16	0.05701	0.00184	0.60803	0.01979	0.07733	0.00108	492	47	482	12	480	6	0.42%
11CO69#101	163	399	0.41	0.06192	0.00213	0.76527	0.02649	0.08961	0.00126	671	50	577	15	553	7	4.34%
11CO69#102	48	309	0.16	0.05927	0.00203	0.74767	0.02574	0.09146	0.0013	577	50	567	15	564	8	0.53%
11CO69#103	50	46	1.09	0.07554	0.01418	0.78013	0.14486	0.0749	0.00209	1083	412	586	83	466	13	25.75%
11CO69#104	51	163	0.31	0.16773	0.00461	11.15641	0.31201	0.48227	0.00667	2535	29	2536	26	2537	29	-0.08%
11CO69#105	65	57	1.14	0.05822	0.00489	0.70987	0.05936	0.0884	0.00148	538	155	545	35	546	9	-0.18%
11CO69#106	82	128	0.64	0.23888	0.00706	3.99403	0.11845	0.12123	0.00177	3113	29	1633	24	738	10	121.27%
11CO69#107	179	246	0.73	0.08787	0.00455	2.35069	0.11633	0.19402	0.00293	1380	102	1228	35	1143	16	20.73%
11CO69#108	117	206	0.57	0.0751	0.00228	1.86931	0.05733	0.18047	0.00254	1071	39	1070	20	1070	14	0.09%
11CO69#109	34	72	0.47	0.06442	0.00538	0.89212	0.07277	0.10044	0.0018	756	182	648	39	617	11	5.02%
11CO69#110	132	284	0.47	0.06996	0.00216	1.47098	0.04583	0.15246	0.00214	927	41	919	19	915	12	0.44%
11CO69#111	74	234	0.32	0.06643	0.00211	1.24285	0.03973	0.13566	0.00192	820	43	820	18	820	11	0.00%
11CO69#112	133	336	0.40	0.0521	0.00207	0.33503	0.0133	0.04663	0.00068	290	64	293	10	294	4	-0.34%
11CO69#113	223	409	0.55	0.05307	0.0018	0.39146	0.01332	0.05348	0.00077	332	51	335	10	336	5	-0.30%
11CO69#114	58	96	0.60	0.07181	0.00256	1.63176	0.05834	0.16477	0.00243	981	49	983	23	983	13	0.00%
11CO69#115	127	203	0.62	0.05856	0.0020	0.724	0.0254	0.08964	0.0013	551	51	553	15	553	8	0.00%

					5		8									
11CO69#116	49	53	0.93	0.09784	0.00322	3.74883	0.12405	0.27781	0.00409	1583	40	1582	27	1580	21	0.19%
11CO69#117	68	222	0.31	0.05846	0.00198	0.7104	0.02418	0.0881	0.00127	547	49	545	14	544	8	0.18%
11CO69#118	201	378	0.53	0.06242	0.00218	0.65748	0.02309	0.07637	0.0011	689	50	513	14	474	7	8.23%
11CO69#119	27	77	0.35	0.07953	0.0027	2.28144	0.0779	0.20799	0.00304	1185	44	1207	24	1218	16	-2.71%
11CO69#120	48	88	0.54	0.05811	0.00262	0.69848	0.03137	0.08715	0.00136	534	71	538	19	539	8	-0.19%
11CO52																
11CO52#01	206	592	0.35	0.0516	0.0013	0.3017	0.00772	0.0424	0.00056	268	35	268	6	268	3	0.00%
11CO52#02	78	292	0.27	0.05182	0.00181	0.31579	0.01104	0.04419	0.00061	277	55	279	9	279	4	0.00%
11CO52#03	183	913	0.20	0.05156	0.00127	0.29732	0.00749	0.04181	0.00054	266	34	264	6	264	3	0.00%
11CO52#04	178	549	0.32	0.05174	0.00165	0.31079	0.00998	0.04356	0.00058	274	49	275	8	275	4	0.00%
11CO52#05	161	315	0.51	0.05166	0.00181	0.30748	0.0108	0.04316	0.0006	270	55	272	8	272	4	0.00%
11CO52#06	242	665	0.36	0.0515	0.00129	0.30486	0.0078	0.04292	0.00056	263	35	270	6	271	3	-0.37%
11CO52#07	65	142	0.46	0.07137	0.002	1.59446	0.04531	0.162	0.00218	968	36	968	18	968	12	0.00%
11CO52#08	202	582	0.35	0.05144	0.00135	0.29947	0.00796	0.04221	0.00056	261	37	266	6	267	3	-0.37%
11CO52#09	96	308	0.31	0.05174	0.0017	0.31115	0.01022	0.04361	0.0006	274	50	275	8	275	4	0.00%
11CO52#10	209	706	0.30	0.05181	0.00124	0.3171	0.00778	0.04438	0.00058	277	33	280	6	280	4	0.00%
11CO52#11	214	295	0.73	0.05166	0.00176	0.30952	0.01053	0.04344	0.00061	270	52	274	8	274	4	0.00%
11CO52#12	106	230	0.46	0.05188	0.00283	0.31665	0.01723	0.04426	0.00063	280	99	279	13	279	4	0.00%
11CO52#13	138	406	0.34	0.05189	0.00164	0.31349	0.00998	0.0438	0.00059	281	48	277	8	276	4	0.36%
11CO52#14	134	279	0.48	0.04943	0.00177	0.29741	0.0107	0.04363	0.0006	168	58	264	8	275	4	-4.00%
11CO52#15	125	198	0.63	0.05197	0.00198	0.3269	0.01243	0.04561	0.00065	284	61	287	10	288	4	-0.35%
11CO52#16	116	333	0.35	0.052	0.0017	0.32088	0.0106	0.04474	0.0006	285	51	283	8	282	4	0.35%

					2		7		1							
11CO52#17	103	397	0.26	0.05184	0.00225	0.29823	0.01291	0.04172	0.0006	278	73	265	10	263	4	0.76%
11CO52#18	100	545	0.18	0.05178	0.00172	0.30605	0.01021	0.04286	0.00058	276	52	271	8	271	4	0.00%
11CO52#19	213	348	0.61	0.05193	0.0018	0.32525	0.01135	0.04541	0.00062	282	55	286	9	286	4	0.00%
11CO52#20	168	515	0.33	0.05195	0.00171	0.31581	0.01045	0.04408	0.0006	283	51	279	8	278	4	0.36%
11CO52#21	162	371	0.44	0.05282	0.00169	0.37148	0.01194	0.051	0.0007	321	48	321	9	321	4	0.00%
11CO52#22	97	198	0.49	0.05175	0.00303	0.30455	0.01777	0.04267	0.00064	274	107	270	14	269	4	0.37%
11CO52#23	111	346	0.32	0.05138	0.00238	0.28752	0.01326	0.04058	0.00059	258	79	257	10	256	4	0.39%
11CO52#24	120	267	0.45	0.05199	0.00235	0.32908	0.01484	0.0459	0.00066	285	77	289	11	289	4	0.00%
11CO52#25	166	406	0.41	0.05204	0.00155	0.33027	0.00989	0.04602	0.00062	287	44	290	8	290	4	0.00%
11CO52#26	585	1008	0.58	0.05175	0.0012	0.31202	0.00742	0.04372	0.00057	274	31	276	6	276	4	0.00%
11CO52#27	139	455	0.31	0.0517	0.00152	0.30652	0.0091	0.04299	0.00057	272	44	271	7	271	4	0.00%
11CO52#28	472	472	1.00	0.05302	0.00144	0.38718	0.01065	0.05295	0.0007	330	39	332	8	333	4	-0.30%
11CO52#29	192	483	0.40	0.05457	0.00174	0.32437	0.01043	0.0431	0.00058	395	48	285	8	272	4	4.78%
11CO52#30	119	377	0.31	0.0522	0.00149	0.33289	0.00961	0.04624	0.00062	294	42	292	7	291	4	0.34%
11CO52#31	180	449	0.40	0.05199	0.00192	0.30013	0.01112	0.04186	0.00058	285	59	267	9	264	4	1.14%
11CO52#32	130	675	0.19	0.05264	0.0015	0.32226	0.0093	0.04439	0.00059	313	42	284	7	280	4	1.43%
11CO52#33	224	331	0.68	0.05205	0.00156	0.33344	0.01007	0.04645	0.00063	288	44	292	8	293	4	-0.34%
11CO52#34	66	335	0.20	0.05238	0.00159	0.33981	0.01039	0.04704	0.00063	302	45	297	8	296	4	0.34%
11CO52#35	236	593	0.40	0.05213	0.0015	0.32542	0.00947	0.04527	0.00059	291	43	286	7	285	4	0.35%
11CO52#36	305	755	0.40	0.0519	0.00122	0.3182	0.00767	0.04445	0.00058	281	32	281	6	280	4	0.36%
11CO52#37	91	276	0.33	0.0518	0.00168	0.32733	0.01066	0.04582	0.00062	277	50	288	8	289	4	-0.35%

11CO52#38	103	262	0.39	0.05181	0.00181	0.31623	0.01107	0.04426	0.00061	277	55	279	9	279	4	0.00%
11CO52#39	179	396	0.45	0.05288	0.00169	0.33457	0.01081	0.04588	0.00062	324	49	293	8	289	4	1.38%
11CO52#40	132	342	0.39	0.06284	0.0042	0.36943	0.02378	0.04264	0.00076	703	146	319	18	269	5	18.59%
11CO52#41	202	633	0.32	0.05259	0.00144	0.32369	0.00899	0.04463	0.00059	311	39	285	7	281	4	1.42%
11CO52#42	257	401	0.64	0.05174	0.00194	0.31132	0.01174	0.04363	0.00059	274	61	275	9	275	4	0.00%
11CO52#43	261	503	0.52	0.05305	0.00163	0.37154	0.01149	0.05079	0.00068	331	46	321	9	319	4	0.63%
11CO52#44	40	68	0.59	0.05217	0.00415	0.33584	0.02653	0.04668	0.00079	293	149	294	20	294	5	0.00%
11CO52#45	59	406	0.15	0.05165	0.00157	0.30924	0.00949	0.04341	0.00059	270	45	274	7	274	4	0.00%
11CO52#46	338	553	0.61	0.0519	0.00157	0.31554	0.00968	0.04408	0.00059	281	46	278	7	278	4	0.00%
11CO52#47	162	666	0.24	0.05214	0.00164	0.31143	0.00986	0.04331	0.00059	292	47	275	8	273	4	0.73%
11CO52#48	216	422	0.51	0.05187	0.00144	0.32014	0.00901	0.04476	0.0006	280	40	282	7	282	4	0.00%
11CO52#49	214	538	0.40	0.05949	0.00139	0.71886	0.01726	0.08762	0.00114	585	30	550	10	541	7	1.66%
11CO52#50	104	114	0.91	0.05142	0.00402	0.30819	0.02402	0.04346	0.00067	260	149	273	19	274	4	-0.36%
11CO52#51	23	170	0.13	0.05545	0.0024	0.53476	0.02322	0.06993	0.00098	430	72	435	15	436	6	-0.23%
11CO52#52	179	827	0.22	0.05258	0.00131	0.35888	0.00914	0.04949	0.00065	311	34	311	7	311	4	0.00%
11CO52#53	87	389	0.22	0.05296	0.00159	0.38672	0.01173	0.05295	0.00071	327	45	332	9	333	4	-0.30%
11CO52#54	409	806	0.51	0.05279	0.00123	0.37163	0.00891	0.05105	0.00067	320	31	321	7	321	4	0.00%
11CO52#55	171	468	0.37	0.05189	0.00161	0.32232	0.01009	0.04504	0.0006	281	47	284	8	284	4	0.00%
11CO52#56	249	487	0.51	0.05189	0.00158	0.31977	0.00985	0.04468	0.0006	281	46	282	8	282	4	0.00%
11CO52#57	107	78	1.38	0.05303	0.00336	0.38859	0.02444	0.05313	0.00086	330	114	333	18	334	5	-0.30%
11CO52#58	168	168	1.00	0.05297	0.00243	0.37812	0.0173	0.05176	0.00074	328	78	326	13	325	5	0.31%
11CO52#59	94	377	0.25	0.0518	0.0022	0.31501	0.0134	0.04409	0.0006	277	72	278	10	278	4	0.00%

							2		2							
11CO52#60	257	829	0.31	0.05205	0.00138	0.32484	0.00876	0.04526	0.0006	288	38	286	7	285	4	0.35%
11CO52#61	276	570	0.49	0.05186	0.0015	0.31466	0.00922	0.044	0.00059	279	43	278	7	278	4	0.00%
11CO52#62	203	1056	0.19	0.05306	0.0014	0.32231	0.00866	0.04405	0.00059	331	37	284	7	278	4	2.16%
11CO52#63	258	331	0.78	0.05183	0.00177	0.31871	0.01095	0.04458	0.00062	278	53	281	8	281	4	0.00%
11CO52#64	113	372	0.30	0.05204	0.00164	0.32579	0.01033	0.04539	0.00063	287	47	286	8	286	4	0.00%
11CO52#65	101	389	0.26	0.05231	0.00166	0.34095	0.01088	0.04726	0.00064	299	48	298	8	298	4	0.00%
11CO52#66	60	306	0.20	0.05197	0.00172	0.31967	0.01063	0.0446	0.00062	284	51	282	8	281	4	0.36%
11CO52#67	198	979	0.20	0.05218	0.00129	0.33292	0.00842	0.04626	0.00061	293	34	292	6	292	4	0.00%
11CO52#68	169	244	0.69	0.05194	0.00222	0.3204	0.0137	0.04473	0.00064	283	71	282	11	282	4	0.00%
11CO52#69	113	357	0.32	0.05185	0.00157	0.31733	0.00966	0.04438	0.00061	279	45	280	7	280	4	0.00%
11CO52#70	141	386	0.37	0.05204	0.00158	0.3293	0.01007	0.04588	0.00062	287	45	289	8	289	4	0.00%
11CO52#71	36	278	0.13	0.05195	0.00184	0.32238	0.01145	0.04499	0.00063	283	56	284	9	284	4	0.00%
11CO52#72	99	102	0.98	0.05917	0.00238	0.82466	0.03318	0.10106	0.00143	573	63	611	18	621	8	-1.61%
11CO52#73	295	764	0.39	0.05189	0.00135	0.3174	0.00838	0.04435	0.00059	281	36	280	6	280	4	0.00%
11CO52#74	116	192	0.61	0.05292	0.00191	0.37777	0.01364	0.05176	0.00074	325	56	325	10	325	5	0.00%
11CO52#75	143	427	0.34	0.05216	0.00155	0.33633	0.01005	0.04675	0.00064	292	43	294	8	295	4	-0.34%
11CO52#76	92	185	0.50	0.05187	0.00216	0.3189	0.01328	0.04458	0.00065	280	68	281	10	281	4	0.00%
11CO52#77	242	430	0.56	0.05319	0.00151	0.39296	0.01129	0.05357	0.00073	337	41	337	8	336	4	0.30%
11CO52#78	215	544	0.40	0.05246	0.00149	0.34837	0.01	0.04815	0.00065	306	41	303	8	303	4	0.00%
11CO52#79	46	152	0.31	0.061	0.00188	0.87817	0.02726	0.10439	0.00145	639	43	640	15	640	8	0.00%
11CO52#80	245	308	0.80	0.05192	0.00176	0.32247	0.01097	0.04504	0.00063	282	52	284	8	284	4	0.00%

11CO52#81	152	331	0.46	0.05194	0.00172	0.32326	0.01075	0.04513	0.00063	283	50	284	8	285	4	-0.35%
11CO52#82	72	154	0.47	0.05223	0.00213	0.34242	0.0139	0.04754	0.0007	295	66	299	11	299	4	0.00%
11CO52#83	244	356	0.69	0.05216	0.00168	0.33349	0.01083	0.04636	0.00064	292	49	292	8	292	4	0.00%
11CO52#84	174	541	0.32	0.05208	0.00152	0.32715	0.00961	0.04554	0.00062	289	42	287	7	287	4	0.00%
11CO52#85	96	219	0.44	0.05221	0.00219	0.33662	0.01408	0.04675	0.00067	295	69	295	11	295	4	0.00%
11CO52#86	232	590	0.39	0.05183	0.00155	0.31019	0.00939	0.0434	0.00059	278	44	274	7	274	4	0.00%
11CO52#87	102	213	0.48	0.05325	0.00214	0.39505	0.01589	0.05379	0.00077	339	65	338	12	338	5	0.00%
11CO52#88	225	396	0.57	0.05212	0.0018	0.33355	0.01155	0.04641	0.00064	291	54	292	9	292	4	0.00%
11CO52#89	132	306	0.43	0.05206	0.0019	0.32251	0.01178	0.04492	0.00063	288	58	284	9	283	4	0.35%
11CO52#90	106	447	0.24	0.05376	0.00178	0.39817	0.01332	0.0537	0.00073	361	51	340	10	337	4	0.89%
11CO52#91	171	507	0.34	0.0517	0.00162	0.30775	0.00973	0.04316	0.0006	272	47	272	8	272	4	0.00%
11CO52#92	53	273	0.19	0.0521	0.00199	0.32744	0.01246	0.04557	0.00066	290	60	288	10	287	4	0.35%
11CO52#93	207	394	0.53	0.05179	0.00184	0.31345	0.01118	0.04388	0.00062	276	56	277	9	277	4	0.00%
11CO52#94	171	241	0.71	0.05201	0.00212	0.32811	0.0133	0.04574	0.00068	286	65	288	10	288	4	0.00%
11CO52#95	211	395	0.53	0.05214	0.00174	0.33669	0.01127	0.04682	0.00066	292	51	295	9	295	4	0.00%
11CO52#96	71	424	0.17	0.0518	0.00187	0.31967	0.01157	0.04475	0.00063	277	57	282	9	282	4	0.00%
11CO52#97	254	283	0.90	0.05203	0.00201	0.32128	0.01238	0.04477	0.00064	287	62	283	10	282	4	0.35%
11CO52#98	169	263	0.64	0.052	0.0023	0.32631	0.0144	0.0455	0.00067	285	74	287	11	287	4	0.00%
11CO52#99	145	240	0.60	0.052	0.0022	0.3238	0.01368	0.04515	0.00067	285	69	285	10	285	4	0.00%
11CO52#100	69	423	0.16	0.0519	0.00172	0.32319	0.01075	0.04515	0.00063	281	51	284	8	285	4	-0.35%
11CO52#101	96	332	0.29	0.05202	0.00188	0.32325	0.01172	0.04505	0.00064	286	57	284	9	284	4	0.00%
11CO52#102	107	374	0.29	0.05202	0.0022	0.31884	0.0137	0.04444	0.0006	286	72	281	11	280	4	0.36%

					4		6		4							
11CO52#103	102	346	0.30	0.05235	0.00196	0.34386	0.0129	0.04762	0.00068	301	59	300	10	300	4	0.00%
11CO52#104	141	448	0.32	0.05211	0.00188	0.33052	0.01197	0.04599	0.00065	290	57	290	9	290	4	0.00%
11CO52#105	58	244	0.24	0.05193	0.0024	0.32264	0.01489	0.04505	0.00067	282	78	284	11	284	4	0.00%
11CO52#106	68	486	0.14	0.0529	0.0018	0.37513	0.01281	0.05142	0.00072	325	52	323	9	323	4	0.00%
11CO52#107	302	505	0.60	0.05292	0.00187	0.37405	0.0133	0.05125	0.00071	325	55	323	10	322	4	0.31%
11CO52#108	396	541	0.73	0.05171	0.00182	0.31075	0.011	0.04358	0.00061	273	55	275	9	275	4	0.00%
11CO52#109	273	380	0.72	0.05334	0.00202	0.40002	0.01519	0.05437	0.00077	343	60	342	11	341	5	0.29%
11CO52#110	169	269	0.63	0.05218	0.00228	0.32894	0.01438	0.04571	0.00067	293	73	289	11	288	4	0.35%
11CO52#111	125	457	0.27	0.05177	0.00201	0.30945	0.01205	0.04334	0.00062	275	63	274	9	274	4	0.00%
11CO52#112	107	145	0.74	0.05311	0.00362	0.39357	0.02672	0.05373	0.00086	333	126	337	19	337	5	0.00%
11CO52#113	259	516	0.50	0.05229	0.00191	0.34017	0.01245	0.04717	0.00067	298	57	297	9	297	4	0.00%
11CO52#114	52	90	0.58	0.05208	0.00358	0.32521	0.02214	0.04528	0.00078	289	124	286	17	285	5	0.35%
11CO52#115	72	323	0.22	0.05214	0.00207	0.33192	0.01317	0.04616	0.00068	292	64	291	10	291	4	0.00%
11CO52#116	156	502	0.31	0.05174	0.00192	0.31552	0.01173	0.04422	0.00063	274	59	278	9	279	4	-0.36%
11CO52#117	381	691	0.55	0.05219	0.00179	0.33341	0.0115	0.04632	0.00065	294	53	292	9	292	4	0.00%
11CO52#118	176	461	0.38	0.05224	0.00194	0.3425	0.01272	0.04754	0.00068	296	59	299	10	299	4	0.00%
11CO52#119	149	190	0.79	0.05309	0.00251	0.39104	0.01838	0.05341	0.00081	333	79	335	13	335	5	0.00%
11CO52#120	24	40	0.62	0.05135	0.01616	0.30129	0.0945	0.04255	0.00125	257	512	267	74	269	8	-0.74%
11CO55A																
11CO55A#01	278	285	0.98	0.05278	0.00162	0.37063	0.01147	0.05093	0.00068	319	46	320	8	320	4	0.00%
11CO55A#02	205	269	0.76	0.05298	0.00171	0.3823	0.01245	0.05233	0.00071	328	49	329	9	329	4	0.00%
11CO55A#03	61	147	0.41	0.05301	0.0027	0.39703	0.0207	0.05431	0.0007	329	93	339	15	341	5	-0.59%

					7		7		7							
11CO55A#04	275	365	0.75	0.05418	0.0017 1	0.3781	0.0120 3	0.0506	0.0006 8	379	47	326	9	318	4	2.52%
11CO55A#05	119	235	0.51	0.05282	0.0015 9	0.37711	0.0114 5	0.05177	0.0007 1	321	44	325	8	325	4	0.00%
11CO55A#06	135	571	0.24	0.05326	0.0013 4	0.38563	0.0098 9	0.05251	0.0006 8	340	35	331	7	330	4	0.30%
11CO55A#07	79	295	0.27	0.05246	0.0016 8	0.35348	0.0113 5	0.04886	0.0006 7	306	48	307	9	308	4	-0.32%
11CO55A#08	87	392	0.22	0.05316	0.0014	0.39481	0.0105 6	0.05386	0.0007 1	336	37	338	8	338	4	0.00%
11CO55A#09	118	302	0.39	0.05527	0.0014 7	0.49966	0.0134 9	0.06556	0.0008 7	423	37	411	9	409	5	0.49%
11CO55A#10	279	384	0.73	0.05264	0.0018 7	0.36413	0.0129 5	0.05016	0.0006 9	313	56	315	10	316	4	-0.32%
11CO55A#11	93	177	0.53	0.05327	0.0018 8	0.39495	0.0139 5	0.05377	0.0007 6	340	54	338	10	338	5	0.00%
11CO55A#12	306	743	0.41	0.05233	0.0011 9	0.37299	0.0087 5	0.05169	0.0006 7	300	31	322	6	325	4	-0.92%
11CO55A#13	198	489	0.40	0.05334	0.0012 7	0.40253	0.0098 1	0.05472	0.0007 2	343	32	343	7	343	4	0.00%
11CO55A#14	327	302	1.08	0.05238	0.0024 7	0.35088	0.0163 5	0.04858	0.0007 7	302	77	305	12	306	5	-0.33%
11CO55A#15	183	611	0.30	0.05262	0.0015 4	0.35635	0.0105 3	0.0491	0.0006 6	312	43	309	8	309	4	0.00%
11CO55A#16	96	327	0.29	0.05192	0.0015 6	0.32266	0.0098 1	0.04506	0.0006 1	282	45	284	8	284	4	0.00%
11CO55A#17	297	661	0.45	0.05517	0.0015 9	0.35152	0.0102 5	0.04621	0.0006 2	419	41	306	8	291	4	5.15%
11CO55A#18	158	279	0.57	0.05265	0.0017 3	0.36383	0.0120 3	0.05011	0.0006 8	314	50	315	9	315	4	0.00%
11CO55A#19	181	523	0.35	0.05144	0.0015 1	0.30492	0.0091	0.04298	0.0005 7	261	44	270	7	271	4	-0.37%
11CO55A#20	120	348	0.34	0.05256	0.0017	0.35474	0.0115 5	0.04894	0.0006 6	310	50	308	9	308	4	0.00%
11CO55A#21	206	1187	0.17	0.05229	0.0011 6	0.34555	0.0078 9	0.04792	0.0006 2	298	29	301	6	302	4	-0.33%
11CO55A#22	188	207	0.91	0.05238	0.0050 4	0.35122	0.0331 4	0.04862	0.0011 7	302	16 9	306	25	306	7	0.00%
11CO55A#23	125	661	0.19	0.05387	0.0017 9	0.36269	0.0120 8	0.04882	0.0006 7	366	50	314	9	307	4	2.28%
11CO55A#24	124	368	0.34	0.0526	0.0013 8	0.37177	0.0098 9	0.05125	0.0006 8	312	37	321	7	322	4	-0.31%

11CO55A#25	130	286	0.45	0.05335	0.00163	0.40464	0.0125	0.055	0.00074	344	46	345	9	345	5	0.00%
11CO55A#26	75	795	0.09	0.05338	0.00117	0.38471	0.00873	0.05226	0.00067	345	29	330	6	328	4	0.61%
11CO55A#27	439	801	0.55	0.05301	0.00113	0.38087	0.00839	0.0521	0.00067	329	28	328	6	327	4	0.31%
11CO55A#28	194	307	0.63	0.05313	0.00182	0.38698	0.01336	0.05282	0.00071	334	54	332	10	332	4	0.00%
11CO55A#29	317	245	1.30	0.0529	0.00179	0.37347	0.01267	0.0512	0.00072	325	51	322	9	322	4	0.00%
11CO55A#30	75	942	0.08	0.05259	0.00112	0.35778	0.0079	0.04933	0.00064	311	28	311	6	310	4	0.32%
11CO55A#31	107	666	0.16	0.05277	0.00121	0.37401	0.0088	0.0514	0.00067	319	30	323	7	323	4	0.00%
11CO55A#32	55	65	0.85	0.19423	0.00352	13.49383	0.25616	0.50378	0.00664	2778	15	2715	18	2630	28	5.63%
11CO55A#33	301	300	1.00	0.05296	0.00158	0.38049	0.01146	0.0521	0.0007	327	44	327	8	327	4	0.00%
11CO55A#34	70	214	0.33	0.05306	0.00183	0.38308	0.01325	0.05236	0.00072	331	53	329	10	329	4	0.00%
11CO55A#35	459	374	1.23	0.053	0.00137	0.37812	0.00994	0.05174	0.00069	329	36	326	7	325	4	0.31%
11CO55A#36	234	537	0.44	0.05282	0.00127	0.3857	0.00948	0.05296	0.00069	321	33	331	7	333	4	-0.60%
11CO55A#37	428	796	0.54	0.05269	0.002	0.36811	0.01395	0.05066	0.00071	315	61	318	10	319	4	-0.31%
11CO55A#38	177	892	0.20	0.05306	0.00113	0.38594	0.00852	0.05274	0.00068	331	28	331	6	331	4	0.00%
11CO55A#39	102	571	0.18	0.05322	0.00131	0.39844	0.01001	0.05429	0.00071	338	34	341	7	341	4	0.00%
11CO55A#40	117	211	0.55	0.05313	0.0017	0.39367	0.01261	0.05373	0.00074	334	48	337	9	337	5	0.00%
11CO55A#41	407	1197	0.34	0.05365	0.00111	0.37422	0.00804	0.05058	0.00065	356	26	323	6	318	4	1.57%
11CO55A#42	99	410	0.24	0.05313	0.00143	0.3824	0.01046	0.05219	0.00069	334	38	329	8	328	4	0.30%
11CO55A#43	262	531	0.49	0.05281	0.00141	0.37695	0.01027	0.05176	0.00068	321	38	325	8	325	4	0.00%
11CO55A#44	159	318	0.50	0.05314	0.00175	0.39056	0.01299	0.0533	0.00071	335	51	335	9	335	4	0.00%
11CO55A#45	99	303	0.33	0.05313	0.00145	0.3957	0.01095	0.054	0.00073	334	38	339	8	339	4	0.00%
11CO55A#46	249	262	0.95	0.05271	0.0020	0.373	0.0145	0.05131	0.0007	316	64	322	11	323	4	-0.31%

					5		5									
11CO55A#47	103	267	0.38	0.05227	0.00149	0.38392	0.01106	0.05326	0.00072	297	41	330	8	335	4	-1.49%
11CO55A#48	111	223	0.50	0.05266	0.00166	0.3785	0.01203	0.05212	0.00071	314	47	326	9	328	4	-0.61%
11CO55A#49	281	556	0.51	0.05315	0.00128	0.37369	0.00923	0.05099	0.00067	335	33	322	7	321	4	0.31%
11CO55A#50	129	277	0.46	0.05311	0.00148	0.38707	0.01093	0.05285	0.00071	333	40	332	8	332	4	0.00%
11CO55A#51	894	1004	0.89	0.05317	0.00123	0.34464	0.00818	0.047	0.00061	336	31	301	6	296	4	1.69%
11CO55A#52	651	367	1.78	0.05291	0.00153	0.36921	0.01079	0.0506	0.00068	325	42	319	8	318	4	0.31%
11CO55A#53	37	88	0.42	0.05435	0.00451	0.3952	0.03269	0.05272	0.00084	386	159	338	24	331	5	2.11%
11CO55A#54	346	395	0.88	0.05276	0.00157	0.3729	0.01126	0.05125	0.00068	318	45	322	8	322	4	0.00%
11CO55A#55	100	164	0.61	0.05319	0.00188	0.39522	0.01398	0.05388	0.00075	337	55	338	10	338	5	0.00%
11CO55A#56	179	325	0.55	0.0531	0.0015	0.3883	0.01113	0.05303	0.00071	333	41	333	8	333	4	0.00%
11CO55A#57	604	393	1.54	0.05287	0.00147	0.37852	0.01064	0.05192	0.00069	323	40	326	8	326	4	0.00%
11CO55A#58	518	531	0.98	0.05305	0.00125	0.38528	0.00927	0.05267	0.00069	331	31	331	7	331	4	0.00%
11CO55A#59	247	547	0.45	0.05292	0.00125	0.3886	0.00942	0.05325	0.0007	325	32	333	7	334	4	-0.30%
11CO55A#60	437	440	0.99	0.05287	0.00134	0.37783	0.00972	0.05182	0.00069	323	35	325	7	326	4	-0.31%
11CO55A#61	60	147	0.41	0.18552	0.00349	11.28663	0.22182	0.44115	0.00571	2703	17	2547	18	2356	26	14.73%
11CO55A#62	154	187	0.82	0.05311	0.00211	0.38965	0.01548	0.0532	0.00074	333	65	334	11	334	5	0.00%
11CO55A#63	80	383	0.21	0.05311	0.00148	0.38588	0.01087	0.05269	0.0007	333	40	331	8	331	4	0.00%
11CO55A#64	166	196	0.85	0.05199	0.00209	0.32057	0.01286	0.04471	0.00064	285	65	282	10	282	4	0.00%
11CO55A#65	334	521	0.64	0.05321	0.00139	0.3951	0.01047	0.05385	0.00071	338	36	338	8	338	4	0.00%
11CO55A#66	199	516	0.38	0.05295	0.0014	0.37887	0.01017	0.05189	0.00069	327	37	326	7	326	4	0.00%
11CO55A#67	192	251	0.77	0.05304	0.00164	0.39245	0.01224	0.05365	0.00073	331	46	336	9	337	4	-0.30%

11CO55A#68	161	393	0.41	0.05286	0.00143	0.37485	0.01026	0.05142	0.00069	323	38	323	8	323	4	0.00%
11CO55A#69	541	438	1.24	0.0531	0.00177	0.38808	0.01299	0.05299	0.00073	333	51	333	10	333	4	0.00%
11CO55A#70	153	323	0.47	0.05319	0.00157	0.38683	0.01152	0.05273	0.00071	337	43	332	8	331	4	0.30%
11CO55A#71	244	223	1.10	0.05313	0.00208	0.38675	0.01519	0.05279	0.00074	334	63	332	11	332	5	0.00%
11CO55A#72	138	214	0.64	0.05127	0.00286	0.29037	0.01616	0.04106	0.00061	253	101	259	13	259	4	0.00%
11CO55A#73	341	645	0.53	0.05167	0.00129	0.32617	0.00829	0.04578	0.0006	271	35	287	6	289	4	-0.69%
11CO55A#74	146	316	0.46	0.05276	0.00161	0.37649	0.01156	0.05175	0.0007	318	45	324	9	325	4	-0.31%
11CO55A#75	194	126	1.54	0.05316	0.00242	0.38722	0.01759	0.05281	0.00077	336	76	332	13	332	5	0.00%
11CO55A#76	273	613	0.45	0.05302	0.00133	0.37819	0.00967	0.05173	0.00068	330	35	326	7	325	4	0.31%
11CO55A#77	64	300	0.21	0.05319	0.00159	0.39206	0.0118	0.05344	0.00072	337	44	336	9	336	4	0.00%
11CO55A#78	155	199	0.78	0.05294	0.0018	0.38298	0.01301	0.05246	0.00074	326	51	329	10	330	5	-0.30%
11CO55A#79	178	410	0.43	0.05238	0.00151	0.34345	0.01003	0.04754	0.00064	302	42	300	8	299	4	0.33%
11CO55A#80	69	206	0.33	0.05321	0.00192	0.38801	0.01404	0.05287	0.00074	338	56	333	10	332	5	0.30%
11CO55A#81	186	639	0.29	0.05276	0.00145	0.37223	0.01037	0.05115	0.00068	318	39	321	8	322	4	-0.31%
11CO55A#82	252	1109	0.23	0.05199	0.0012	0.32723	0.00774	0.04564	0.0006	285	31	287	6	288	4	-0.35%
11CO55A#83	119	229	0.52	0.05338	0.00178	0.40101	0.01342	0.05448	0.00076	345	50	342	10	342	5	0.00%
11CO55A#84	134	230	0.58	0.05335	0.00173	0.39916	0.01302	0.05425	0.00074	344	49	341	9	341	5	0.00%
11CO55A#85	151	819	0.18	0.05253	0.00141	0.34536	0.00941	0.04768	0.00063	309	38	301	7	300	4	0.33%
11CO55A#86	81	130	0.62	0.051	0.00214	0.36932	0.01544	0.0525	0.00077	241	69	319	11	330	5	-3.33%
11CO55A#87	804	850	0.95	0.05461	0.00134	0.29733	0.00742	0.03948	0.00052	396	33	264	6	250	3	5.60%
11CO55A#88	230	218	1.05	0.05308	0.00189	0.39247	0.01399	0.05362	0.00075	332	55	336	10	337	5	-0.30%
11CO55A#89	272	533	0.51	0.05303	0.0014	0.38926	0.0105	0.05322	0.0007	330	38	334	8	334	4	0.00%

					2		6		1							
11CO55A#90	38	47	0.80	0.07912	0.00247	2.36284	0.07365	0.21654	0.00312	1175	39	1231	22	1264	17	-7.04%
11CO55A#91	95	815	0.12	0.05258	0.0013	0.37047	0.00933	0.05109	0.00068	311	34	320	7	321	4	-0.31%
11CO55A#92	147	398	0.37	0.05302	0.00162	0.39113	0.01205	0.0535	0.00073	330	45	335	9	336	4	-0.30%
11CO55A#93	411	639	0.64	0.05383	0.00195	0.31538	0.0114	0.04248	0.00061	364	55	278	9	268	4	3.73%
11CO55A#94	159	130	1.22	0.05279	0.00366	0.36824	0.02546	0.05058	0.00078	320	130	318	19	318	5	0.00%
11CO55A#95	92	419	0.22	0.05236	0.00151	0.37677	0.01097	0.05218	0.00071	301	42	325	8	328	4	-0.91%
11CO55A#96	305	447	0.68	0.05321	0.00148	0.3901	0.01095	0.05316	0.00072	338	39	334	8	334	4	0.00%
11CO55A#97	38	424	0.09	0.0532	0.00175	0.39696	0.0131	0.05411	0.00074	337	50	339	10	340	5	-0.29%
11CO55A#98	133	524	0.25	0.05311	0.00154	0.38526	0.01124	0.0526	0.00072	333	41	331	8	330	4	0.30%
11CO55A#99	373	680	0.55	0.05144	0.00169	0.26001	0.00858	0.03665	0.0005	261	51	235	7	232	3	1.29%
11CO55A#100	474	1145	0.41	0.0532	0.00141	0.36108	0.00972	0.04922	0.00066	337	37	313	7	310	4	0.97%
11CO55A#101	359	932	0.38	0.06041	0.00149	0.65253	0.01633	0.07832	0.00104	618	32	510	10	486	6	4.94%
11CO55A#102	387	897	0.43	0.05359	0.0014	0.39908	0.01055	0.054	0.00072	354	36	341	8	339	4	0.59%
11CO55A#103	112	475	0.24	0.05283	0.00157	0.37259	0.01115	0.05114	0.0007	322	43	322	8	322	4	0.00%
11CO55A#104	202	699	0.29	0.05231	0.00145	0.33636	0.00938	0.04663	0.00063	299	39	294	7	294	4	0.00%
11CO55A#105	169	393	0.43	0.05233	0.00161	0.34042	0.01052	0.04717	0.00065	300	45	297	8	297	4	0.00%
11CO55A#106	124	295	0.42	0.05294	0.00186	0.37881	0.01335	0.05189	0.00072	326	55	326	10	326	4	0.00%
11CO55A#107	112	284	0.39	0.05288	0.00176	0.38015	0.01268	0.05212	0.00073	324	50	327	9	328	4	-0.30%
11CO55A#108	297	354	0.84	0.05242	0.004	0.34768	0.0261	0.04809	0.00097	304	135	303	20	303	6	0.00%
11CO55A#109	325	524	0.62	0.05295	0.00153	0.39915	0.0116	0.05466	0.00074	327	42	341	8	343	5	-0.58%
11CO55A#110	94	319	0.29	0.05426	0.00212	0.38943	0.01522	0.05204	0.00074	382	62	334	11	327	5	2.14%

11CO55A#111	171	464	0.37	0.05239	0.00164	0.34169	0.01077	0.04729	0.00065	302	47	298	8	298	4	0.00%
11CO55A#112	359	553	0.65	0.05274	0.00166	0.36511	0.01151	0.0502	0.0007	318	46	316	9	316	4	0.00%
11CO55A#113	293	409	0.72	0.05271	0.00204	0.35345	0.01363	0.04862	0.00071	316	61	307	10	306	4	0.33%
11CO55A#114	266	470	0.57	0.05334	0.00161	0.40054	0.01215	0.05445	0.00075	343	44	342	9	342	5	0.00%
11CO55A#115	185	412	0.45	0.05308	0.00164	0.39518	0.01225	0.05398	0.00075	332	45	338	9	339	5	-0.29%
11CO55A#116	96	694	0.14	0.05304	0.00151	0.37985	0.01087	0.05193	0.00071	331	40	327	8	326	4	0.31%
11CO55A#117	111	206	0.54	0.05311	0.00226	0.39362	0.01671	0.05374	0.00078	333	70	337	12	337	5	0.00%
11CO55A#118	98	95	1.04	0.05369	0.00266	0.42008	0.02064	0.05673	0.00089	358	82	356	15	356	5	0.00%
11CO55A#119	26	54	0.48	0.05866	0.00343	0.72762	0.04205	0.08994	0.00155	555	96	555	25	555	9	0.00%
11CO55A#120	141	392	0.36	0.05311	0.00161	0.39326	0.01199	0.05369	0.00074	333	44	337	9	337	5	0.00%

Highlights

Detrital zircon from turbidites of the Balagne and Piedmont nappes of Alpine Corsica

Late Cretaceous and Early Eocene detrital zircon provenance is investigated

5 samples yielded U-Pb age spectra ranging from Neoarchean to Late Paleozoic

494 points of Lu-Hf isotopic analysis with continental model ages from 3.5 - 1.0 Ga

European Tethyan margin origin of the Balagne nappe and Piedmont Narbinco flyschs